DISCLAIMER

This report was prepared as an account of work sponsored by an agency of the United States Government. Neither the United States Government nor any agency thereof, nor any of their employees, makes any warranty, express or implied, or assumes any legal liability or responsibility for the accuracy, completeness, or usefulness of any information, apparatus, product, or process disclosed, or represents that its use would not infringe privately owned rights. Reference herein to any specific commercial product, process, or service by trade name, trademark, manufacturer, or otherwise does not necessarily constitute or imply its endorsement, recommendation, or favoring by the United States Government or any agency thereof. The views and opinions of authors expressed herein do not necessarily state or reflect those of the United States Government or any agency thereof. Reference herein to any social initiative (including but not limited to Diversity, Equity, and Inclusion (DEI); Community Benefits Plans (CBP); Justice 40; etc.) is made by the Author independent of any current requirement by the United States Government and does not constitute or imply endorsement, recommendation, or support by the United States Government or any agency thereof.

Ammonium Looping with Membrane Absorber and Distributed Stripper for Enhanced Algae Growth

Final Technical Report

Project Period:
10/1/2020-3/31/2025

Principal Authors:
Bradley Irvin, Kunlei Liu and Mark Crocker

Report Issued
June 2025

Work Performed Under Award Number
DE-FE0031921

SUBMITTED BY
University of Kentucky Research Foundation
109 Kinkead Hall, Lexington, KY 40506-0057

PRINCIPAL INVESTIGATORS
Kunlei Liu, Ph.D., Institute for Decarbonization and Energy Advancement
Phone: (859) 257-0293, Email: Kunlei.Liu@uky.edu
Mark Crocker, Ph.D., Center for Applied Energy Research
Phone: (859) 257-0295, Email: Mark.Crocker@uky.edu

DOE PROJECT MANAGER
Gregory Imler
Gregory.Imler@NETL.DOE.GOV

SUBMITTED TO
U.S. Department of Energy National Energy Technology Laboratory

ACKNOWLEDGEMENT: The University of Kentucky (UK) is grateful to the U.S Department of Energy National Energy Technology Laboratory for the support of this project. UK is also grateful to Trimeric, Vanderbilt University and Colorado State University for support and partnership.

The project team is also grateful to the many UK research personnel for assistance with the project, as listed below.

John Adams
Hashem Altamneh
Saloni Bhatnagar
Matthew Burton
Norman Chan
Mark Crocker
Reynolds Frimpong
Feng Zhu
Xin Gao
Len Goodpaster
Brian Hogston
Bradley Irvin
Kim Knorr
Kunlei Liu
Marshall Marcum
Madeline McDermott
Margaret Moore
Chin Ng
Heather Nikolic
Lisa Richburg
Steve Summers
Otto Hoffman
Jesse Okorafor
Julia Parker
Robert Pace
Roger Perrone
Michael Renfro
Benjamin Sears
Aaron Smith
Shi Su
Jesse Thompson
Xiaoshuai Yuan
Fritz Vorisek
Yaying Ji

Contents

1. EXECUTIVE SUMMARY 6
1.1 Overview 6
1.2 Key Results 9
1.3 Key Challenges 12
2. BACKGROUND AND TECHNOLOGY DESCRIPTION 13
2.1 Project Objective and Background 13
2.2 Process Description 14
2.3 Overview of Technology 15
3. DESIGN, FABRICATION, INTEGRATION WITH EXISTING IDEA BENCH CO_2 CAPTURE UNIT, MEMBRANE DEVELOPMENT, AND INITIAL ALGAE STUDY 17
3.1 Design of Absorber Loop 17
3.2 Membrane Development 20
3.2.1 Hollow Fiber Membrane from Compact Membrane Systems 20
3.2.2 Flat Sheet Membrane from Sterlitech 22
3.2.3 Hollow Fiber Membrane from Mann+Hummel 23
3.3 Advanced Membrane Development ..... **Error! Bookmark not defined.**
3.4 Lab-scale Membrane Absorber Performance Evaluation 25
3.5 Parametric Testing Results 26
3.7 Algae Study 32
3.7.1 Introduction 32
3.7.2. Experimental 35
3.7.3. Results and Discussion 36
3.7.4. Summary 45
4. DESIGN AND FABRICATION OF FULLY INTEGRATED PROCESS, AND LONG TERM CAMPAIGN RESULTS 45
4.1 Integrated Process Design Basis 46
4.2 Integrated Process Design Package: 47
4.3 Integrated Process Construction: 48
4.4 Gas Sampling 51
4.5 Long-term Campaign, Process Performance 53
4.6. Algae, Outdoor Evaluation 56
4.6.1. Overview 56
4.6.2. Experimental 56

4.6.3. Results and Discussion 57
4.6.4. Summary 66
4.7 Long-term Campaign, Algae Production 66
4.7.1. Introduction 66
4.7.2. Experimental 67
4.7.3. Results and Discussion 68
4.7.4. Summary 78
5. SUMMARY OF TECHNOLOGY MATURATION PLAN 78
6. SUMMARY OF TECHNOLOGY GAP ASSESSMENT 79
7. SUMMARY OF TECHNO- ECONOMIC ANALYSIS 83
8. LESSONS LEARNED 93
9. TECHNICAL BENEFITS AND SHORTCOMINGS 93
10. FUTURE DEVELOPMENT 94
11. References 94
12. LIST OF ACRONYMS 98

1. EXECUTIVE SUMMARY

The objective of this project is to conduct a comprehensive investigation to develop and demonstrate a practical, reliable, and cost-effective integrated carbon dioxide (CO_2) capture and biofixation process for algae production. This process utilizes a chemical hindered ammonium solution (NH_4OH) as both a capture reagent and an algae nutrient. The membrane absorber employed in the system ensured minimal ammonia (NH_3) emissions in the treated flue gas. Additionally, distributed solar-energy powered strippers located near the bioreactor modules facilitate solvent regeneration and enable just-in-time delivery of CO_2 and NH_3 to the algae, thereby minimizing the pH swing for enhanced productivity. The proposed membrane CO_2 absorber and solar-powered stripper is designed and seamlessly integrated with the existing 0.1 MWth bench-scale CO_2 capture system (CCS) and open raceway ponds (ORPs) at the University of Kentucky Center for Applied Energy (UK CAER) campus. The entire integrated process has undergone construction, operation, testing, and analysis. Furthermore, technology has been evaluated with a techno-economic analysis (TEA), technology gap analysis (TGA), life-cycle analysis (LCA), and a technology maturation plan (TMP).

This project was performed within two budget periods, 54 months in duration. There are fourteen Project Tasks, twelve Milestones and four Success Criteria.

1.1 Overview

The overall goal of this project is to create a CO_2 capture system with onsite utilization for enhanced algae growth—eliminating costly CO_2 transportation costs. The generalized concept is shown in **Exhibit 1.1.1**. This technology can be used in proximity to algae production in conjunction with the onsite point source CO_2 generation, such as power or heat generation, chemical production, and energy-intensive industries, etc. Atmospheric CO_2 is an option, but only under certain algae growth requirements. The CO_2 capture system is an aqueous process, CO_2 is scrubbed from the point source emitter using a 0.5-2 mol/kg ammonium solution. During solvent regeneration, a product stream of CO_2 and NH_3 is produced at a molar ratio of about 10 to 1. This stream is then fed to nearby algae ponds as a nutrient and carbon source. The regeneration of the solvent is driven by solar-thermal energy, thereby eliminating the requirement for excess capital equipment, such as boilers, turbines, their auxiliary equipment, and their operating cost to provide steam and electricity to the solvent regeneration unit. This application not only reduces the capital expenditure associated with the process, but also eliminates additional CO_2 emission from solvent regeneration. The direct connection between the outlet of the CO_2 capture process and the bioreactor avoids long distance delivery and reduces associated capital and gas compression costs. Overall, the integrated process can offer environmental benefits by converting captured CO_2 into value-added products, reducing CO_2 emissions, and contributing to a more circular and sustainable economy in a simple and cost-effective way.

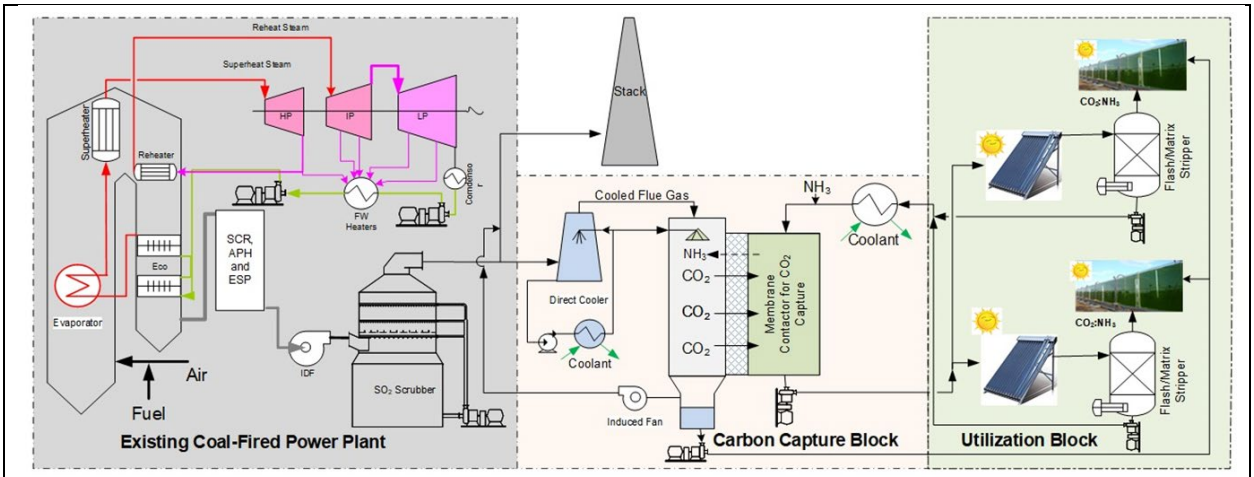

Exhibit 1.1.1. Generalized concept of the ammonium looping process for enhanced algae growth. CO_2 is generated in the point source emitter block, captured by the carbon capture block, and fed directly to the algae in the utilization block eliminating the need for CO_2 gas compression, transportation, delivery, and storage.

The UK integrated post-combustion CO_2 capture and utilization system for a point-source emitter builds on aqueous carbon capture technology with key attributes of ammonium solvent applied as both capture reagent and algae nutrient, indirect contact of flue gas and solvent in membrane absorber with downward flow in over-saturated environment to ensure long-term operation, solar-thermal energy powered solvent regenerators, just-in-time CO_2/NH_3 supply control strategy and utilization by the algae in photobioreactors. These techniques intensify the capture and conversion process towards significantly lower capital and operating costs and provide a clear pathway to reduce capture capital and operating costs by 50% and boost algae production by 50%.

From the point source emitter, flue gas enters the ammonium looping process and passes through the hollow fiber membrane absorber, CO_2 is absorbed and the now rich ammonium solvent travels through a series of heat exchangers, as shown in **Exhibit 1.1.2**. The first heat exchanger is the primary heat exchanger, a heat recovery unit, where heat transfer occurs between the cold rich and hot lean solvents. Further downstream the warm rich solvent is split into two separate streams. One is heated by solar water heater, up to stripping temperatures, becoming the hot rich stream and the other is sent directly into the flash stripper at pre-determined temperatures as the warm rich stream to control CO_2/H_2O molar ratio at the stripper gas outlet. The hot rich solvent enters the flash stripper through a spray nozzle with a 40° cone shaped spray angle. Due to the drop in temperature pressure flashing occurs and CO_2 is stripped from the solvent along with gaseous ammonia. The warm rich stream enters the top of the stripper and is sprayed onto the gaseous CO_2 and ammonia via a 65° spray nozzle which condenses excess ammonia, increasing the richness of CO_2 in the eventual product stream sent to the algae ponds. The now lean solvent is pumped back through the process, completing the loop.

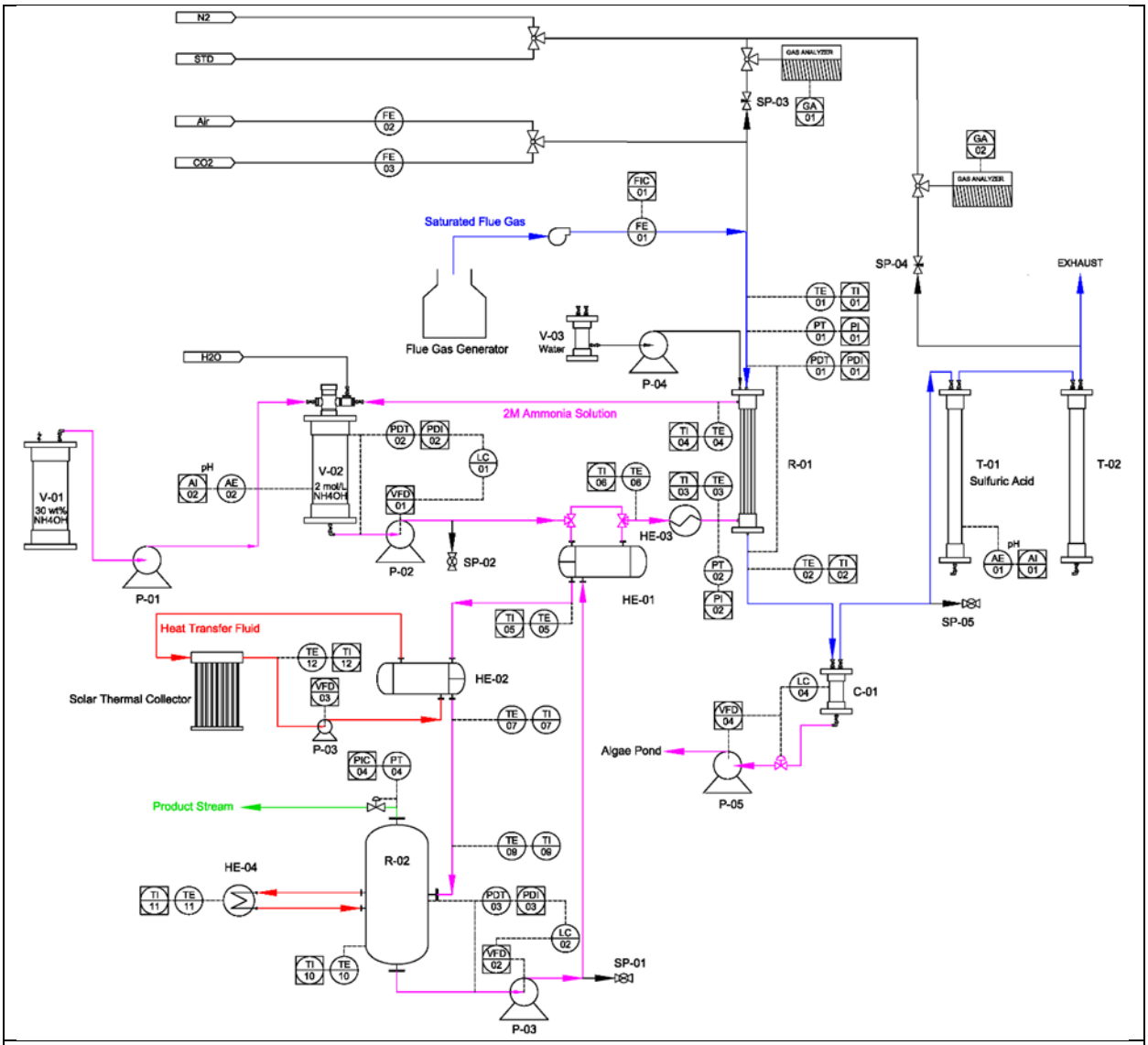

Exhibit 1.1.2. Process flow diagram for the ammonium looping process.

According to the NH_3-CO_2-H_2O ternary phase diagram, **Exhibit 1.1.3**, ammonium carbamate, a sticky solid, is the only product between NH_3 and CO_2 in the absence of water vapor. However, non-sticky ammonium carbonate, a compound that is very soluble in water, will be formed at a saturated gas condition when the CO_2 concentration is much higher than the NH_3 concentration, as exists in the proposed scenario. Downflow condensate from the saturated flue gas in the application resulting from heat transfer will continuously dissolve and wash away the NH_4^+ salts as they form and prevent fouling of the membrane.

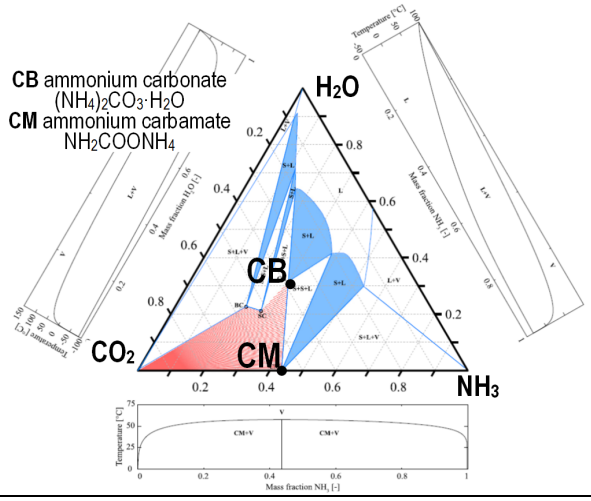

Exhibit 1.1.3. The NH_3-CO_2-H_2O Ternary Phase Diagram. (53)

Algae is less productive when under chemical stress, which is the practical case resulting from intermittent intake of NH_4^+, HCO_3^- and CO_3^{2-}, or when there is an imbalance in the C:N ratio in the algae growth medium as shown in **Exhibit 1.1.4**. At high C:N ratios, consumption of N by the culture (in parallel with CO_2 consumption) will result in a pH decrease, whereas at low C:N ratios the pH increases. Hence, there is a strong incentive to target the stoichiometric C:N ratio in the solution fed to the culture to minimize fluctuations in pH. To address this, distributed solvent regenerators will be operated individually via controlling the stripper exhaust temperature to deliver just-in-time CO_2 and NH_3 to the bioreactor as needed and at the appropriate ratio. Given that the molar C:N ratio of rich ammonium solution exiting the membrane contactor is between 0.5-1 (0.5 corresponding to ammonium carbonate and 1 corresponding to ammonium bicarbonate) without any regeneration, and 147 when the regenerator outlet is set at 210 °F and 59 psi, the stoichiometric C:N ratio (~7) for Scenedesmus acutus (UTEX B72), the algae strain to used in the proposed study, is readily achievable by adjusting the stripper pressure and exhaust temperature.

$\underline{NH_4^+ \text{ consumption - excess } CO_2 \text{ present } (NH_4^+ \text{ limiting}):}$

$(NH_4)_2CO_3 \rightarrow\rightarrow H_2CO_3;\ NH_4HCO_3 \rightarrow\rightarrow H_2CO_3$

$\underline{CO_2 \text{ consumption - excess } NH_4^+ \text{ present } (CO_2 \text{ limiting}):}$

$(NH_4)_2CO_3 + H_2O \rightarrow\rightarrow 2NH_4OH;\ NH_4HCO_3 \rightarrow\rightarrow NH_4OH$

Exhibit 1.1.4. NH_4^+ and CO_2 Consumption.

1.2 Key Results

In Budget Period (BP) 1, the absorber membrane loop was designed, constructed, and tested as a standalone unit and integrated with the University of Kentucky Institute for Decarbonization and Energy Advancement (UK IDEA) bench CO_2 capture unit. This was done to test the capture of the membrane and ensure adequate performance before being integrated into the standalone process constructed in BP 2 for onsite capture and delivery of nutrients for enhanced algae growth. The membrane was studied and engineered to reduce ammonia slippage to below 1000 ppm that will react with CO_2 at the gas-side passage and then be dissolved in the flue gas condensate. Algae was

grown at the laboratory scale in 800 mL tubular photobioreactors with bottled CO_2 feed and nitrogen-based nutrients delivered as needed. This allowed the team to study the effects that varying nutrient feed rates and CO_2:NH_3 ratios have on algae growth rate and pond pH. This was necessary to establish optimal feeding conditions in BP2.

- 0.5M NH_4OH was used as the primary capture solvent. Given the target feed rates needed for BP 2 evaluation, the absorber loop easily meets the performance requirements.
- Ammonia slippage from the membrane absorber was kept below 1000 ppm with hollow fiber membrane used in the final integrated process. It was determined that slippage is dependent on free ammonia concentration in the solvent, lower concentrations yield lower slippage.
- NH_3 concentrations in absorber exhaust and product stream were measured using the EPA wet-chemistry method. This method being time consuming and costly, a real-time estimation method was developed by correlating solution pH with concentration. While the EPA method was still used to get precise measurements, the pH method was invaluable for real-time feedback during process operation. This was later adopted into the advanced process control scheme developed for long term testing in BP 2.
- Demonstrated stable operation via ammonium salts formed on gas side of membrane being washable by flue gas condensate.
- Growth of *Scenedesmus acutus* was obtained using gaseous CO_2/NH_3 as a C- and N-source for algae cultivation, a CO_2/NH_3 mole ratio of ~10 being optimal with respect to algae productivity and the utilization of CO_2 and NH_3.
- The composition of resulting algae biomass was notable for its low ash content and high protein content. These characteristics suggest that the biomass should be well suited for the production of bioplastics or for use as animal feed.
- To avoid the toxic effects of high dissolved NH_3 concentrations (>2.0 mM) in the algae culture, it is necessary to balance the NH_3 supply with the algae growth rate so that excessive NH_3 accumulation is prevented.

The integrated process was evaluated with solvent and real fossil fuel-derived flue gas. A long-term campaign of 80 days was conducted with natural gas combusted flue gas. TEA, a TMP, and TGA were also performed. The BP 2 parametric and long-term campaigns demonstrated the following.

- Splitting the rich feed into a hot and warm feed to the stripper is effective to control the product stream CO_2:NH_3 molar ratio of 10 via adjusting the gas exhaust temperature. Experimental and simulation results for product stream ratios aligned.
- Target stripping conditions were achievable with the solar thermal heater.
- The advanced smart operating system was able to control the process while reaching and maintaining target product stream requirements.
- In conclusion, the productivity of the test ponds (ORPs 1 and 2), when averaged over the whole dataset (80 days), exceeded that of the reference ponds (ORPs 3 and 4), validating our hypothesis concerning the benefits of using CO_2/NH_3 for algae culturing. Not only were algae growth rates higher in the test ponds, the algae cultures proved more robust with respect to the reference ponds. This can be attributed, in part at least, to the suppression of rotifers in the test ponds, resulting from the presence of free NH_3.

The TEA showed:

- UK's ammonium looping technology provides a great opportunity for the dual use of ammonia, a commercially available bulk, oxidation-stable chemical as a CO_2 capture solvent and feedstock to promote algal biomass growth.
- While significant progress was demonstrated in developing suitable membranes for the application, some uncertainty still exists around the membrane availability with large bore size, operability, and cost that needs to be resolved through additional testing.
- There is no technical risk associated with generating concentrated solar power for solvent regeneration. However, the current scale of the technology is too small to realize economies of scale.
- Capital cost could potentially be reduced by replacing the direct contact cooler (DCC) with water spray in the flue gas duct to remove superheat from the flue gas as the DCC tower together with ancillary equipment like the heat exchanger and pumparound would not be required.
- Additionally, capital costs are directly proportional to the capacity of the CO_2 capture unit, which is sized based on the peak algae CO_2 utilization. The process simplification and optimization should be reviewed and evaluated for cost reduction, including buffer storage of CO_2, standalone rich and lean storage tanks, and/or enlarged absorber and regenerator sumps. This would allow the capture unit to have a design rate closer to the average algae demand rate, and it would increase the system utilization.

The LCA showed:

- A significant amount of carbon is sequestered by the biomass during cultivation (-109 g CO_{2e} MJ^{-1}). However, most of this sequestered carbon is redistributed across different hydrothermal liquefaction (HTL) product streams, with portions released in the gas-phase (13 g CO_{2e} MJ^{-1}) and aqueous-phase (23 g CO_{2e} MJ^{-1}).
- Assessment of the contributions of different process stages to the global warming potential (GWP) showed that cultivation-related emissions, particularly those linked to CO_2 capture and delivery, are the largest contributors to overall GWP.
- A comparison of the ammonium looping system with the conventional CO_2 compression and sparging method showed that the CO_2 sparging scenario exhibits significantly higher emissions from cultivation due to its greater energy intensity, stemming from the compression and sparging process required for CO_2 delivery. The ammonium looping system, however, benefits from emissions offsets through carbon sequestration in biochar and the recovery of ammonia in the aqueous phase of HTL, both of which help reduce its net impact. Conversion and transportation emissions were found to remain relatively similar across both scenarios, contributing to 30% of the total net GWP in the ammonium looping system.
- An analysis of the sensitivity of GWP to carbon utilization efficiency (CUE) and productivity considering the impact of CO_2 on the net greenhouse gas emissions of algal biofuel production, showed that increasing both CUE and productivity significantly reduces GWP, with values decreasing from approximately 75 g CO_2e MJ^{-1} at 50% CUE and 10 g m^{-2} d^{-1} productivity to below 55 g CO_2e MJ^{-1} at 70% CUE and 28 g m^{-2} d^{-1} productivity. The steepest reductions in GWP occur when both parameters are optimized, highlighting the importance of improving CO_2 conversion efficiency and biomass growth rates to enhance the sustainability of algal biofuel systems.

1.3 Key Challenges

The key technical challenge encountered in BP 1 was a suitable sampling method to determine ammonia slip in the hollow fiber membrane absorber. While experimenting with different membrane materials and operating the absorber loop, it became clear that a real-time method for determining ammonium concentrations in the process would be needed for optimal operation. **Exhibit 1.3.1** shows that by correlating concentration to pH a reasonable determination of ammonium concentration can be easily obtained in real-time.

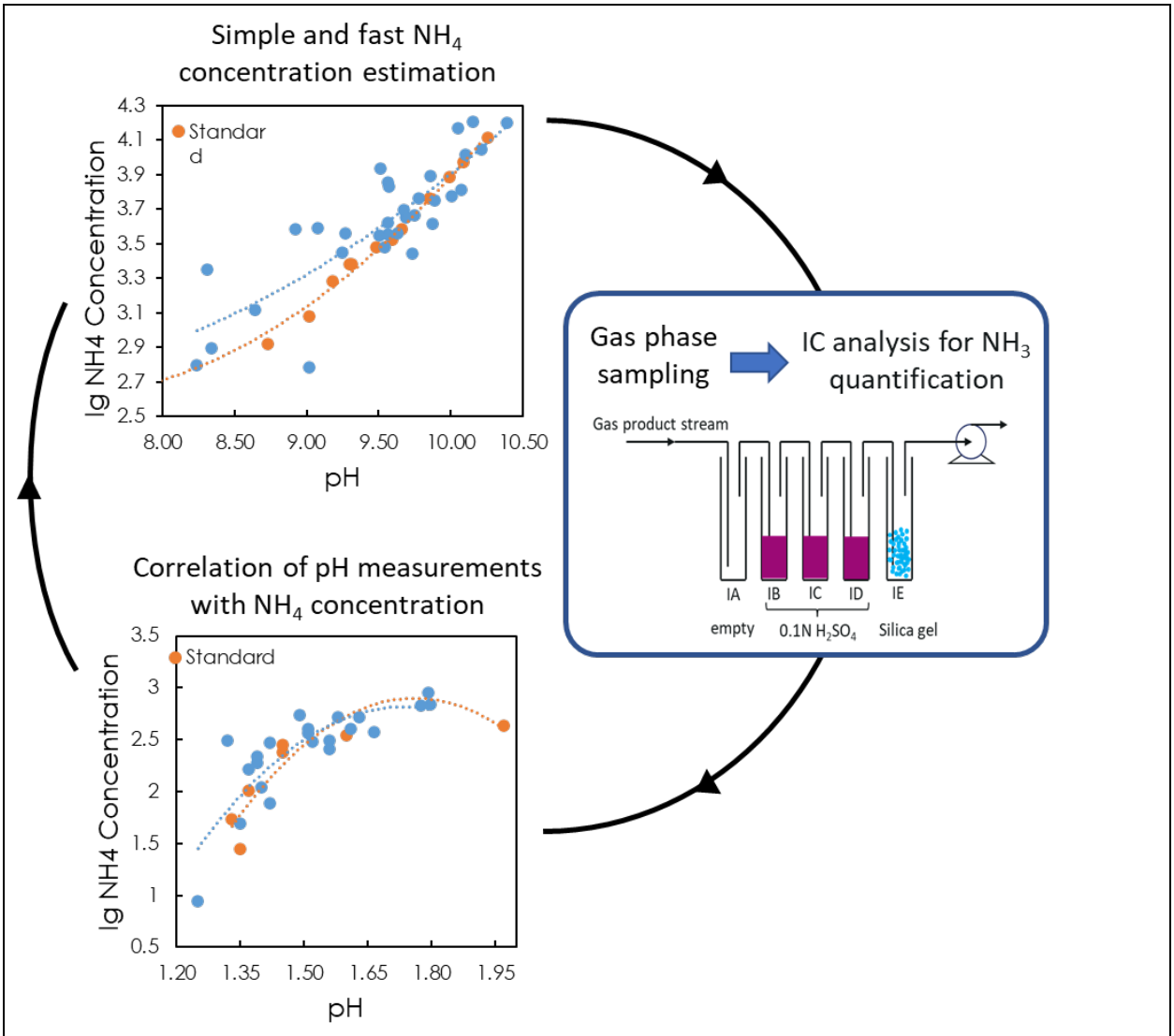

Exhibit 1.3.1. Correlating ammonia concentrations with pH to replicate gas sampling for fast real-time feedback. Note: the off-line IC analysis is time-consuming step

The key technical challenge encountered in BP 2 was to deliver a product stream ratio of 10:1 CO_2:NH_3. Initially, a condenser was included in the design of the stripper but was removed due to concerns of ammonium carbonate formation. As a result, high ammonia vapor existing in the product stream, results in a product stream ratio below the target level of 10:1. To solve this

problem, the rich solvent feed to the stripper after lean/rich heat exchanger was split into two streams fed into different locations along the regenerator named a hot and warm rich feed respectively. The warm rich stream is fed to the top of the regenerator while the hot rich stream was sent through the solar thermal heater to reach stripping temperatures, as shown in **Exhibit 1.3.2**. The warm feed was directed into the top of the stripper and through a wide-angle nozzle. This acted as an in-situ condenser to control the gas temperature at stripper exhaust without direct contact to any metal surface thus eliminating the potential solid formation, and an ammonia in-process absorber to readjust the CO_2 and NH_3 vapor pressure by already being at a high carbon loading in the liquid. Additionally, this modification has the added benefit of improving energy utilization efficiency by reducing the temperature of the product stream, keeping the heat inside the stripper. This method has been tested and proven on other UK IDEA CO_2 capture processes.

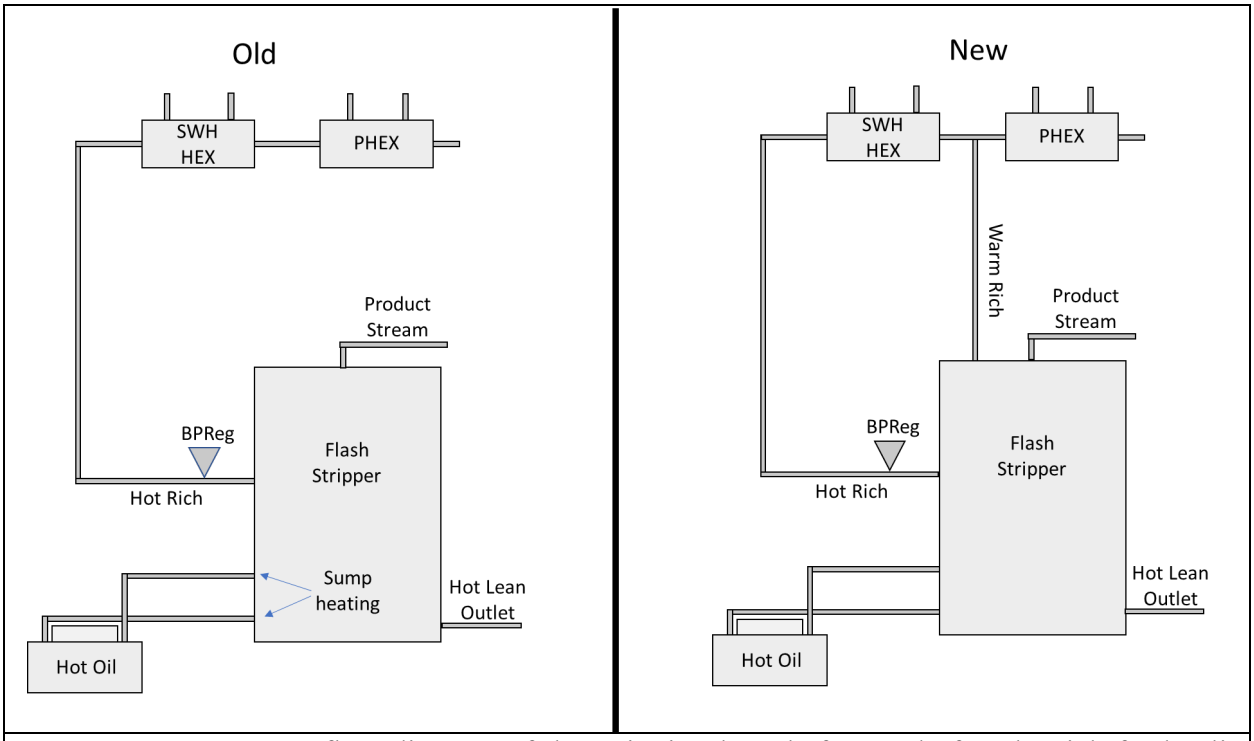

Exhibit 1.3.2. Process flow diagram of the stripping loop before and after the rich feed split flow modification.

2. BACKGROUND AND TECHNOLOGY DESCRIPTION

2.1 Project Objective and Background

Objectives

- Demonstrate effectiveness of the membrane CO_2 absorber using an ammonium solution with chemical additives in terms of CO_2 capture and minimal NH_3 slip with no blockage on the membrane surface.
- Demonstrate increased algae production by continuous feed of CO_2:NH_3 in the proper ratio.

• Demonstrate effectiveness and operability of the solar-powered solvent regenerator in terms of producing the instantaneous product stream with proper CO_2:NH_3 ratio. • Evaluate the feasibility and economics of the proposed technology by completing a TEA, TGA, LCA and TMP.
Exhibit 1.1.1. Project Objectives.

To meet the Department of Energy (DOE)'s performance and cost targets for CO_2 capture and utilization, innovative approaches that provide a pathway for the realization of the goals have to be adopted. With technological improvements geared towards significant capital and operating cost reduction, energy savings and performance enhancements, UK IDEA validated an ammonium looping integrated CO_2 capture and utilization technology as highlighted in **Exhibit 2.1.1.** First, a thermally- and oxidatively-stable, dual-function, ammonium solution is used as both the CO_2 capture absorbent and an algae nutrient. Second, a membrane CO_2 absorber using an ammonium solution with chemical additives in terms of CO_2 capture and minimal NH_3 slip, is demonstrated effective with no blockage on the membrane surface and flue gas passage. The down-flow condensate from the saturated flue gas continually dissolves and washes solid formed on the gas side of the membrane absorber to ensure long-term operation. A capture capital and operating costs savings of 50% is achievable by eliminating flue gas pretreatment for cooling/SO_2 removal, steam extraction for solvent regeneration and CO_2 compression for distribution to algae ponds. Third, algae production increased by 50% by continuously supplying CO_2:NH_3 in the proper ratio compared to a state-of-the-art (SOA) intermittent, decoupled feeding system. Fourth, effectiveness and operability of solvent regeneration is demonstrated in the integrated ammonium looping CO_2 capture and utilization process, eliminating steam extraction typical in SOA aqueous CO_2 capture technologies.

The bench-scale integrated system consists of UK IDEA's existing CO_2 capture system (replacing the absorber) and algae bioreactor to demonstrate CO_2 capture and utilization from coal-, natural gas (NG)-, and industrial-flue gas, as illustrated in **Exhibit 3.1.2**. A stripping loop was then constructed, and the entire process was relocated to the site with algae ORP's, NG boiler, and an advanced process control program, forming a fully integrated process, as shown in **Exhibit 4.3.1**. The experimental information gathered served as inputs for modelling to optimize the membrane capital and operation cost for scale-up by Vanderbilt University. The data generated by UK IDEA and Vanderbilt University was sent to Colorado State University and Trimeric Corporation to conduct the TEA and LCA analyses. The developed simplified ammonium looping for large quantity algae production can significantly reduce complexity and cost of CO_2 capture and biofixation from all sources (fossil-fueled power generation, cement plants and chemical plants). The project, as a whole, can result in continued utilization of fossil fuels for reliable electricity production while affordably managing environmental concerns and increase public confidence in capture and utilization technology that could be self-financing and sustainable.

2.2 Process Description

The proposed ammonium looping CO_2 capture and fixation integrated system, **Exhibit 1.1.1**, combines expertise from UK IDEA's aqueous CO_2 capture and UK CAER's algae-utilization research areas. The integrated capture and utilization UK IDEA system comprises real flue gas generators (coal and NG), a hydrophobic membrane CO_2 absorber, a solar powered flash stripper,

bioreactors, auxiliary pumps, NH_3 and water make-up systems, heat exchangers, valves, instrumentation, and advanced process controls.

In detail, at the scale under investigation funded by this cooperative agreement, the integrated capture and utilization system use 15 cfm flue gas produced from either coal or NG combustion. Flue gas enters a flue gas pre-conditioning device for SO_2 removal when needed and cooling via water spray. A fan is then used to boost the pressure before flowing downward through the membrane CO_2 absorber. CO_2 is captured through the membrane by ammonium solution. Treated flue gas flows through a water-wash column to remove any NH_3 slip prior to stack emission. The washed solution combining with flue gas condensate in the absorber is sent to algae ponds as make-up water. The CO_2-rich solution exiting from the absorber flows through a pump, a heater powered by solar thermal energy, and a solvent regenerator followed by a rich-lean heat exchanger, is pressurized by a pump and recirculates through a lean solvent temperature polisher to CO_2 membrane absorber. The product stream at solvent regenerator exhaust with a just-in-time feed of CO_2 and NH_3 is injected to algae reactor via sparging under just-in-time supply control strategy. A 2 or 0.5 M ammonium solution is used as capture reagent and N nutrient for algae growth. Two 900L ORPs are used to evaluate the performance of the integrated system.

The indirect contact between the flue gas and capture solvent in the membrane absorber reduces or even eliminates the flue gas cooling and pretreatment requirement. Using the solar thermal energy for the solvent regeneration eliminates the need for the excess generation capacity that is usually needed to provide steam and electricity and its associated CO_2 emission. The direct connection between the outlet of CO_2 capture process and the bioreactor eliminates the CO_2 compression and transportation cost.

2.3 Overview of Technology

The intensified process addresses four scientific challenges faced by SOA technologies of CO_2 capture and fixation by algae: 1) the high cost of capturing CO_2 using aqueous solvents due to high energy consumption and large capital investment; 2) CO_2 delivery and feed, due to the large footprint (10-20 of acres/1000 tonnes utilized annually) of the algae bioreactor and the high pressure drop across the gas spargers required for high CO_2 utilization efficiency; and 3) inhibition of algae growth resulting from frequent pH swings in the bioreactor due to unbalanced (intermittent) feeding systems for CO_2 and N.; and 4) short-term planned or unplanned disruptions in flue gas/CO_2 supply to the algae bioreactor.

1. Membrane CO_2 Absorber

<u>Reduced Cost of CO_2 Captured to Bioreactor:</u>
Approximately 25% of the cost of aqueous post-combustion (PC) CO_2 capture is associated with flue gas pretreatment, steam extraction, and CO_2 compression, which are all eliminated in the proposed process. Advantage is taken of the flue gas condensate in the indirect-contact low-thermally conducting membrane absorber, eliminating the need for a cooling (maintaining the water balance in the typical aqueous systems) and SO_2 removal pretreatment (reducing the thermal stable salt formation in the conventional aqueous systems) step. Solvent regeneration is powered by solar energy, eliminating the need for steam extraction from additional fossil fuel combustion. The integrated solvent regenerator with bioreactor eliminates the need to compress a CO_2 product

stream. A preliminary TEA conducted by team members, Colorado State University and Trimeric, has indicated that 20-50% of the cost of algae production is from CO_2 cost and distribution depending on the source (coal or natural gas, respectively), the way CO_2 is supplied, and the distance transported.

Dual-functional Ammonium Looping:

NH_3 has been used for CO_2 capture and as an algae nutrient respectively but hasn't been integrated as one loop. For CO_2 capture it is inexpensive, has a low regeneration energy, zero degradation and a viscosity near that of water. Numerous studies have shown that the scrubbing capacity of NH_3 is approximately 0.9-1.2 kg of CO_2/kg of NH_3, with a CO_2 removal efficiency of ~99% and half the solvent regeneration energy than that of 30 wt% MEA [1-3]. However, the main drawback is the high NH_3 emission. Hydrophobic membranes have been studied for CO_2 capture using an aqueous ammonium solution [4,5]. However, even though significant reduction of the NH_3 slip has been achieved, there is still a critical challenge regarding long-term performance stability in industrial applications due to crystallization of ammonium (NH_4^+) salts on the lumen side of the membrane due to the reverse permeation of NH_3 from liquid side to gas side then reacting with gaseous CO_2. In this project, three ways were adopted to manage NH_3 slip.

1) A carbon-loaded low concentration of NH_3 (0.5-2 M) solvent with additives is employed to lower the NH_3 vapor pressure. The species partial pressure is proportional to the concentration in the liquid. Hence, lowering the free ammonia concentration will lower the partial pressure.
2) The counter movement of ammonia and CO_2 across the membrane provides opportunity to form ammonium carbonate in the presence of water vapor, that acts as an ammonia recovery unit.
3) A downflow flue gas configuration was utilized since flue gas is entering the membrane at a saturated condition, forming liquid film along the membrane wall due to heat transfer. Experiments performed using water-saturated simulated flue gas showed a benefit to anti-fouling and NH_3 slip recapture from the water condensate liquid phase formed on the gas-side [5]. The downflow orientation will allow the condensate to continuously wash ammonium salts from the membrane surface when formed. The collected condensate will be fed to the algae as makeup water and supplemental nutrients.
4) A nanoporous, dense membrane was utilized. To reduce NH_3 slip, a set of chemically resistant composite fibers have been utilized, made of a thin dense layer that is highly permeable to CO_2 but less permeable to NH_3. It was found that fluorinated polymers are effective for this purpose by increasing the NH_3 mass transfer resistance [6]. Further development of the membrane material will be conducted to depress the NH_3 permeability.

2. Algae Production

Preferable Growth Media with Just-in-time C:N Delivery at Appropriate Ratio:

In the regenerators, the amount of CO_2 and NH_3 in the product stream can be adjusted and controlled by a combination of the stripper pressure and its exit temperature assisted with the feed of warm rich stream. During the project execution, a pressure of 20 psi and a temperature of 135 °F after the overhead condenser was determined to deliver a product stream with C:N molar ratio of ~10, as preferred by the algae culture. Algae biomass typically contains 45-50% C, 7-8% N, and 1.4% P, varying according to species and growth conditions. Numerous studies have suggested

that the effects of N on algae production and composition may depend on the source and chemical composition of N added to the growth medium [7,8]. Additionally, the thermally compressed CO_2/NH_3 stream from the stripper could facilitate sparging of this stream with fine gas bubbles into the bioreactor modules for high ammonia and CO_2 utilization efficiency.

Disruptions of CO_2 Original Source:
The NH_3 solvent loop of the proposed technology can continue to circulate with regeneration occurring for short periods during interruption of the flue gas supply. In this case, the solvent may be over-stripped, but the algae feed should remain continuous.

3. DESIGN, FABRICATION, INTEGRATION WITH EXISTING IDEA BENCH CO_2 CAPTURE UNIT, MEMBRANE DEVELOPMENT, AND INITIAL ALGAE STUDY

3.1 Design of Absorber Loop

The piping and instrumentation diagrams (P&IDs) for the integration of membrane absorber into the existing bench-scale CO_2 unit was prepared as shown in **Exhibit 3.1.1**. Membrane absorber tie-ins to the existing CCS has been accomplished, as shown in **Exhibit 3.1.2**. Three major components are included in the process, namely the aqueous ammonia tanks (V-01/02), the membrane absorber (R-01) and the acid tower (T-01). Concentrated 30 wt% aqueous ammonium solution from V-01 is pumped by P-01 into V-02 and diluted to 3 wt% (1.76M). The liquid exits V-02 from the bottom and is pumped by P-02 to the shell-side of R-01 and circulates back to V-02 at the beginning stage. After absorbing CO_2 and reaching the targeted carbon loading, the liquid exiting V-02 is pumped to the existing stripper for regeneration. The lean solvent from outlet of stripper is sent back to R-01 for CO_2 absorption. The liquid exiting from R-01 is pumped back to V-01 for continuous operation. Coal or NG derived flue gas is fed to R-01, CO_2 diffuses from the gas side to the liquid side through the membrane and gets absorbed in the ammonium solution. The ammonia in the solution could diffuse to the gas side, as ammonia slip, and reacts with CO_2 in the gas stream or mixes with treated flue gas exiting R-01 to the condenser (C-01). To prevent the NH_3 emission to the atmosphere at bench-scale investigation, an acid tower, T-01, is used to scrub the ammonia in the treated flue gas.

Liquid samples are taken manually at the inlet and outlet of the stripper via sample points SP-01 and SP-02, for off-line analyses to measure alkalinity and carbon loading. Gas phase composition is monitored on-line via sample points SP-03 and SP-04 for CO_2 and NH_3 concentration determined by gas analyzer, and a gas phase sample is collected at point SP-05 for off-line NH_3 slip determination by wet-chemistry method using ion chromatography (IC). To maintain the solution alkalinity, samples are collected from V-02 ammonia tank for off-line total alkalinity analysis to determine the amount of 30 wt% ammonium solution to be added to maintain the 3 wt% concentration in V-02. The equipment and instrumentation used in the bench-scale unit are given in **Exhibit 3.1.3.** The control system and electrical layout is given in **Exhibit 3.1.4**. The main equipment and instrumentation include pumps, gas analyzers, and the control system computer.

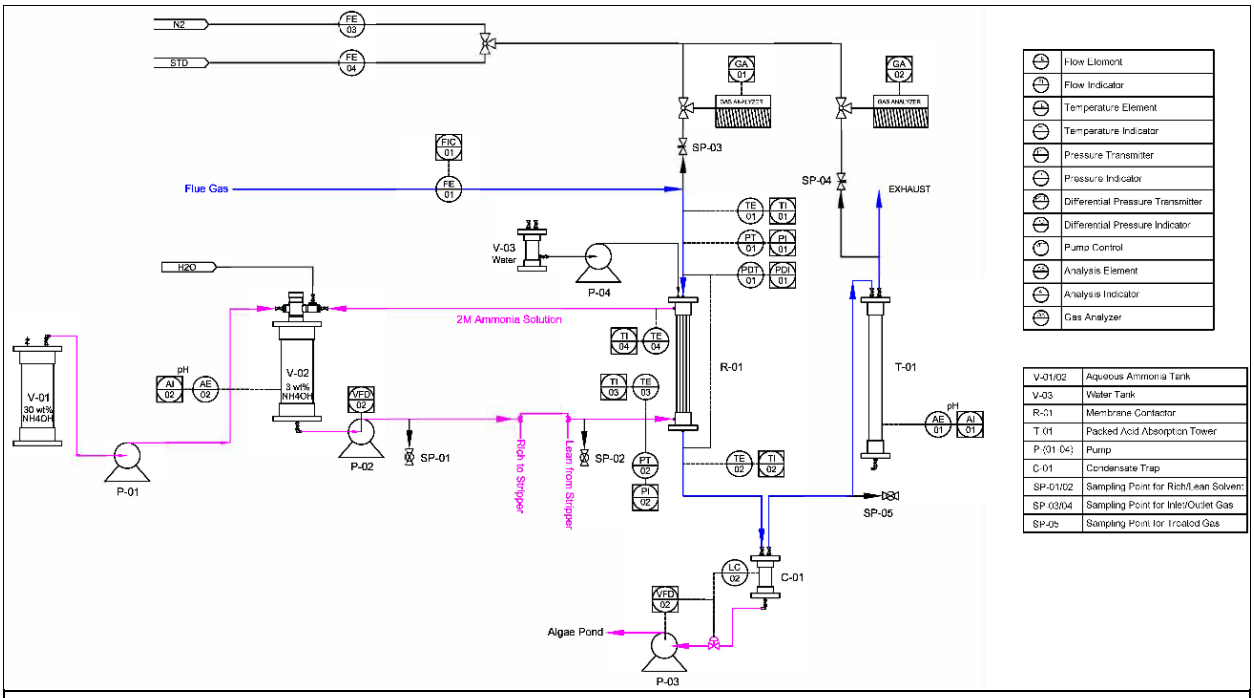

Exhibit 3.1.1. P&ID for bench-scale absorption unit.

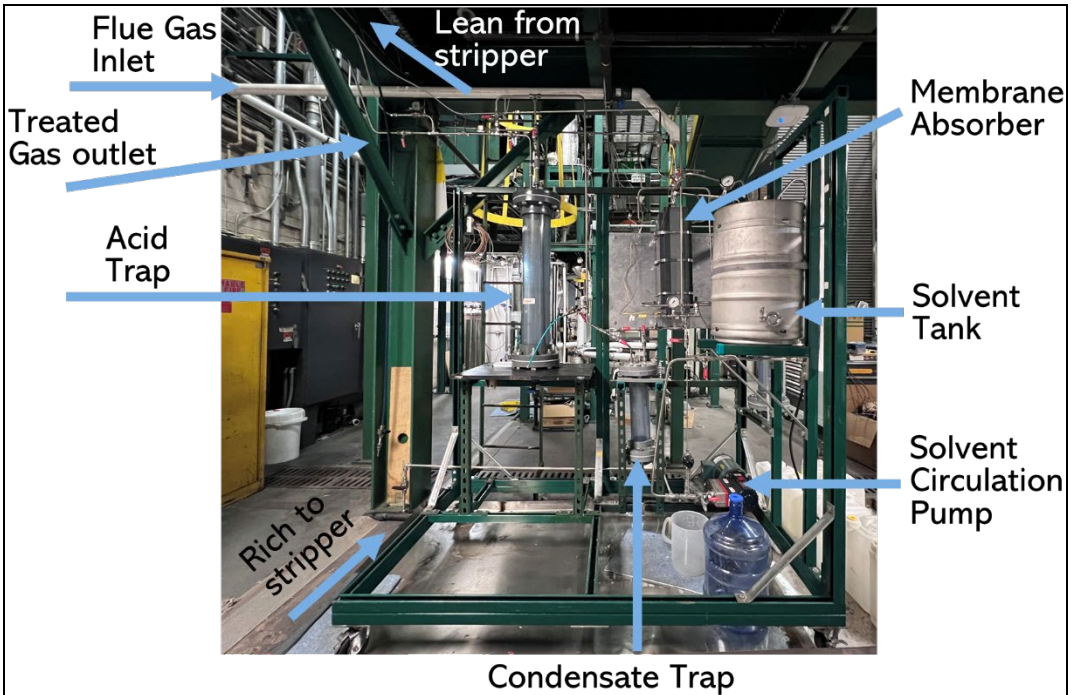

Exhibit 3.1.2. Integration of membrane absorber and existing CCS.

Exhibit 3.1.3. Equipment and instrumentation list.

Name	Description	Stream/Drawing No.	Quantity	Material

Aqueous Ammonia Tank	50 L stainless steel tank	V-02	1	Stainless steel
Acid Tower	PVC column, built in-house	T-01	1	PVC
Membrane Module	Hollow fiber membrane module (CMS, Mann+Hummel), flat sheet (Sterlitech) customized module,	R-01	1	
Pumps	Hydra-cell pumps	P-01, P-02, P-03, P-04	4	
Stripper column	Existing unit		1	Stainless steel
Condenser	PVC column, built in-house	C-01	1	PVC
Control valves	Stripper solvent inlet and gas outlet		2	
Gas analyzer	HORIBA CO_2 gas analyzer	GA-01, GA-02	2	
Flow elements	Mass flow controllers	FE-01, FE-02, FE-03, FE-04	4	
Pressure elements	Pressure transducers	PT-01, PT-02	2	
Differential pressure elements	Differential pressure transducer	PDT-01	1	
pH elements	Inline pH probes	AE-01, AE-02		
Temperature elements	Thermocouples	TE-01, TE-02, TE-03, TE-04	4	

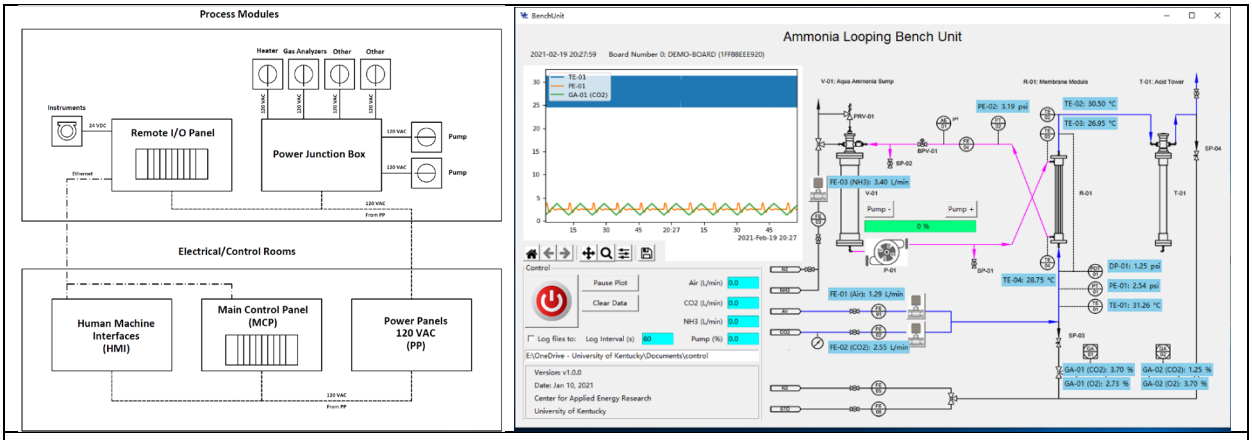

Exhibit 3.1.4. Control system electrical layout and system interface.

Membrane Absorber Performance Evaluation

Membrane CO_2 absorber was first evaluated on the lab-scale and bench-scale units using aqueous NH_3-based solvent and simulated flue gas to initially understand membrane properties, absorber

configuration, effect of chelating additives in solvents on the ammonia slip rate and demonstrated >500 hours of stable operation. The complete absorber loop process was then designed, fabricated, constructed by integration of membrane absorber and solvent regenerator in the UK IDEA 0.1 MWth large bench CCS for evaluation. Baseline tests were first conducted as batch running without solvent regenerator for reference comparisons and assessment of the individual components. A parametric campaign, over ~100 hours, was then conducted with ammonia absorber loop tied into the bench CCS process to evaluate the system operational limits and demonstrated controllable CO_2:NH_3 ratios with varying stripper temperature, pressure, and solvent carbon loading.

3.2 Membrane Development

Hollow fiber membranes with different bore size from Compact Membrane Systems (CMS) and Mann+Hummel were selected and purchased. Flat sheet membrane was purchased from Sterlitech and developed in UK IDEA labs. A customized flat-sheet membrane module was designed and constructed to achieve a low gas pressure drop in the bench scale unit. Process Flow Diagrams (PFDs), piping and instrumentation diagrams (P&IDs), equipment and instrumentation list, electrical layout, control and data acquisition system were completed for the bench unit and solvent regeneration integration unit. Membrane absorber tie-ins with the existing CCS were completed according to design specifications for supply of real fossil fuel derived flue gas.

3.2.1 Hollow Fiber Membrane from Compact Membrane Systems

Prior to purchasing a bench-scale membrane module, a lab-scale testing unit was built and used to collect and refine the membrane requirement specifications, shown in **Exhibit 3.2.1**. A mini module containing fluorinated polymer hollow fiber membranes from CMS was applied. A 2 M ammonium hydroxide solution without additives, as the worst-case scenario for ammonia slip, was circulated between the solvent vessel and shell side of the membrane. Simulated flue gas was used, controlled by mass flow controller and fed into the tube side of the membrane. When dry feed gas was used and fed directly to the membrane absorber, the membrane clogged within several hours, as expected, due to the reaction between CO_2 and NH_3 slip producing ammonium salt precipitate in the confined space inside hollow fiber with a bore size of ~200 μm. When feed gas was saturated with water at 55 °C before entering membrane module, >500 hours of operation were demonstrated without membrane clogging by flushing ammonium salts formed during operation. To decrease the amount of free ammonia in the solution, lower the NH_3 vapor pressure and reduce the slip, 50% of ammonium hydroxide was replaced by ammonium carbonate ($(NH_4)_2CO_3$), simulating the CO_2 capture in the membrane reactor. As shown in **Exhibit 3.2.2**, the NH_3 slip was reduced from 2653 ppm to 1282 ppm.

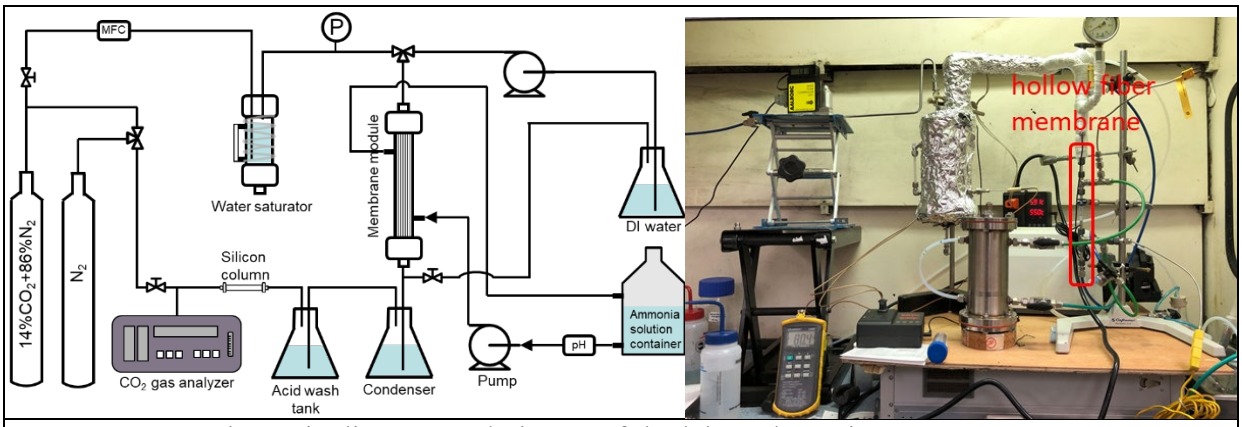

Exhibit 3.2.1. Schematic diagram and picture of the lab-scale testing system.

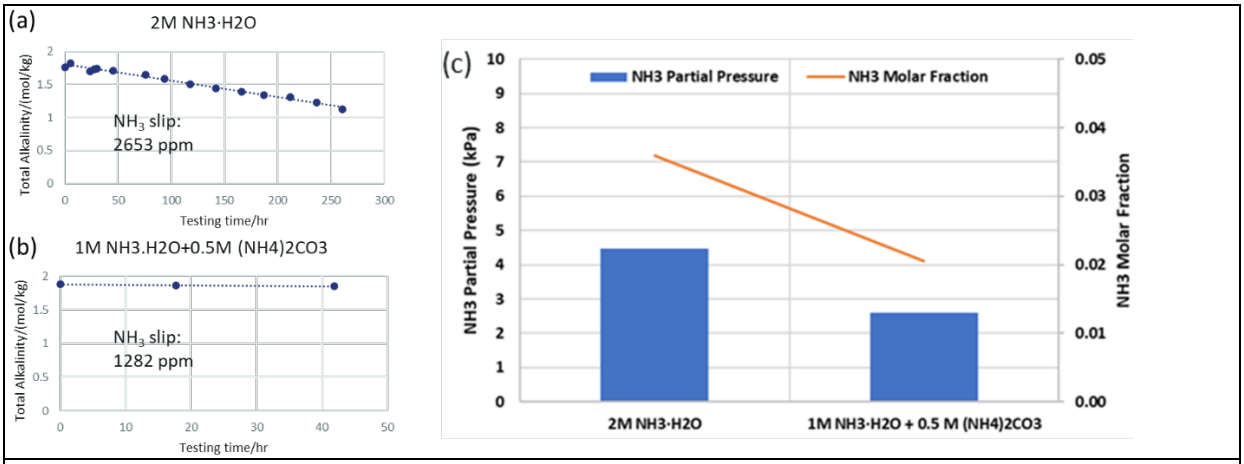

Exhibit 3.2.2. Total alkalinity of solvent vs. testing time for (a) 2 M ammonium hydroxide solution and (b) 1 M ammonium hydroxide+0.5 M ammonium carbonate solution; (c) Ammonia partial pressure and molar fraction in both solutions simulated by Aspen Plus.

The membrane modules that CMS can provide along with the parameters are shown in **Exhibit 3.2.3**. The 4-inch membrane module was selected and procured for installation in the bench-scale unit for initial testing.

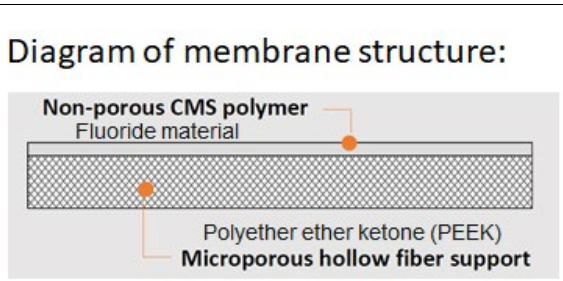

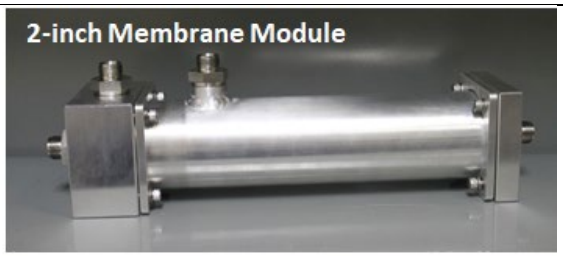

Membrane Module Type	Length (inch)	Surface Area (m^2)	N_2 flow rate at 20 psig (cfm)
¼-inch Mini Module	8	0.0014	0.013
2-inch Module	16	0.72	0.318
4-inch Module	20	1.3	1.907

Exhibit 3.2.3. Diagram and parameters of CMS membrane structure and membrane module.

3.2.2 Flat Sheet Membrane from Sterlitech

Sterlitech was chosen as an alternative polytetrafluoroethylene (PTFE) flat sheet membrane vendor to construct the bench scale membrane contactor to achieve a lower gas side pressure drop across membrane contactor. Lab-scale ammonia slip testing unit for flat sheet membrane is shown in **Exhibit 3.2.4**. The absorption solvent in liquid phase was 1 M NH_4OH + 0.5 M $(NH_4)_2CO_3$ with a flow rate of 80 mL/min. The gas phase was saturated flue gas containing 14% CO_2 with a flow rate of 115 mL/min. PTFE flat-sheet membranes with different pore size (0.1, 0.2 μm) from Sterlitech were evaluated for NH_3 slip rate with a result of 80 ppm (0.1 μm pore size) and 733.8 ppm (0.2 μm pore size). The membrane with 0.1 μm pore size was selected and procured for bench-scale testing.

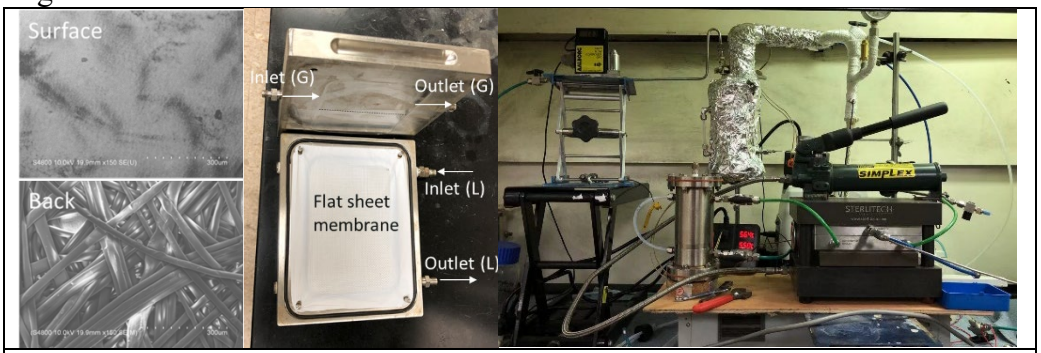

Exhibit 3.2.4. Morphology of Sterlitech PTFE membrane (left); Configuration of testing cell for flat-sheet membrane (middle); Lab-scale system for evaluation of NH_3 slip through flat sheet membranes (right).

A symmetric membrane CO_2 absorber was designed and constructed for the bench unit to produce a pressure drop lower than 0.1 psi with a feed gas flow rate of 5 cfm. The liquid phase is sent through the outside chambers at an inlet pressure ~7 psig. Separated by the flat membrane, the gas phase flows through the center chamber at atmospheric pressure. Given the pressure difference across the membrane, metal grills are included on the gas phase side to support the membrane. The membrane absorber is 6 inches wide and 24 inches deep, designed for 15 cfm feed gas and 2 second residence time. The outside liquid phase sections have a 1 x 6 inch flow area and the gas phase section has a 3 x 6 inch flow area. Machined chlorinated polyvinylchloride (CPVC) material was used as the housing.

3.2.3 Hollow Fiber Membrane from Mann+Hummel

Due to the limited membrane area per volume for the customized flat sheet membrane module a hollow fiber membrane (Microdyn-MD-063-CU-2N) with a 9 times larger bore size (bore size = 1.8 mm) compared to the previous CMS hollow fiber membrane (bore size = 0.2 mm) was acquired from Mann+Hummel and evaluated in the bench scale unit, as shown in **Exhibit 3.2.6**. This feature enables testing of the hollow fiber membrane at a feed flow rate similar to the flat sheet membrane, but with a higher surface area per volume. Two CO_2 concentrations (5 and 14%) and three different feed flow rates (1.15, 2.41, and 3.67 cfm) were used to investigate the CO_2 capture efficiency. The change of capture efficiency is linear with the change of feed flow rate, which indicates that the residence time in the membrane module (e.g. reaction kinetics) is the limiting factor for the CO_2 capture efficiency (**Exhibit 3.2.7**). NH_3 slip results are shown in **Exhibit 3.2.8**. The pore size of this membrane is 0.2 μm, which is higher than the Sterlitech flat sheet membrane and CMS hollow fiber membranes with 0.1 μm pore sizes. The larger pore size leads to high ammonia slip. However, after adding a certain amount of ammonium carbonate in the solvent to raise the carbon loading, the NH_3 slip dropped to around 1000 ppm. An alternative hollow fiber membrane module (MICRODYN-MD-150-CU-2M) with 6.3 m^2 membrane area and 46 cm^2 cross-section flow area was ordered to provide lower pressure drop and longer residence time. This was also used in the integrated system with algae.

Exhibit 3.2.6. Comparison of membrane module parameters

Model No.	MD-063-CP-2N	MD-150-CU-2M

Membrane inner diameter	1.8 mm	1.8 mm
Membrane nominal pore size	0.2 µm	0.2 µm
Membrane area	0.75 m^2	6.3 m^2
Free flow area	5 cm^2	46 cm^2
Residence time at 5 cfm feed flow rate	0.16 s	1.46 s
Evaluation Conditions		
Inlet CO_2 concentration	5%, 14%	N/A
Gas feed flow rate	1.15 CFM, 2.41 CFM, 3.67 CFM	
Liquid inlet pressure	1 psig	
Gas inlet pressure	~ 0.5 psig	

Exhibit 3.2.7. NH_3 slip and carbon loading along with testing time for batch operation of bench-scale unit with customized flat sheet membrane module.

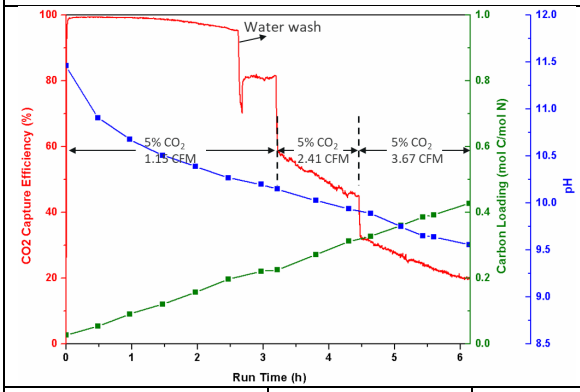

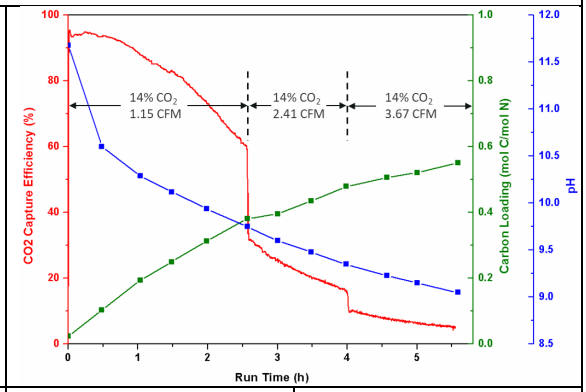

	CO_2 Capture Efficiency Before (%)	**CO_2 Capture Efficiency After (%)**	**CO_2 Capture Efficiency Before (%)**	**CO_2 Capture Efficiency After (%)**
Feed flow change from 1.15 CFM to 2.41 CFM	82	58	60	32
Feed flow change from 2.41 CFM to 3.67 CFM	45	33	17	10

Exhibit 3.2.8. Ammonia slip summary for the bench-scale unit tests with MICRODYN hollow fiber membrane module.

Solvent	**Carbon Loading (mol C/mol N, beginning)**	**Carbon Loading (mol C/mol N, ending)**	**NH_3 Slip (ppm)**
2M NH_4OH	0.393	0.428	6792
	0.506	0.552	4449
0.5M NH_4OH+0.75M $(NH_4)_2CO_3$	0.640	0.669	1218

3.4 Lab-scale Membrane Absorber Performance Evaluation

A lab-scale test unit was built to collect preliminary ammonia slip data and demonstrate >500 hours of stable operation with water saturated feed gas. Test and sampling plans and SOPs for ammonia slip measurements and integrated system operation were established. Ammonia slip was evaluated using the CMS ¼-inch hollow fiber membrane module in lab scale unit with the following conditions. Gas phase: 14% CO_2; Liquid phase: 1 M NH_4OH + 0.5 M $(NH_4)_2CO_3$ solution; Gas flow rate: 100 mL/min; Liquid flow rate: 80 mL/min. Three batches of solution were tested to verify the repeatability of testing methods. As shown in **Exhibit 3.4.1**, the pressure drop was maintained between 3 and 3.5 psi, the volume in the acid trap at the gas phase outlet of membrane increased from 100 to 125 mL after 100 hr testing, as gas condensate accumulated. The water condensate flowing downward on the tube side of membrane washes out the precipitation, as expected when saturated flue gas was applied. An average of 5850 ppm NH_3 slip was estimated as shown in **Exhibit 3.4.2.**

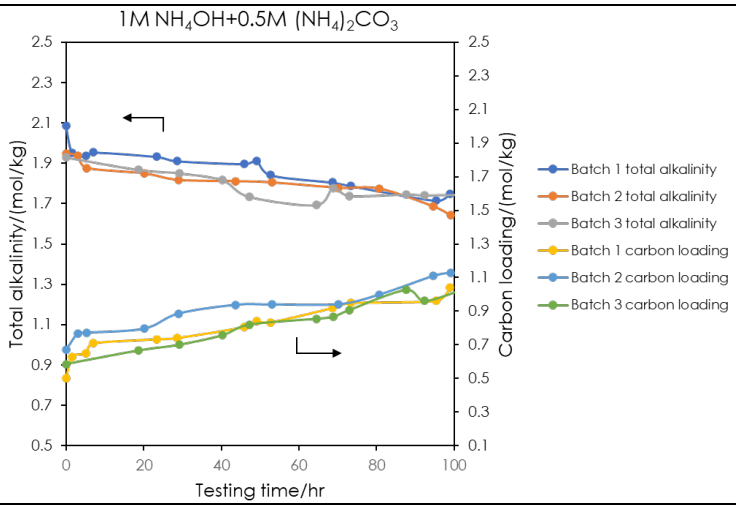

Exhibit 3.4.1. Total alkalinity and carbon loading along with testing time for batches 1-3.

Exhibit 3.4.2. Ammonia slip summary for batches 1-3.

Batch	Solvent	Testing time (hr)	Ammonia slip (ppm)
1	1 M NH_4OH + 0.5 M $(NH_4)_2CO_3$	100	6345
2	1 M NH_4OH + 0.5 M $(NH_4)_2CO_3$	100	5409
3	1 M NH_4OH + 0.5 M $(NH_4)_2CO_3$	100	5795

To minimize ammonia slip, 1 wt% and 20 wt% tetraethylene glycol dimethyl ether (TGDE) (batches 4 and 5, respectively) and 10 wt% 2-amino-2-methyl-1-propanol (AMP) (batch 6) were introduced into the ammonium solvents as chelating additives. As shown in **Exhibit 3.4.3**, each batch of solvent was tested for 50 hr with stable pressure drop around 4 psi. The ammonia slip was reduced by ~20%, with an average of 4826 ppm NH_3 slip achieved when 10 wt% AMP was added, as shown in **Exhibit 3.4.4.**

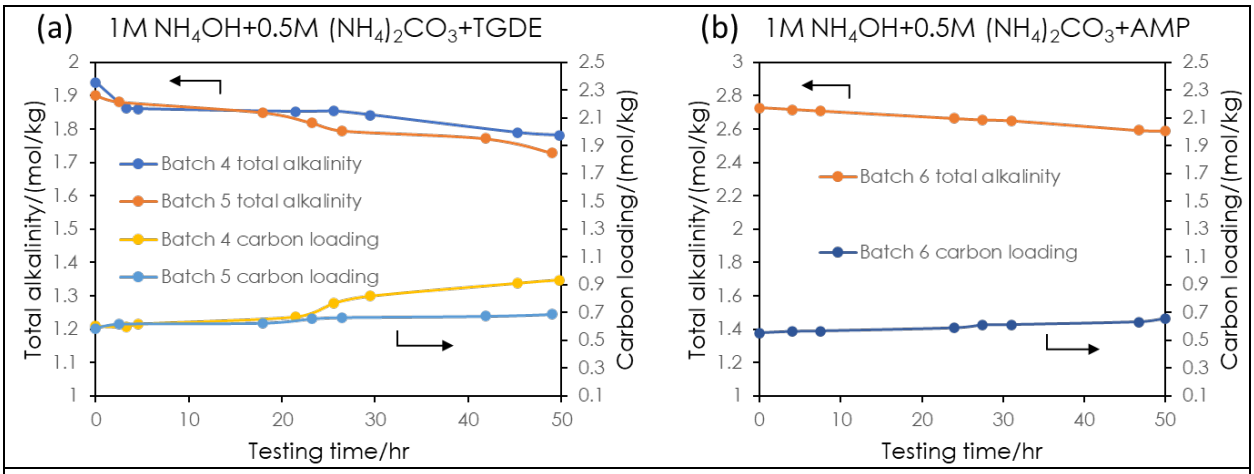

Exhibit 3.4.3. Total alkalinity and carbon loading along with testing time for batches 4-6.

Exhibit 3.4.4. Ammonia slip summary for batches 4-6.

Batch	Solvent	Testing Time (hr)	Ammonia Slip (ppm)
4	1 M NH_4OH + 0.5 M $(NH_4)_2CO_3$ + 1 wt% TGDE	50	5953
5	1 M NH_4OH + 0.5M $(NH_4)_2CO_3$ + 20 wt% TGDE	50	5049
6	1 M NH_4OH + 0.5M $(NH_4)_2CO_3$ + 10 wt% AMP	50	4826

3.5 Parametric Testing Results

Batch operation was conducted with both the hollow fiber and flat sheet membrane modules and the inhibition effect of chelating additives on ammonia slip was validated. The flat sheet membrane exhibited lower ammonia slip rate compared to hollow fiber membrane demonstrated by a similar ammonia slip observed with both membrane modules at significantly lower carbon loading and therefore higher free ammonia content for the flat sheet membrane module.

The bench scale membrane absorber unit for batch running without solvent regeneration was completed, as shown in **Exhibit 3.5.1**. Operations were conducted to evaluate ammonia slip through the CMS 4-inch hollow fiber membrane module (membrane area ~ 1.3 m^2). An aqueous ammonium solution with a total inventory of about 6 gals was used for batch running. The liquid flow rate was 0.6 GPM and the gas flow rate was 6.1 L/min (14 vol% CO_2 balanced with N_2). The feed gas was saturated with water vapor in the saturator at the temperature of 55 °C. Gas samples for ammonia slip analysis were collected after a stable inlet CO_2 concentration was measured.

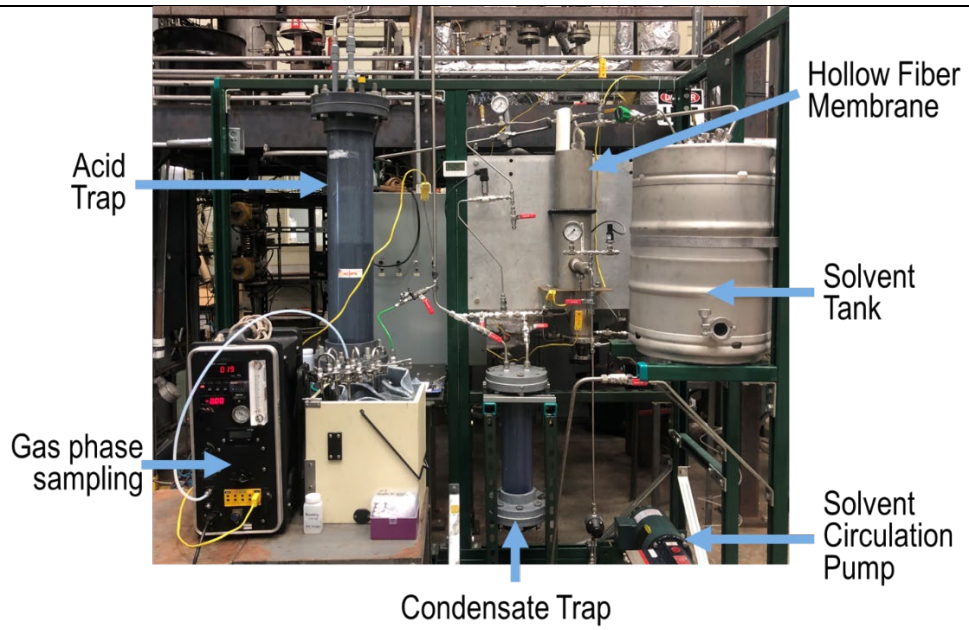

Exhibit 3.5.1. Completed bench-scale membrane absorber unit used for batch testing.

Different concentrations of glycerol, AMP and tris(hydroxymethyl)aminomethane (THAM or Tris), were added as chelating additives to reduce the ammonia slip. The CO_2 capture efficiency and pressure drop during the tests are given in **Exhibit 3.5.2**. With the addition of THAM, the initial capture efficiencies tend to be lower because the additive bonds with ammonia and reduces the free ammonia concentration in the solution. When the CO_2 loading of the solution is higher, the ammonia bonded with the additives may also contribute to the CO_2 capture resulting in a higher capture efficiency. The pressure drops for all the experiments are higher at the beginning and tend to decrease with run time. This is caused by initial ammonium salt formation on the tube side of the hollow fiber membranes due to high concentration of free ammonia, which increases the resistance of the gas flow. The pressure drop decreases along with run time as the salts are washed out by the water condensate, validating the downward flow membrane design concept of this technology. As shown in **Exhibit 3.5.3**, alkalinity decreased from 4.00 mol/kg to 0.62 mol/kg with run time. The alkalinity is higher initially as more salts are dissolved and lower later as less salts are dissolved. The pressure drop change with run time was further investigated by analyzing the collected flue gas condensate. Pressure drop started at ~20 kPa with relatively higher alkalinity and carbon loading found in the condensate solution. The pressure drop gradually fell to ~15 kPa with decreasing alkalinity and carbon loading found in the condensate solution as ammonium salts were washed out by water as it condensed on the membrane from the saturated flue gas. **Exhibit 3.5.2 a** shows the typical change of CO_2 capture efficiency and carbon loading. At the beginning stage, the capture efficiency is high and stable until all the free ammonia is converted to ammonium carbamate. Then the capture efficiency decreases and carbon loading increases as ammonium carbamate is converted to ammonium carbonate.

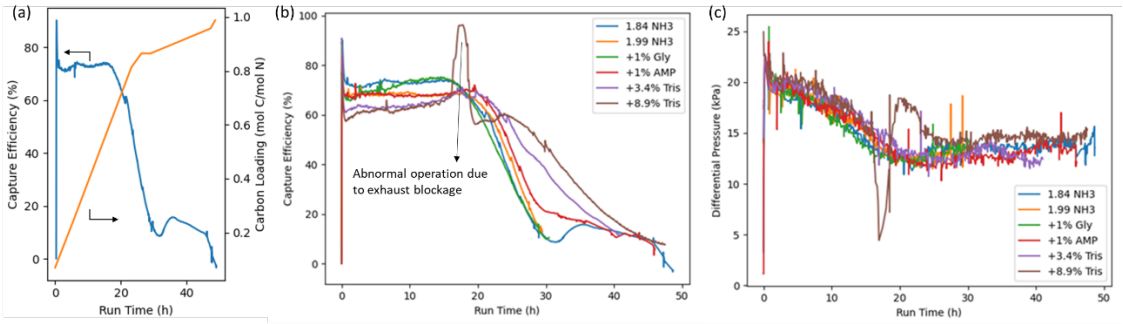

Exhibit 3.5.2. CO_2 capture efficiency, carbon loading, and pressure drop for the bench-scale unit tests with hollow fiber membrane module. In these figures Tris is THAM.

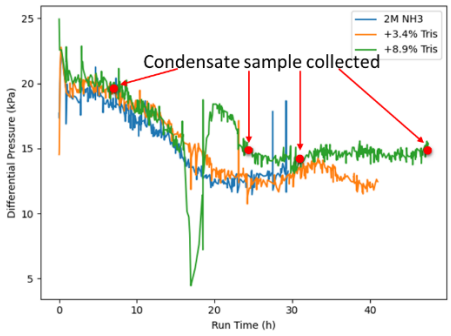

Time (h)	6.5	23	30.5	47.5
Mass (g)	391	851	410	895
Rate (g/h)	60	52	55	53
Alkalinity (mol/kg)	4.00	3.16	1.08	0.62
Carbon Loading (mol/kg)	2.42	1.90	0.84	0.64

Solvent: 2M NH_4OH+8.9 wt% tris(hydroxymethyl)aminomethane

Exhibit 3.5.3. Differential pressure between inlet and outlet of membrane module on gas side along with testing time (left) and analysis results of condensate solution samples (right).

Gas phase sampling, following EPA method CTM-027, was conducted to collect the gas at the membrane module outlet. The sampling system is composed of one empty impinger followed by three impingers containing ~150 g 0.1 N standard H_2SO_4 acid and one impinger containing ~170 g silica gel. When collecting gas samples, any NH_3 present reacts with the H_2SO_4 to form $(NH_4)_2SO_4$, and the concentration is measured by ionic chromatography (IC). If NH_4 is detected in the last H_2SO_4 impinger then results may be unreliable as some NH_3 may have broken through all impingers. For quality assurance/quality control (QA/QC), the IC results from the last acid containing impingers were found to be below the limit of detection, indicating that breakthrough did not occur. The gas samples for ammonia slip measurement are collected when the capture efficiency starts to decrease, as shown in **Exhibit 3.5.4**. At the beginning stage of each run, the NH_3 slip was 7000-10000 ppm due to the high concentration of free ammonia in the fresh solvent with a partial pressure of ~4 kPa (**Exhibit 3.5.2 c**), which contributes to 40000 ppm free ammonia. When the free ammonia is consumed and converted to ammonium carbonate, the NH_3 slip was observed to be fairly consistent at around 900 ppm until ammonium bicarbonate was formed. When the solvent was almost saturated with CO_2, the NH_3 slip dropped to ~300 ppm. The IC analysis results show that the lower the solvent carbon loading is, the higher the NH_3 slip will be. More details are provided in the highlighted rows of **Exhibit 3.5.4** to show that trend with the addition of chelating additives. The same NH_3 slip can be achieved at lower carbon loading, which means the additive inhibits the effect of free ammonia in the solvent. For example, 1000 ppm NH_3 slip can be achieved at 0.6 C/N with addition of 8.9 wt% THAM instead of 0.8 C/N in 2M NH_4OH.

This was used for guidance in selecting appropriate chelating additive concentration for future experiments.

Exhibit 3.5.4. Ammonia slip summary for the bench-scale unit tests with hollow fiber membrane module.

Solvent	Outlet CO_2 (%, begin)	Outlet CO_2 (%, end)	Carbon loading (mol C/mol N, begin)	Carbon loading (mol C/mol N, end)	NH_3 slip (ppm)
2M NH_4OH	4.22	4.31	0.095	0.231	10422
	7.66	10.48	0.813	0.855	932
	11.59	12.24	0.865	0.875	878
	13.06	14.10	0.958	0.988	273
2M NH_4OH	4.82	4.88	0.083	0.134	8771
	6.77	8.39	0.735	0.798	1001
	10.54	11.98	0.820	0.845	961
2M NH_4OH+1 wt% glycerol	5.00	4.88	0.082	0.126	7341
	4.60	4.69	0.197	0.219	9926
	9.31	10.81	0.757	0.777	807
	11.67	12.23	0.764	0.780	817
2M NH_4OH+1 wt% AMP	4.85	4.89	0.071	0.104	8399
	4.54	5.29	0.605	0.670	2471
	7.01	8.89	0.729	0.800	1985
	12.28	12.81	0.920	0.934	788
2M NH_4OH+3.4 wt% THAM	4.55	4.96	0.470	0.524	2376
	5.80	6.40	0.590	0.635	2517
2M NH_4OH+8.9 wt% THAM	6.94	7.76	0.596	0.606	1050

Solvent	Total alkalinity (mol/kg)	Carbon loading (mol/kg)	Carbon loading (mol C / mol N)	Outlet CO_2 (%)	NH_3 slip (ppm)
2M NH_4OH	1.718-1.706	1.26-1.36	0.733-0.797	6.77-8.39	1001
2M NH_4OH+3.4 wt% THAM	1.882-1.875	1.11-1.19	0.590-0.634	5.80-6.40	2517

2M NH_4OH+8.9 wt% THAM	2.295-2.281	1.36-1.39	0.592-0.609	6.94-7.76	1050

In addition to the CMS polymeric membrane module, the UKy customized flat sheet membrane module was tested, as shown in **Exhibit 3.2.5**, aiming to lower the pressure drop on gas side. The membrane module was installed in the bench scale unit, as shown in **Exhibit 3.5.5**. An existing steam generator was integrated with the simulated flue gas to generate a water-saturated feed stream. Membrane testing was conducted at 8.2 m^3/hr feed flow rate with 5% CO_2. A gas side pressure drop of 0.7 kPa was observed. The steam flow rate was kept at ~2.15 lb/hr to achieve a stable temperature and water concentration in the feed stream. A higher gas flow rate applied with (8.2 m^3/hr) and lower membrane area (0.2 m^2) of the flat sheet membrane module compared to the hollow fiber membrane module (0.36 m^3/hr and 1.3 m^2) resulted in a lower CO_2 capture efficiency obtained with the flat sheet membrane module, as shown in **Exhibit 3.5.6**. The ammonia slip tested at C/N of 0.24-0.30, shown in **Exhibit 3.5.7**, is comparable to the results tested on hollow fiber membrane at C/N of 0.59-0.80, as shown in **Exhibit 3.5.4**, which implies the flat sheet membrane can exhibit the similar ammonia slip inhibition at higher concentration of free ammonia.

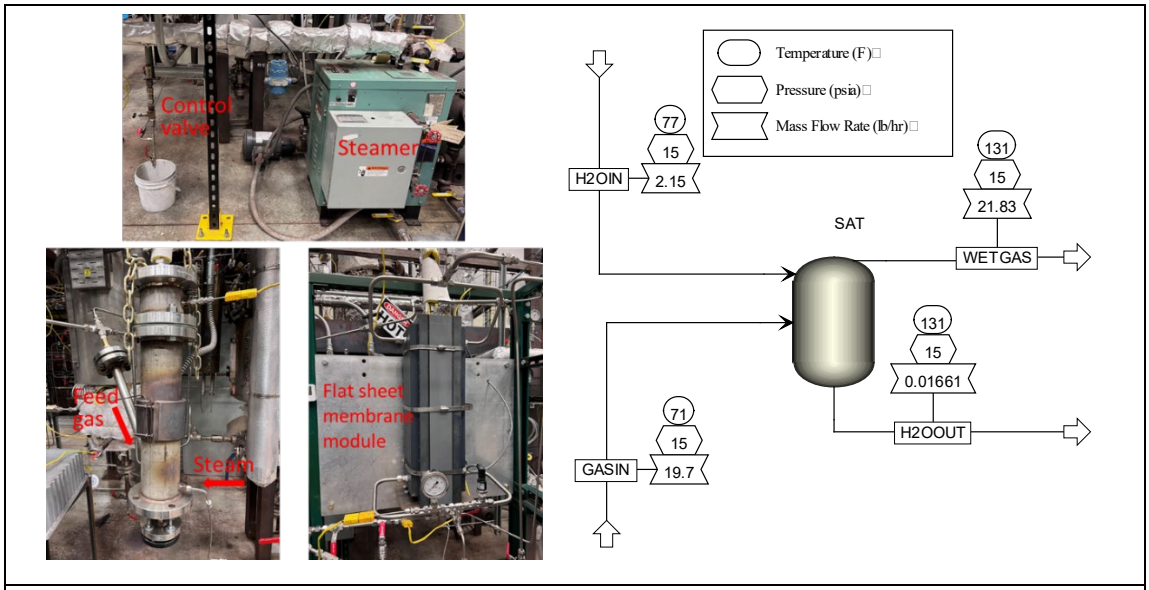

Exhibit 3.5.5. Integration of the steam generator with the bench unit operated with the customized flat sheet membrane module (left) and simulation of operating conditions for steam generator to produce a water-saturated feed gas (right).

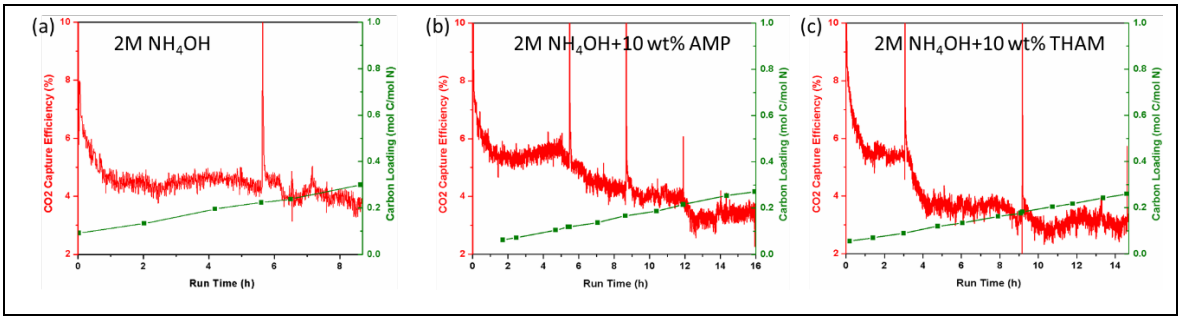

Exhibit 3.5.6. CO_2 capture efficiency and carbon loading along with testing time for the bench-scale unit tests on customized flat sheet membrane module, solvent content: (a) 2 M NH_4OH; (b) 2 M NH_4OH+10 wt% AMP; (c) 2 M NH_4OH+10 wt% THAM.

Exhibit 3.5.7. Ammonia slip summary for the bench-scale unit tests with customized flat sheet membrane module.

Solvent	Total alkalinity (mol/kg)	Carbon loading (mol/kg)	Carbon loading (mol C / mol N)	Outlet CO_2 (%)	NH_3 slip (ppm)
2 M NH_4OH	1.273-1.115	0.30-0.35	0.238-0.299	4.79-4.81	1925
2 M NH_4OH+10 wt% AMP	1.892-1.832	0.48-0.50	0.254-0.270	4.77-4.79	1559
2 M NH_4OH+10 wt% THAM	1.598-1.568	0.39-0.41	0.242-0.260	4.79-4.83	1364

Batch running was conducted to establish a baseline of carbon loading and NH_3 slip, as shown in **Exhibit 3.5.8**. After 30-hour operation, the solvent carbon loading increased from 0.55 to 0.70 mol C/mol N and the NH_3 slip dropped from 600 to 400 ppm. NH_3 slip through the hollow fiber membrane, evaluated at the same range of carbon loading (0.55-0.70 mol C/mol N), shown in **Exhibit 3.5.4**, was >1000 ppm. The flat sheet membrane shows better inhibition of NH_3 slip, while resulting in a much lower operational pressure drop (~0.1 psi).

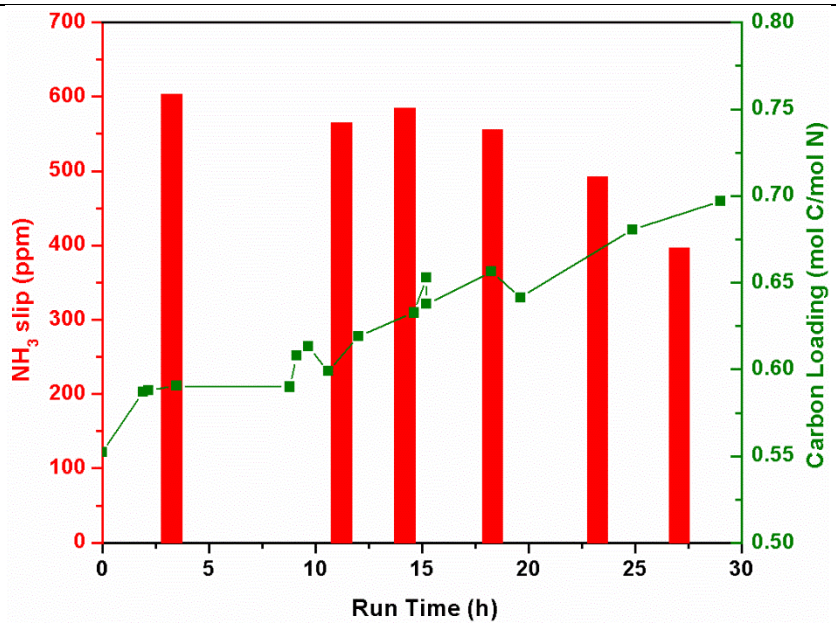

Exhibit 3.5.8. NH_3 slip and carbon loading along with testing time for batch running on bench-scale unit with customized flat sheet membrane module.

3.6 Parametric Campaign

Parametric campaign was conducted to evaluate the system operational limits and establish the typical membrane absorber performance. Controllable CO_2:NH_3 ratios in product stream can be achieved by using different stripper temperature, pressure, and solvent carbon loading. Parametric campaign test was conducted in complete integrated system with Microdyn-MD-063-CU-2N hollow fiber membrane absorber and solvent regeneration with two different L/G ratio. L/G=13.7 was the same as batch running, gas feed flow rate: 3.3 cfm, liquid feed flow rate: 206 lb/hr. L/G=5.4 was determined by Aspen simulation, gas feed flow rate: 5.0 cfm, liquid feed flow rate: 121 lb/hr. Different stripper temperature, pressure, solvent carbon loading were adjusted to control CO_2:NH_3 ratio in the gas product stream. Stripper bottom temperature was adjusted within 90-120 °C. The CO_2 capture efficiency was around 15% to 25% due to short residence time, which is 0.24 s and 0.16 s for 3.3 cfm and 5.0 cfm feed gas flow rate. With the increase of stripper temperature and decrease of carbon loading, the CO_2:NH_3 ratio decreased. According to the CO_2:NH_3 ratio study for algae, the ideal ratio is between 10-18 and the data indicates that CO_2:NH_3 = 18 shows slightly higher growth rate than ratios 10 and 12. In the parametric campaign, the CO_2:NH_3 ratio did not reach lower than 18 due to the limit of CO_2 capture efficiency by the membrane module, which cannot provide long enough residence time to absorb CO_2 and maintain the solvent carbon loading, so it gets more and more lean. As can be seen in **Exhibit 3.6.1**, the carbon loading was already lower than 0.2 when stripper bottom temperature was 123 °C.

Exhibit 3.6.1. Parametric campaign results of ammonium looping tests.

Stripper pressure (psia)	Stripper bottom temperature (°C)	Stripper top temperature (°C)	Lean carbon loading (mol C/mol N)	Rich carbon loading (mol C/mol N)	CO_2/NH_3 (mol/mol)
26.66	104.40	68.84	0.28	0.33	18.47
15.59	93.78	68.09	0.34	0.39	58.32
14.81	88.93	60.90	0.32	0.36	64.22
34.21	122.71	115.96	0.11	0.18	44.92
32.43	104.53	64.09	0.39	0.44	72.03
32.11	104.91	66.86	0.39	0.44	80.92
32.91	104.82	63.05	0.41	0.42	140.40

3.7 Algae Study

3.7.1 Introduction

Published studies have shown that CO_2 can account for 20-25% of operating costs in algae production, a finding that highlights the importance of understanding and integrating the costs associated with CO_2 delivery and utilization [9-16]. Typical sources of CO_2 considered for algal cultivation are waste streams from power or chemical manufacturing plants. These sources of CO_2 range in concentration from low, approximately 3-5 vol% and 10-15 vol% from natural gas and coal-fired power plants, respectively, to high, at 99 vol% from ethanol plants or other chemical plants, such as ammonia or hydrogen plants. According to Somers and Quinn [17], direct utilization of a pure CO_2 source is optimal with utilization efficiencies of 20-30% required, whereas the integration of algal growth facilities with lower purity CO_2 streams requires much higher utilization efficiencies for economic viability.

In terms of the state-of-the-art, there are essentially two options for introducing CO_2 into algae cultures: 1) compression and subsequent bubbling of the CO_2-containing gas directly into the algae growth system; and 2) production of a concentrated aqueous stream saturated or supersaturated with dissolved carbon that is supplied to the cultivation system.
Bubbling compressed CO_2 is a tried and tested method for the carbon supplementation of algae cultures that has been proven effective with both photobioreactors and raceway ponds. However, sparging in traditional raceways has a low mass transfer efficiency [18-21]. This results in limited CO_2 absorption and outgassing. To overcome these limitations, a wide variety of materials have been used to introduce CO_2 into algae cultures, including hollow fiber modules, laser-cut silicon tubing and porous ceramic disks [18-21]. In general, these materials have advantages and disadvantages in terms of capital (material cost) and operating (pressure drop) expenses. For example, a material that produces smaller bubbles – which would increase mass transfer efficiency – may prove undesirable from an economic and life cycle assessment standpoint due to the energy penalty associated with overcoming the associated pressure drop.

The alternative method mentioned above, in which an aqueous stream typically containing Na_2CO_3 (pH > 7) is pre-saturated with CO_2 [22,23], shows potential for lowering operating costs and increasing the viable distance between an algae farm and the CO_2 emission source. Once the resulting aqueous HCO_3^- has been consumed by the algae (regenerating the Na_2CO_3), the liquid can be recycled for loading with more CO_2. An additional benefit of this approach is that after CO_2 scrubbing, the exhaust gas can be returned to the main emissions stack, avoiding potential issues with air permitting. However, this method could run into issues with equipment fouling by algae in the return loop/CO_2 scrubbing section unless appropriate precautions are taken.
A modification of this approach, similarly designed to integrate CO_2 capture with its utilization in algae culturing, utilizes aqueous ammonia as the CO_2 scrubbing medium [24,25] without the algae culture directly contacting the flue gas loop. According to this concept, flue gas that has been treated to remove SOx, NOx and particulate matter using conventional scrubbers is contacted with aqueous ammonia in a CO_2 absorber (membrane or conventional packed column), forming ammonium (bi)carbonate. The resulting solution is then pumped to distributed solar-energy powered strippers located close to algae cultivation modules (open ponds or photobioreactors) for solvent regeneration and just-in-time gaseous CO_2 and NH_3 delivery at an optimal molar ratio for algae cultivation. The regenerated solvent is then returned to the CO_2 capture unit for re-use. In the case of a membrane absorber, any NH_3 that crosses the membrane to the flue gas side is converted to ammonium salts (e.g., ammonium (bi)carbonate or ammonium sulfite) that are recovered with condensate from the unit; these salts can also be fed to the algae culture.

The use of aqueous ammonia is particularly attractive for CO_2 scrubbing for several reasons, including its low cost and low viscosity. The scrubbing capacity of NH_3 is approximately 0.9-1.2 kg of CO_2/kg of NH_3, while the solvent regeneration energy is about half that required for 30 wt% monoethanolamine (MEA) [26,27]. Moreover, it has long been recognized that algae are able to utilize NH_4^+ as a source of nitrogen, an essential nutrient required for amino acid/protein synthesis [28-30]. Hence, a gaseous CO_2/NH_3 mixture can in principle function as the required C- and N-source for algae cultivation. Algae biomass typically contains 45-50% C, 7-8% N, and 1.4% P, albeit the elemental composition can vary significantly according to the species of algae and growth conditions. The foregoing composition is consistent with the Redfield molar elemental ratio (106:16:1 C:N:P) on a mass basis (40:7:1 C:N:P) [31]. From this it follows that the required

stoichiometric C:N ratio for algae cultivation is ~6.63, although attainment of this value in the algae culture may require a higher C:N ratio in the gas feed due to the lower solubility of CO_2 compared to NH_3, i.e., the CO_2 partial pressure may have to be increased relative to the NH_3 component.

Unlike the consumption of nitrate ions which results in an increase in pH, during the growth of algae using ammonium ions, the pH decreases due to the release of H^+ ions into the medium [32]. However, excessive supply of NH_3 will result in an increase in pH, while excessive supply of CO_2 will result in acidification of the medium. Hence, there is a need to ensure that the supply of CO_2 and NH_3 is balanced, i.e., an optimal CO_2/NH_3 ratio is employed. Moreover, the feed rate must be balanced with algae growth, such that excessive concentrations of NH_3/NH_4^+ do not accumulate, which might prove toxic. In addition, practical considerations dictate that the choice of microalga will be important, given that it must be able to flourish under basic conditions and should be able to withstand fluctuations in pH in the case of operational upsets. In this respect, *Scenedesmus acutus* (UTEX B72) represents an ideal choice, given that in previous work we have observed that it flourishes at basic pH values, while also showing good growth under acidic conditions (pH 5.5-7) [33].

To date there appears to have been only one report of algae cultivation using both gaseous CO_2 and NH_3. In order to evaluate the possible use of algae for mitigating emissions from animal production operations, Kang and Wen [34] studied the growth of *Scenedesmus dimorphus* in a flat panel photobioreactor aerated with ammonia- and CO_2-laden air. It was found that at the NH_3 feed rate utilized (0.041-0.042 g/L/day) – and within the range of the CO_2 feed rates investigated (0.64 to 5.49 g/L/day) – the majority of the ammonia (80-90%) was removed by algal cell assimilation, with a small portion (10-12%) being removed via liquid dissolution. It should also be noted that culturing algae in the presence of a low concentration of free NH_3 may prove beneficial given that pests such as rotifers are inherently more sensitive to the toxic effects of NH_3 than are algae. For example, while *Scenedesmus obliquus* has been reported to tolerate free NH_3 at concentrations up to 2 mM [35,36], *Brachionus* rotifer reproduction is inhibited at NH_3 concentrations of 0.14 mM [37] and complete mortality is observed at concentrations above 0.29 mM [38]. Indeed, exposure of algae cultures to NH_3 has recently been demonstrated as a practical method of suppressing rotifers to ensure culture health [39]. Care must be taken, however, to avoid exposure of algae cultures to excessive concentrations of NH_3. In principle, ammonia toxicity in water can be due to the effects of both free NH_3 and its ionized form, i.e., NH_4^+. However, ammonia is considered to be by far the most toxic form because it is uncharged and lipid soluble and easily diffuses across membranes [32].

Against this background, Task 5.1 took as its starting point the hypothesis that gaseous CO_2/NH_3 can be used as a C- and N-source for algae cultivation, thereby facilitating a new, integrated approach to flue gas CO_2 capture and utilization. Specific points of interest were the identification of the optimal CO_2/NH_3 ratio for algae productivity – within the range of CO_2/NH_3 ratios readily obtainable from the CO_2 capture portion of the process – and the efficiency with which CO_2 and NH_3 can be utilized by algae cultures. Low CO_2 uptake efficiencies would render the integrated process unviable from an economic standpoint, while low NH_3 uptake would be environmentally unacceptable if it resulted in NH_3 emissions to the atmosphere. Consequently, experiments were performed with the objective of (i) confirming that good algae productivity can be obtained using

NH_3 as a nutrient, (ii) determining the optimal CO_2/NH_3 ratio for algae productivity, and (iii) determining the optimal CO_2/NH_3 ratio with respect to maximizing the efficiency with which CO_2 and NH_3 are utilized by the culture.

3.7.2. Experimental

Algae Culturing

For the culturing experiments, 800 mL tubular photobioreactors were employed, which were seeded with *Scenedesmus acutus* (UTEX B72) from one 10 L photobioreactor. BG-11 was used as the culture medium, the $NaNO_3$ component being omitted. The photobioreactors were bubbled with a gas blend sourced from house N_2, 0.25% CO_2/N_2 and 0.1 % NH_3/N_2 at ambient temperature; the measured culture temperature was 23.3 ± 0.6 °C. The total gas flow rate used was set at a value of 0.1 L/min per reactor, which was sufficient to ensure good mixing in the reactors. Using this flow rate, flows of N_2, 0.25% CO_2/N_2 and 0.1 % NH_3/N_2 were initially adjusted using mass flow controllers (Brooks; Hatfield, PA, USA) to provide sufficient C and N to support an algae growth rate of 0.2 g/L/day, corresponding to 0.74 mmol NH_3 and 5.2 mmol CO_2 per reactor per day (CO_2/NH_3 mole ratio of 7). In subsequent experiments, the CO_2 flow rate was increased (at the expense of the N_2 balance), while maintaining the same NH_3 and total gas flow rates. In this manner, a series of experiments were performed in which the CO_2/NH_3 mole ratio was varied between 7 and 18. For experiments in which the CO_2/NH_3 flow rate was increased at a fixed CO_2/NH_3 mole ratio of 10, the flows of CO_2 and NH_3 were both increased by 50% and by 100% over the standard values of 7.4 mmol CO_2 and 0.74 mmol NH_3 per reactor per day, while adjusting the flow of N_2 balance gas to maintain the same total gas flow rate.

The light source consisted of T5 35-watt cool white fluorescent bulbs (90 μmol/m^2/s), cycling 24 hours a day. Experiments were performed for multiple growth/harvest cycles, ~80% of the algae being removed at each harvest. Harvesting was performed when the algae concentration reached a minimum value of 1 g/L, the concentration after harvesting being ~0.2 g/L. In this manner, the cultures remained in the log phase of growth. After each harvest, the nutrients and water were replenished, the water being filtered through a 1 μm filter using a 10" whirlpool canister and then sterilized using a UV system. The nutrient solution was similarly sterilized. Cultures were sampled three times a week and analyzed for pH and for culture density by means of UV-vis spectrophotometry (absorption at 680 nm) and dry mass measurements [40]. In addition, the gas flow exiting the photobioreactors was sampled once a day and analyzed for residual CO_2 using a refinery gas analyzer (Inficon 3000 micro-GC) equipped with 5Å molecular sieve, PoraPLOT U, alumina and OV-1 columns. In selected cases the exit gas was also analyzed for the presence of NH_3 using Kitagawa tubes (minimum detection level of 0.2 ppm); in all cases, NH_3 was not detected.

Productivity (P, g/L/d) was obtained using the equation $P = (X_t - X_0)(t - t_0)^{-1}$ where X_t is the biomass concentration (g/L) at t (d) and X_0 is the biomass concentration at inoculation (t_0) [41].

Determination of NH_3 and NH_4^+ in algae cultures

Detection and quantitation of ammonium ions was performed with a Dionex ICS-3000 Ion Chromatography system (Dionex-ThermoScientific, Sunnyvale, CA). The cation system consisted of a CERS 500 suppressor, EGC III MSA (methansulfonic acid) eluent generator, IonPac CS17 analytical column and an CG17 guard column operated at 30 °C. The ammonium ions were eluted

using an isocratic gradient of MSA at 10 mM concentration for 12 minutes. The conductivity detector was maintained at 30 °C and an injection volume of 20 µL was used.

A certified ammonium standard was obtained from Environmental Express (Charleston, SC) for preparation of the calibration standards by diluting the standard solution with 18.2 MΩ water. A check standard solution of ammonium ions was obtained from VHG (Manchester, NH). The samples were prepared with 18.2 MΩ water to a 50 times dilution factor. Each sample was analyzed in triplicate. Peak identification and integration were performed manually using Dionex Chromeleon chromatography management system software version 6.80.

From the measured concentration of NH_4^+ ions, the concentration of free ammonia in solution was calculated according to eqns. 1 and 2 [42]:

$$X_{NH3} = \frac{1}{10^{(pKa-pH)}+1} \quad (1)$$

$$pK_a = 0.0902 + \frac{2729.92}{T_k} \quad (2)$$

X_{NH3} is the mole fraction of free ammonia in solution (i.e., the fraction that is not protonated), T_k is the temperature in Kelvin, and pH refers to the measured pH of the sample.

Analysis of algae biomass

Biomass was analyzed at the University of Kentucky (UK) for elemental analysis (CHN, ASTM D5373) and moisture and ash content (ASTM D7582). Analyses were performed in triplicate. The protein content of the biomass was calculated by multiplying the nitrogen content by a conversion factor of 4.78 as described in the literature [43]. Based on the C and N content of the biomass and the algae productivity, the CO_2 and NH_3 utilization was calculated for each growth/harvest cycle of the various experiments according to eqns. 3 and 4:

$$\eta_{CO2} = \frac{100*m_{SA}*X_C}{m_{CO2}} \quad (3)$$

$$\eta_{NH3} = \frac{100*m_{SA}*X_N}{m_{NH3}} \quad (4)$$

η_{CO2} is the %CO_2 utilization, m_{SA} is the mass of algae produced, X_C is the C fraction in the algae, and m_{CO2} is the mass of CO_2 fed. η_{NH3} is the %NH_3 utilization, X_N is the N fraction in the algae, and m_{NH3} is the mass of NH_3 fed.

Statistical analysis

Differences in the data reported as significant were compared at the 95% confidence level by one-way analysis of variance (ANOVA) using GraphPad Prism 9 software. To compare mean values between pairwise combinations of datasets, Tukey's HSD test was applied.

3.7.3. Results and Discussion

Cultivation of Scenedesmus acutus using gaseous CO_2/NH_3 in different mole ratios

Scenedesmus acutus was cultured using gaseous CO_2/NH_3 in mole ratios varying from 7 to 18. **Exhibit 3.7.1a** shows the measured pH values during culturing for two representative experiments (CO_2/NH_3 = 7 and 14). For the first growth cycle (i.e., the period up to the first harvest), the cultures

displayed an initial pH value of ~7.0, which increased with time for the first five days. After reaching a maximum of ~10.3 in both cases, the pH started to decrease until almost leveling out at the point of harvest (13 days after initiation of the experiment); at this point, the next growth/harvest cycle commenced. For both experiments, the pH trend was very reproducible from one cycle to the next, although in line with the acidic nature of CO_2 a slightly lower pH value was typically observed in the case of the CO_2/NH_3 ratio of 14 compared to the CO_2/NH_3 ratio of 7.

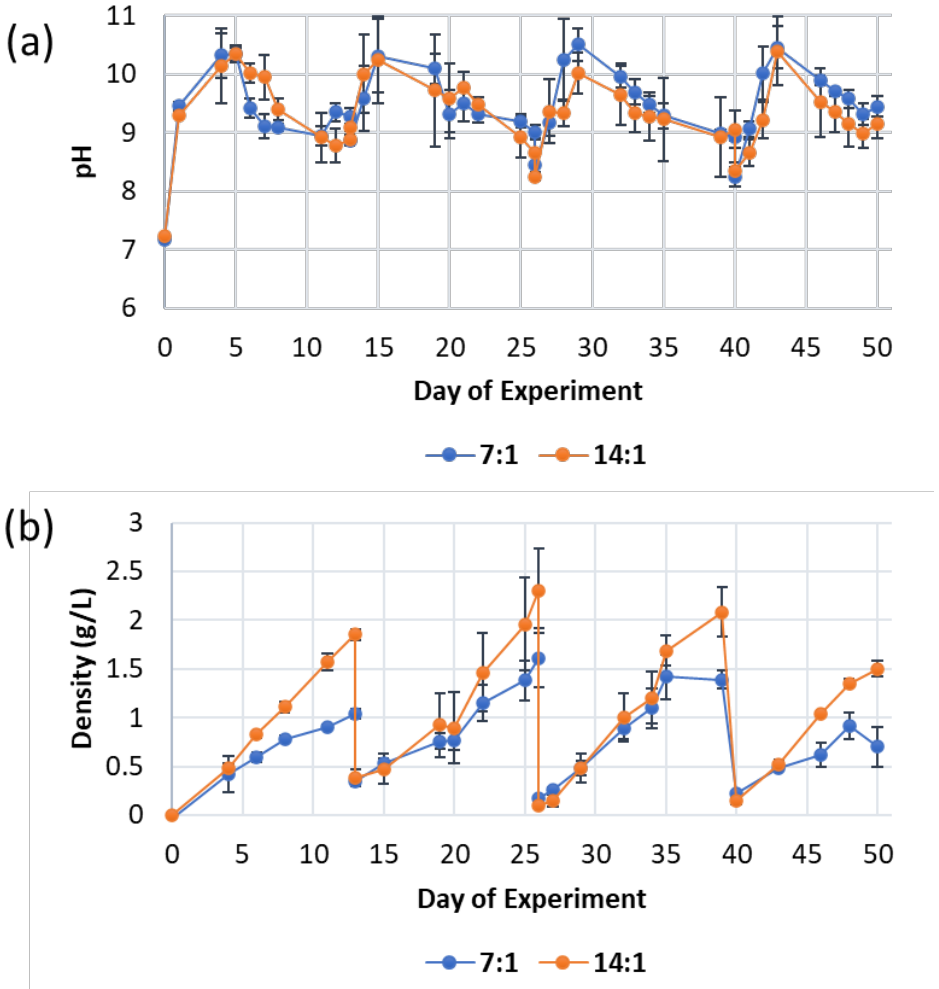

Exhibit 3.7.1. (a) pH values and (b) culture density during consecutive growth/harvest cycles. Error bars represent the st. dev. (n=3). CO_2/NH_3 mole ratios of 7 and 14 were used.

The initial increase in culture pH mirrors that observed when CO_2/NH_3 is bubbled through the culture medium in the absence of algae and reflects the accumulation of NH_3/NH_4^+ in solution. The occurrence of algae growth during this phase can be attributed to the presence of intracellular nitrogen remaining from the previous growth cycle. Four to five days after the initiation of culturing, or after harvesting, the pH declined as the accumulated NH_4^+ started to be utilized by the algae cells. Quantitative analysis of algae growth was performed using dry mass measurements, **Exhibit 3.7.1b** displaying the evolution of culture density for each growth/harvest cycle. Continuous growth of the cultures was observed in both cases, the CO_2/NH_3 = 14 experiment displaying consistently faster algae growth than the CO_2/NH_3 = 7 experiment.

Exhibit 3.7.2 shows a comparison of the measured maximum pH values during all of the culturing experiments, as well as the pH values observed immediately prior to harvesting. In general, the observed trends follow those for the CO_2/NH_3 = 7 and 14 experiments and as expected, increasing the CO_2/NH_3 ratio resulted in generally lower pH values due to the acidifying effect of dissolved CO_2.

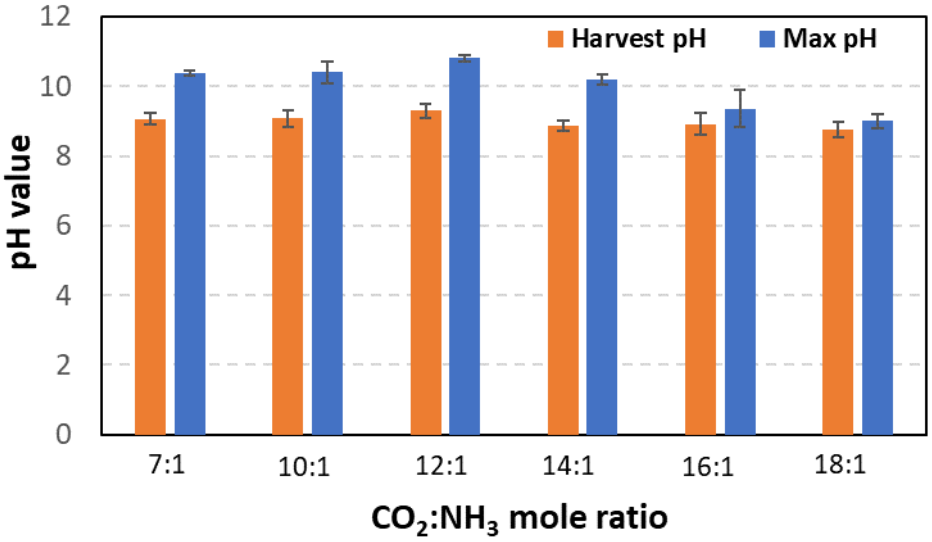

Exhibit 3.7.2. Average maximum culture pH and pH at culture harvest as a function of molar CO_2/NH_3 ratio for multiple growth/harvest cycles. Error bars represent the st. dev. (n = 3 for the 7:1, 10:1, 14:1 and 18:1 experiments; n = 2 for the 12:1 and 16:1 experiments). Applying Tukey's HSD test, the difference in maximum pH for the following mole ratio comparisons are significant: 7 vs 18, 10 vs 16, 10 vs 18, 12 vs 16, 12 vs 18, 14 vs 18.

Exhibit 3.7.3 displays culture productivity as a function of the CO_2/NH_3 mole ratio and of the different growth/harvest cycles. Application of Tukey's HSD test to the data revealed the differences in productivity obtained using the 7:1 CO_2/NH_3 mole ratio and those obtained using the 10:1, 14:1, 16:1 and 18:1 ratios to be significant. From these results it is evident that within the range studied, the optimal CO_2/NH_3 ratio in terms of algae productivity lies in the range 10 – 18, with the 12:1 experiment indicated to be an outlier. Culture productivity for this mole ratio was slightly lower than expected, while the maximum pH values measured for this experiment (**Exhibit 3.7.2**) were higher than for the other runs.

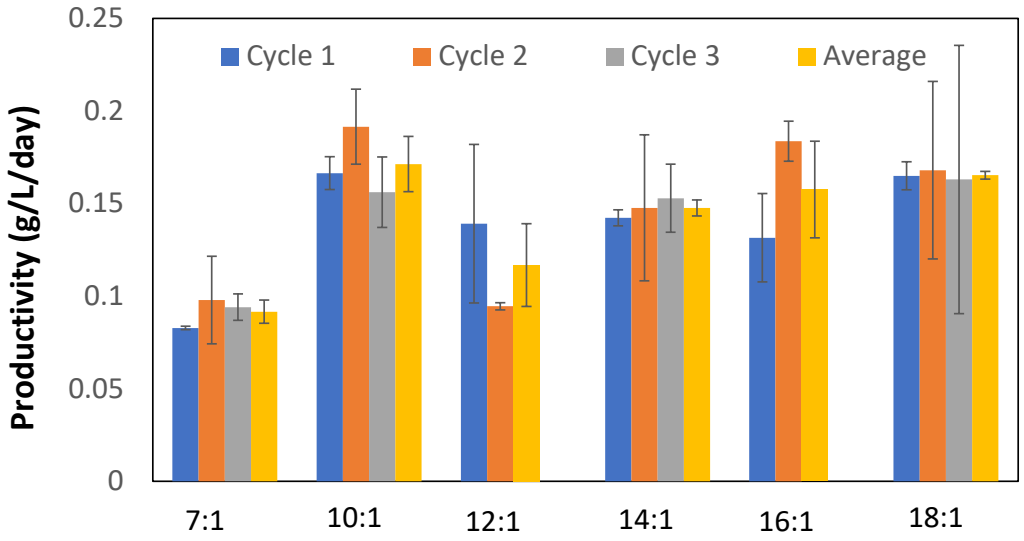

Exhibit 3.7.3. Average culture growth rate as a function of molar CO_2/NH_3 ratio and growth/harvest cycle. Error bars represent the st. dev. (n = 3)

Overall, these results demonstrate that excellent growth of *Scenedesmus acutus* can be obtained using gaseous CO_2/NH_3 as the C- and N-source. Indeed, the average growth rate for CO_2/NH_3 = 10 of 0.171 ± 0.015 g/L/day exceeds that obtained for *Scenedesmus acutus* grown with 1% CO_2/N_2 and urea as the N-source (0.099 ± 0.28 g/L/day; $p < 0.05$) and is comparable with that obtained using 1% CO_2/N_2 and urea as the N-source (0.144 ± 0.025 g/L/day, see **Exhibit 3.7.4** for details).

Exhibit 3.7.4. Comparison of *Scenedesmus acutus* (UTEX B72) productivity cultured with different nitrogen sources[1]

Urea medium[2] (g/L/day)	**BG-11, $NaNO_3$ (g/L/day)**
0.099 ± 0.028	0.144 ± 0.025

[1] 1% CO_2/N_2 bubbled at 0.1 L/min per reactor (n = 3). Other conditions as given in experimental section.

[2] Nutrient recipe as given in Crofcheck *et al*., *J. Biochem. Tech.*. 2012, 4(2): 589-594.

Assessment of CO_2 and NH_3 utilization efficiency

To assess the degree of NH_3 and CO_2 utilization during the experiments, algae biomass harvested from select experiments was subjected to microcombustion analysis. **Exhibit 3.7.5** summarizes the results. Based on the C and N content of the produced algae and the amount of CO_2 and NH_3 fed, the utilization of CO_2 and NH_3 can be estimated according to eqns. 3 and 4. Utilization efficiencies of 43.7 ± 0.9% and 49.3 ±1.0% were obtained for CO_2 and NH_3, respectively, for CO_2/NH_3 = 7. With increase of the CO_2/NH_3 ratio to 10, CO_2 and NH_3 utilization both increased, the CO_2 utilization ranging from 56.8 ±6.9% to 71.9 ±7.6%, depending on the growth/harvest cycle, while the NH_3 utilization was close to 100% in all cases. These results are consistent with the improved algae growth rate obtained at CO_2/NH_3 = 10, such that even though the amount of

CO_2 fed was increased, the CO_2 was utilized to a greater extent. In turn, these findings indicate that at $CO_2/NH_3 = 7$ algae growth is CO_2-limited, likely due to the fact that not all of the CO_2 dissolves in the culture medium under these conditions; in other words, the actual solution CO_2/NH_3 ratio is < 7, i.e., less than the stoichiometrically required ratio. Consistent with this inference is the fact that the NH_3 utilization efficiency in this case is only 49%, i.e., only half of the NH_3 fed was utilized for algae growth. Hence, increasing the CO_2/NH_3 ratio is beneficial, albeit this effect can be expected to diminish as the ratio is increased and the equilibrium concentration of CO_2 in solution represents an excess over that required.

For the 14:1 and 18:1 mole ratio experiments, CO_2 utilization decreased relative to the 10:1 mole ratio experiment (**Exhibit 3.7.5**), a consequence of the fact that these higher ratios represent an excess of CO_2. However, the NH_3 utilization remained at high levels (>80%), reflecting the good growth rates obtained.

Notably, the nitrogen content of the biomass resulting from the 10:1 mole ratio experiment consistently amounted to ~9.8 wt%, corresponding to a rather high protein content of 47 wt%. Indeed, all of the experiments afforded biomass with high protein content (as high as 59 wt%),

Exhibit 3.7.5. CO_2 and NH_3 utilization efficiencies calculated from algae elemental analysis and productivity data.

CO_2/NH_3 mole ratio	**Growth cycle no.**	**Algae analysis by microcombustion, ± st. dev. (n =3)**				**Algae growth rate, ± st. dev. (n= 3)**	**Total in algae (g/day)**		**Total in feed (g/day)**		**Utilization (%)**	
		C (wt%)	**N (wt%)**	**H (wt%)**	**Ash (wt%)**	**(g/L/day)**	**C**	**N**	**C**	**N**	**CO_2**	**NH_3**
7	1	51.62 ± 0.88	9.72 ± 0.15	7.78 ± 0.13	4.43 ± 0.08	0.083 ± 0.001	0.083 ± 0.002	0.016 ± 0	0.191	0.032	43.7 ± 0.9	49.3 ± 1.0
10	1	52.55 ± 0.22	9.86 ± 0.09	7.72 ± 0.03	2.89 ± 0.03	0.162 ± 0.009	0.166 ± 0.009	0.031 ± 0.002	0.273	0.032	62.5 ± 3.4	100.4 ± 5.5
	2	52.51 ± 0.35	9.56 ± 0.06	7.79 ± 0.11	3.0 ± 0.04	0.191 ± 0.02	0.196 ± 0.021	0.036 ± 0.004	0.273	0.032	71.9 ± 7.6	112.1 ± 11.9
	3	50.93 ± 0.50	9.90 ± 0.05	7.58 ± 0.06	3.58 ± 0.01	0.156 ± 0.019	0.155 ± 0.019	0.030 ± 0.004	0.273	0.032	56.8 ± 6.9	94.6 ± 11.5
14	1	51.99 ± 0.30	9.32 ± 0.11	7.82 ± 0.04	2.77 ± 0.05	0.142 ± 0.004	0.144 ± 0.005	0.026 ± 0.001	0.382	0.032	38.2 ± 1.2	82.1 ± 2.8
	2	51.46 ± 0.17	11.5 ± 0.04	7.71 ± 0.02	2.64 ± 0.01	0.148 ± 0.039	0.148 ± 0.039	0.033 ± 0.009	0.382	0.032	38.9 ± 10.4	104.2 ± 27.8
	3	52.63 ± 0.46	9.65 ± 0.13	7.97 ± 0.12	2.9 ± 0.04	0.153 ± 0.18	0.157 ± 0.019	0.029 ± 0.004	0.382	0.032	41.1 ± 5.0	90.4 ± 11.0
18	2	53.66 ± 0.30	11.29 ± 0.11	7.82 ± 0.04	2.95 ± 0.03	0.168 ± 0.048	0.176 ± 0.05	0.037 ± 0.011	0.491	0.032	35.8 ± 10.2	116.1 ± 33.1
	3	53.79 ± 0.16	12.35 ± 0.13	7.66 ± 0.05	2.28 ± 0.03	0.163 ± 0.072	0.171 ± 0.076	0.039 ± 0.017	0.491	0.032	34.8 ± 15.5	123.2 ± 54.7

from which it follows that the biomass should be well suited for the production of bioplastics [44] or for use as animal feed. The low ash content of the biomass (< 3.6 wt%) is also favorable for these applications.

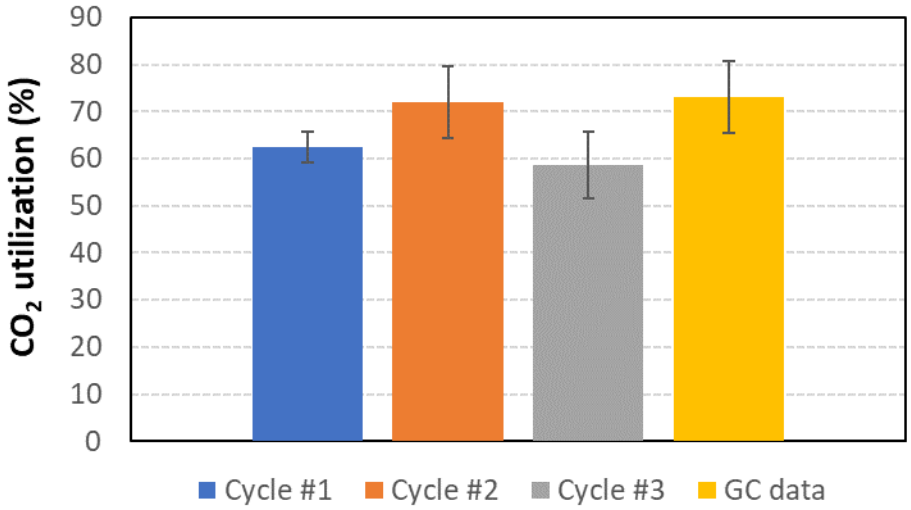

Exhibit 3.7.6. CO_2 utilization calculated from elemental analysis data and algae productivity data for three growth/harvest cycles and from GC analysis of feed gas and reactor effluent for 3rd cycle; $CO_2/NH_3 = 10$. Error bars represent the st. dev. (n = 3 for algae productivity data and n = 8 for GC data).

CO_2 utilization was also estimated based on GC analysis of the gas at the entrance and exit of the photobioreactors. **Exhibit 3.7.6** presents a comparison of these results with those presented in **Exhibit 3.7.5**, the GC results representing the average of measurements taken every day during the third growth/harvest cycle. It should be noted that the GC-based calculation does not take account of CO_2 that dissolved in the culture but was not consumed by the algae. Nevertheless, excellent agreement is observed between the results of the two calculation methods, the CO_2 utilization estimated from GC data amounting to 73%; indeed, the differences in CO_2 utilization values between the two methods are insignificant ($p > 0.05$). Taken together, these findings indicate that the optimal mole ratio of CO_2 to NH_3 is around 10 with respect to both culture productivity and the utilization of the supplied CO_2 and NH_3

Effect of varying the CO_2/NH_3 feed rate on algae productivity

In an effort to increase algae productivity, the effect of increasing the CO_2/NH_3 feed rate was investigated, using a fixed CO_2/NH_3 mole ratio of 10 (corresponding to the previously determined optimal value). As shown in **Exhibit 3.7.7a**, for the feed rates of x1.0 and x1.5 (relative to the feed rate used in above), the pH followed the trends discussed earlier, while for the x2.0 feed rate relatively little variation in pH was observed. Absorbance and dry mass measurements (**Exhibits 3.7.7b** and **3.7.7c**) indicated a continuous increase in culture density for the x1.0 and x1.5 feed rates during each cultivation/harvest cycle, consistent with healthy algae growth. In the case of the x2.0 experiment, however, poor growth was observed (the experiment being terminated at the end of the second growth/harvest cycle).

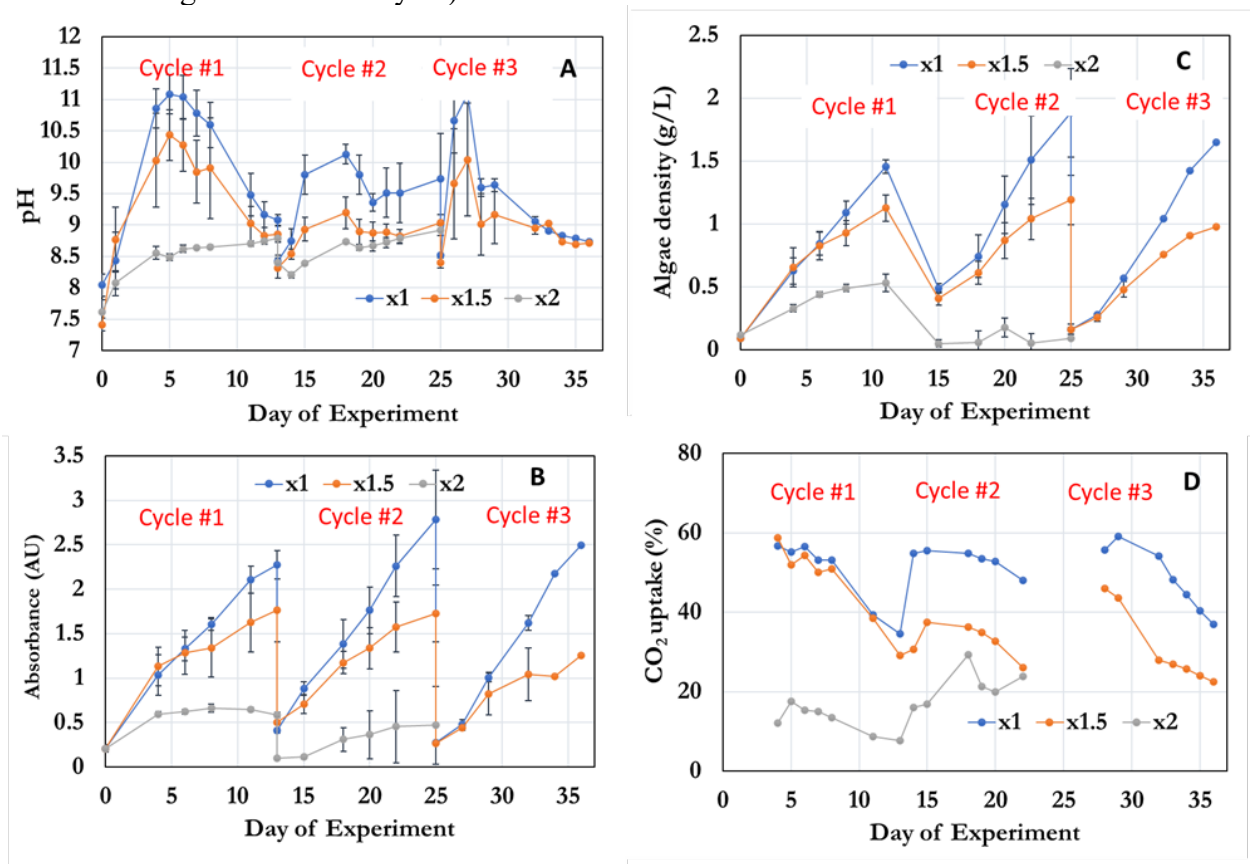

Exhibit 3.7.7. (a) Culture pH; (b) culture absorbance at 680 nm; (c) culture density (dry mass basis); (d) CO_2 conversion based on gas analyses by GC. Three growth/harvest cycles were performed, except for the x2.0 run which was terminated after the second cycle. CO_2/NH_3 mole ratio = 10, N_2 as balance, total gas flow rate = 100 mL/min for each 800 mL PBR. Error bars represent the st. dev. (n = 3)

GC analysis of the gas exiting the photobioreactors revealed much higher CO_2 uptake at the lower feed rates (x1.0 and x1.5) compared to the x2.0 experiment (see **Exhibit 3.7.7d**). It was also noticeable that for the x1.0 and x1.5 experiments, the CO_2 utilization tended to decline towards the end of each growth/harvest cycle (data not shown). This decline coincided with decreased algae growth at high algae densities (>1 g/L), indicating that the growth curve was no longer linear at these higher culture densities.

Exhibit 3.7.8 compares the productivity of the cultures during the successive growth/harvest cycles, the three feed rates employed giving rise to significant differences in algae productivity ($p < 0.05$). At the feed rate of x1.0 good productivity was consistently achieved, whereas increasing the feed rate inhibited the algae growth as depicted in **Exhibits 3.7.7b** and **3.7.7c.** When the flow rate was increased by 50%, a decrease in the overall growth rate of ~40% was observed, corresponding to an average rate of ~0.09 g/L/day. An even more significant drop occurred when doubling the feed rate, with almost no algae growth occurring during the second growth/harvest cycle.

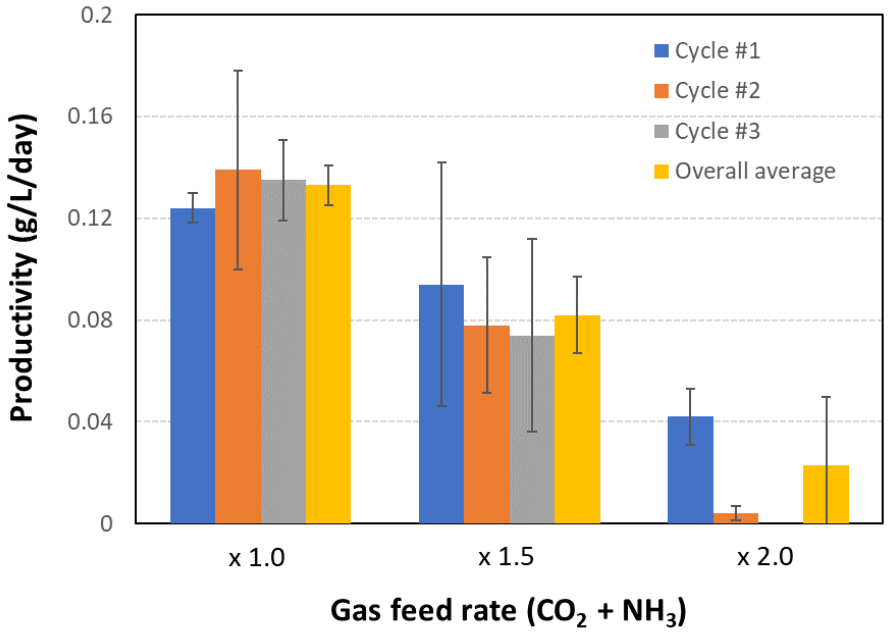

Exhibit 3.7.8. Productivity of algae cultures at different CO_2/NH_3 feed rates; CO_2/NH_3 mole ratio = 10. Error bars represent the st. dev. (n = 3).

To understand the effect of CO_2/NH_3 feed rate on algae growth, ion chromatography (IC) was used to analyze the ammonium ion concentration in the cultures during the second cultivation/harvest cycle of each experiment. From this value the free ammonia concentration was calculated according to eqns. 1 and 2. **Exhibit 3.7.9** shows the ammonium ion concentrations as analyzed by IC and the calculated free ammonia concentrations at the different feed rates during the ninth day of the second growth/harvest cycle. As shown, both the NH_4^+ and free NH_3 concentrations increased with the feed rate. At the feed rate of x1.0, average values of 1.4 - 1.6 mM for both NH_4^+ and free NH_3 were present, these values increasing to values of 17.1 and 3.91 mM for NH_4^+ and free NH_3, respectively, when the feed rate was doubled. In the case of the measured NH_4^+ concentrations, the observed differences in concentration are significant ($p < 0.05$), whereas differences in the NH_3 concentrations are not ($p > 0.05$). However, barring major differences in pH, from eqn. 1 it follows that higher NH_4^+ concentrations will result in increased concentrations of free ammonia. Research by Abeliovich and Azov [35] has shown that free ammonia concentrations in excess of 2 mM can inhibit the growth of *Scenedesmus obliquus*. Indeed, the toxicity of NH_3 at high concentrations appears to be common to all types of algae [32,35,36] and would therefore include the *Scenedesmus acutus* strain used in this study. Hence, for practical

applications, a CO_2/NH_3 feed control strategy would be required that takes into account the ammonium ion concentration in solution and the pH to avoid significant concentrations of free ammonia.

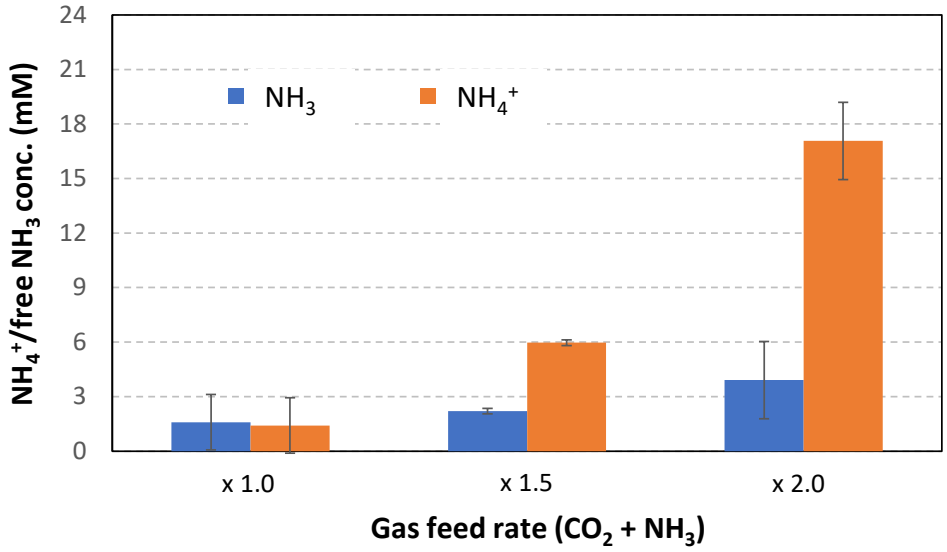

Exhibit 3.7.9. Measured ammonium ion and calculated free ammonia concentrations in algae cultures during 2nd growth/harvest cycle. CO_2/NH_3 = 10; error bars represent the st. dev. (n= 3).

3.7.4. Summary

Growth of *Scenedesmus acutus* was obtained using gaseous CO_2/NH_3 as a C- and N-source for algae cultivation, a CO_2/NH_3 mole ratio of ~10 being optimal with respect to algae productivity and the utilization of CO_2 and NH_3. The composition of resulting algae biomass was notable for its low ash content and high protein content. These characteristics suggest that the biomass should be well suited for the production of bioplastics or for use as animal feed. The CO_2/NH_3 feed rate represents another critical parameter for successful algae cultivation; to avoid the toxic effects of high NH_3 concentrations (>2.0 mM), it is necessary to balance the NH_3 supply with the algae growth rate so that excessive NH_3 accumulation is prevented. Consequently, for practical applications, a CO_2/NH_3 feed control strategy would be required that takes into account the ammonium ion concentration in solution and the pH to avoid significant concentrations of free NH_3.

4. DESIGN AND FABRICATION OF FULLY INTEGRATED PROCESS, AND LONG TERM CAMPAIGN RESULTS

The design basis and detailed process design package were completed based on the experience and lessons learned from UK IDEA's in-house fundamental studies and batch testing investigations, including Heat and Mass Balance (H&MB) stream tables, PFDs, P&IDs, General Arrangement (GAs), equipment and controls lists, utility and electrical requirements, equipment, instrument and piping specification sheets, foundation requirements, electrical line and installation layout, control system layout, and electrical and controls system specifications.

4.1 Integrated Process Design Basis

The process design basis was developed including site characteristics, available utilities and flue gas supply conditions, a process equipment general layout and identification of tie-in locations.

The existing flue gas generators were used to supply flue gas to the capture and integrated unit via a 4-inch pipe tied-in to the existing flue gas supply line. The flue gas characteristics are given in **Exhibit 4.1.1**. The electric power was tied-in to the distribution box behind the coal-fired flue gas generator. The control system of the integrated unit was tied-in to the control system of the flue gas generator.

Exhibit 4.1.1. Flue gas characteristics, dry basis.					
Coal-fired Flue Gas			**Natural Gas-fired Flue Gas**		
Component	**Units**	**Value**	**Component**	**Units**	**Value**
CO_2	vol%	12	CO_2	vol%	8.5
O_2	vol%	6-8	O_2	vol%	4-6
N_2 and Ar	balance		N_2 and Ar	balance	
NO_x	ppm	200-300	NO_x	ppm	30-50
SO_2	ppm	50-150			

Evaluation of site characteristics included an evaluation of the solar energy available for solvent regeneration. At the UK CAER campus, the average daily incident shortwave solar energy experiences significant seasonal variation over the course of the year as shown in **Exhibit 4.1.2**. The brighter period of the year lasts for 4.3 months, from April 24 to September 3, with an average daily incident shortwave energy per square meter above 5.7 kWh. The brightest month of the year in Lexington-Fayette is July, with an average of 6.6 kWh. The darker period of the year lasts for 3.0 months, from November 9 to February 9, with an average daily incident shortwave energy per square meter below 2.9 kWh. The darkest month of the year in Lexington-Fayette is December, with an average of 2.0 kWh.

Exhibit 4.1.2. Average Daily Incident Shortwave Solar Energy in Lexington, Kentucky [1]												
	Jan	**Feb**	**Mar**	**Apr**	**May**	**Jun**	**Jul**	**Aug**	**Sep**	**Oct**	**Nov**	**Dec**
Solar Energy (kWh)	2.2	3.1	4.3	5.5	6.2	6.6	6.6	6.2	5.2	3.9	2.6	2.0

The piping and instrumentation diagram of the bench CO_2 capture and utilization system was shown in **Exhibit 1.1.2**. The integrated capture and utilization system used 5 cfm flue gas produced from either coal or NG combustion and a spiral-wound polymeric membrane for CO_2 preconcentration to simulate an industrial CO_2 source. Other process equipment includes the membrane CO_2 absorber, a solar powered flash stripper, bioreactors, and auxiliary pumps, NH_3 and water make-up systems, heat exchangers, valves, instrumentation, and controls. When coal fired flue gas is applied, flue gas desulfurization is applied to lower SO_2 content to ~30 ppm. A

[1] https://weatherspark.com/y/15790/Average-Weather-in-Lexington-Fayette-Kentucky-United-States-Year-Round#Sections-SolarEnergy

fan is then used to boost the pressure before flowing downward through the membrane CO_2 absorber. Treated flue gas flows through an acid column to remove any ammonia slip prior to stack emission. The CO_2-rich solution exiting from the absorber flows through a pump, a heater powered by solar thermal energy, and a solvent regenerator followed by a rich-lean heat exchanger, is pressurized by a pump, and recirculated through a lean solvent temperature polisher to CO_2 membrane absorber. The product stream at solvent regenerator exhaust was injected to algae bioreactor via sparging for the just-in-time utilization strategy. A 2 M ammonium solution was used as both the capture agent and nutrient for algae growth. Modularized bioreactors with approximately 10 m^2 were used to evaluate the performance of algae production.

4.2 Integrated Process Design Package:

A process model was developed for the ammonium looping integrated CO_2 capture and utilization system using an Aspen Plus controlled equilibrium method to match bench scale experimental results. All columns, heat exchangers and major pumps are included. Complete stream condition specification is supplied with temperatures, pressures, flowrates, and chemical compositions. The flow sheet for the Aspen Plus model is given in **Exhibit 4.2.2**. A RadFrac model is used to simulate the membrane absorber. An additional condenser is added before the absorber column to remove the water vapor in the flue gas and calculate the heat released by the condensation of water vapor.

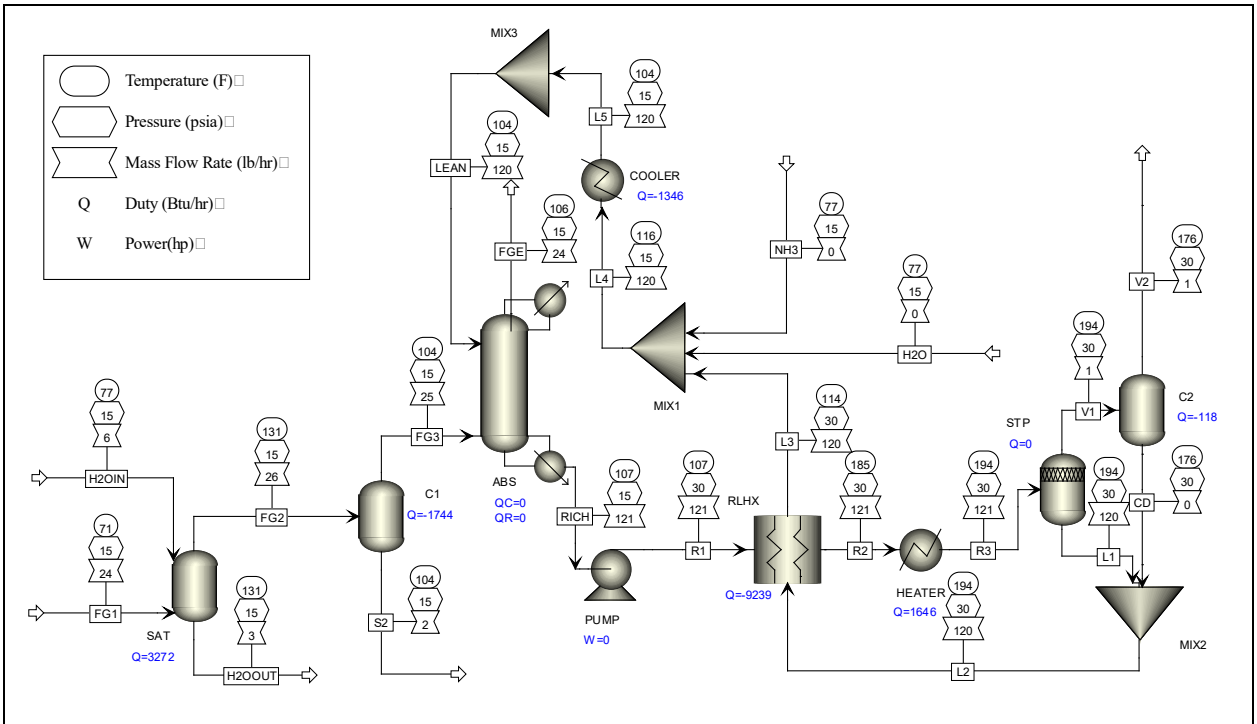

Exhibit 4.2.2. Process model with 5 cfm inlet flue gas.

The membrane module and related equipment were located in the greenhouse, adjacent to the algae ORPs. The solar thermal collectors were installed outside the greenhouse and next to the ORPs. The flue gas generator, cooling equipment, and blower were installed in shed on the backside of the greenhouse. One of the existing ORPs was also moved to this area, totaling 4 ORPs, to ensure

just-in-time CO_2 and NH_3 delivery. The general layout for the integrated absorber and stripping loops are shown in **Exhibit 4.2.3**.

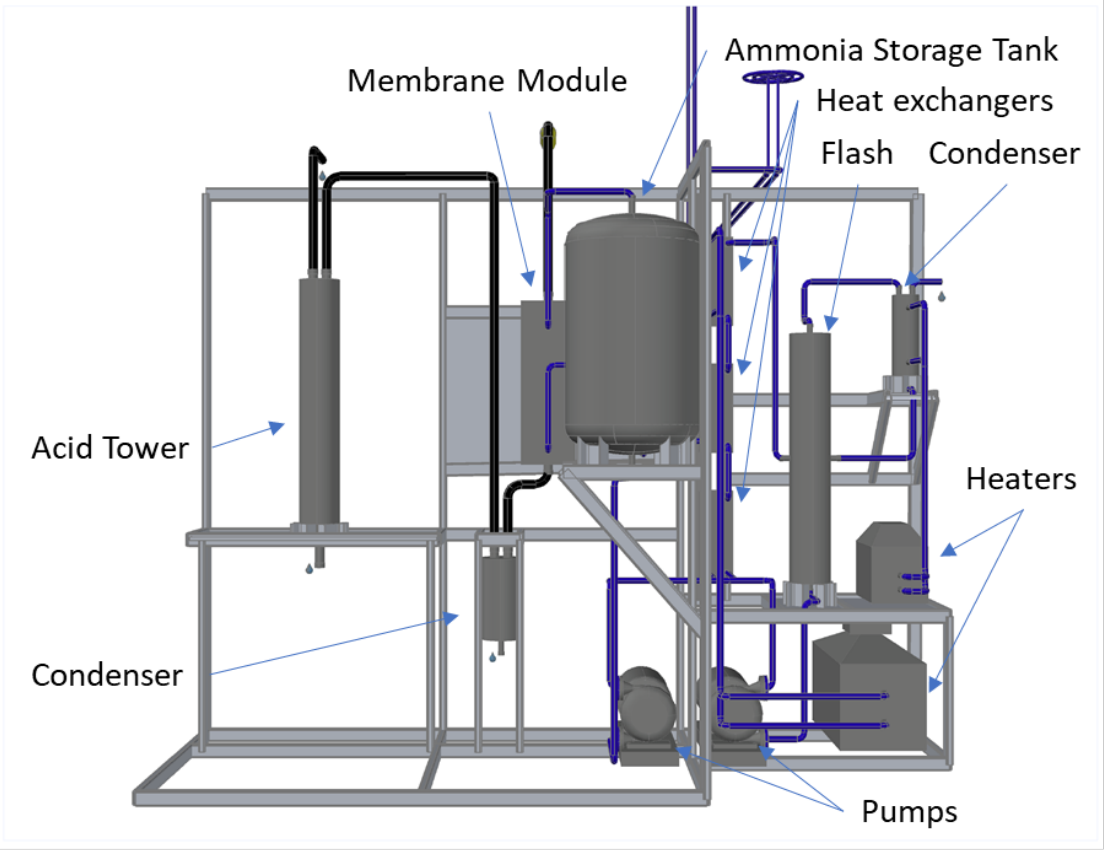

Exhibit 4.2.3. 3D rendering of the ammonium looping integrated process.

4.3 Integrated Process Construction:

Exhibit 4.3.1 shows the different parts of the process that have been constructed and integrated together.

- LF Boiler: A natural gas boiler was installed with a glycol dry cooler to remove heat generated during combustion which enabled continuous operation. The generated flue gas was piped to integrated process via a variable frequency drive blower.
- Stripping Loop: The loop was installed onto the existing ammonium looping process platform. This loop included 3 heat exchangers, a polishing chiller, hot oil bath, plumbing to solar water heater, back pressure regulator, controls and sensory equipment, and a variable frequency drive (VFD) pump.
- Solar Water Heater: The heater was installed outside with tubes facing the most direct path to the sun with a plexiglass blast shied to protect the fragile glass tubes from debris. Also installed was a hot oil pump with insulated piping.

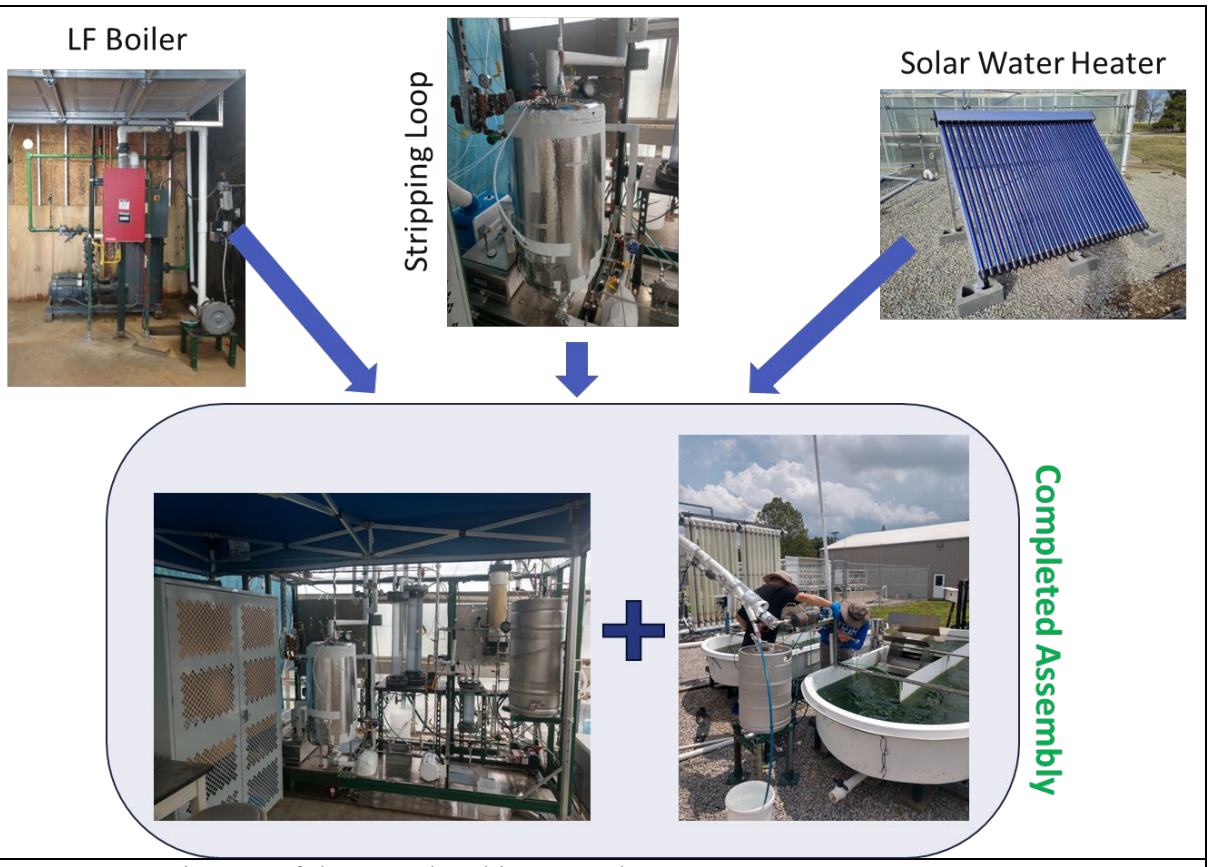

Exhibit 4.3.1. Pictures of the completed integrated process.

Integration with algae ORPs

CO_2:NH_3 stream was produced in the flash stripper and was sent to a knock out drum to reduce liquid entrainments after which it is split 3-ways to Test ORP 1 or 2, or the stack, as shown in **Exhibit 4.3.2** Rotameters were installed before both ORPs to ensure proper and consistent delivery of nutrients while the bulk of the product stream was sent to the stack. Each pond requires 317g of CO_2 and 13.6g of NH_3 every 24 hours, with a CO_2:NH_3 ratio of 10:1 in the product stream. Additionally, a steady flow of 750 mL/min of CO_2 was continuously supplied to the algae ponds 24/7 to ensure the algae's survival but without additional N-nutrient being fed on top of ammonia. The integrated system was operated simultaneously for 12 weeks with stable gas flow rate.

Exhibit 4.3.2. Images of the product stream delivery and interface with the algae ORPs.

Monitoring and control of the ammonium looping process was done with a suite of sensors configured with a National Instruments LabVIEW data aquisition rig and complementary LabVIEW program. The process control program was developed in house and displays all process sensors, records data, and has control loops for automated process control, as shown in **Exhibit 4.3.3**. Inlet and outlet flu gas stream were sampled using a Horiba single channel CO_2 analyzer and 5 channel CO_2, O_2, CO, NO_X, and SO_X analyzer respectively. To prevent equipment damage from the high temperatures in the greenhouse, the instrument cabinet housing the gas analyzers, sample pumps, and data acquisition rig was climate controlled with a portable spot chiller.

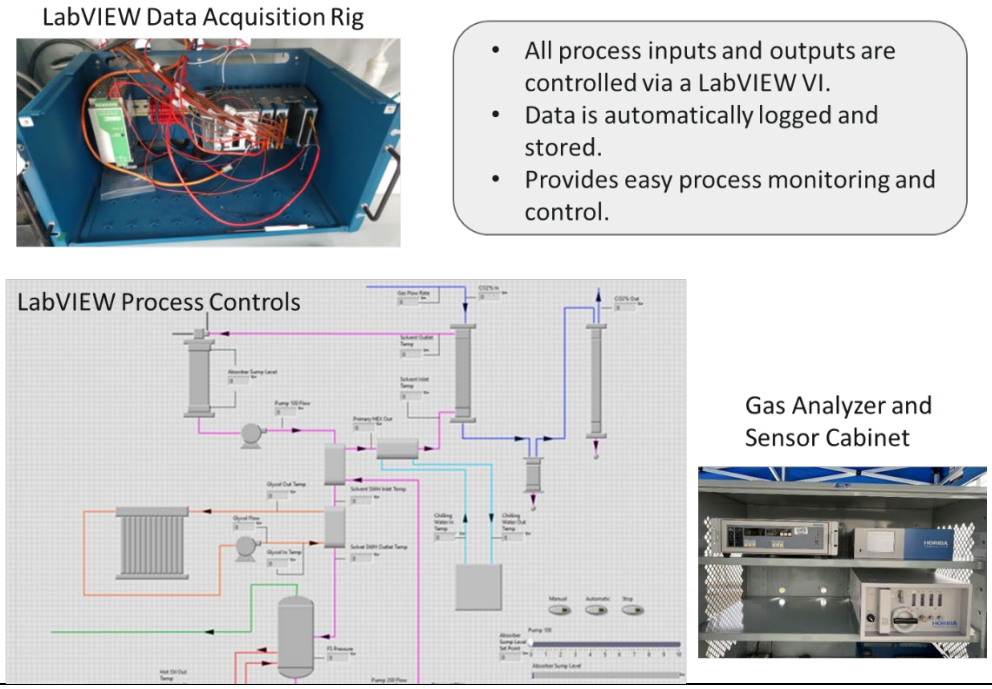

Exhibit 4.3.3. LabVIEW process control program, data acquisition rig, and gas analysis cabinet with climate control.

4.4 Gas Sampling

While the installed process controls suite can automate the basic operation of the ammonium looping process there is no feedback loop between the process, product stream, and algae ponds. Making these connections is critical for future commercial development and smart process automation/optimization. To determine the product stream ratio being delivered to the algae ponds physical gas sampling using the impinger train method and with IC analysis must be done. This is a lengthy process which is not conducive to a responsive process. To improve on this, Aspen simulation results are used to guide process operating parameters to achieve a desired CO_2:NH_3 ratio, but a guide is not a physical measurement. To get an instantaneous and accurate product stream measurement, a high concentration CO_2 probe was installed on the product stream to directly measure the CO_2 and H_2O content, the product ratio was calculated from this information. **Exhibit 4.4.1** shows the evolution from Aspen guided conditions to physical gas sampling to fully automated real time measurements.

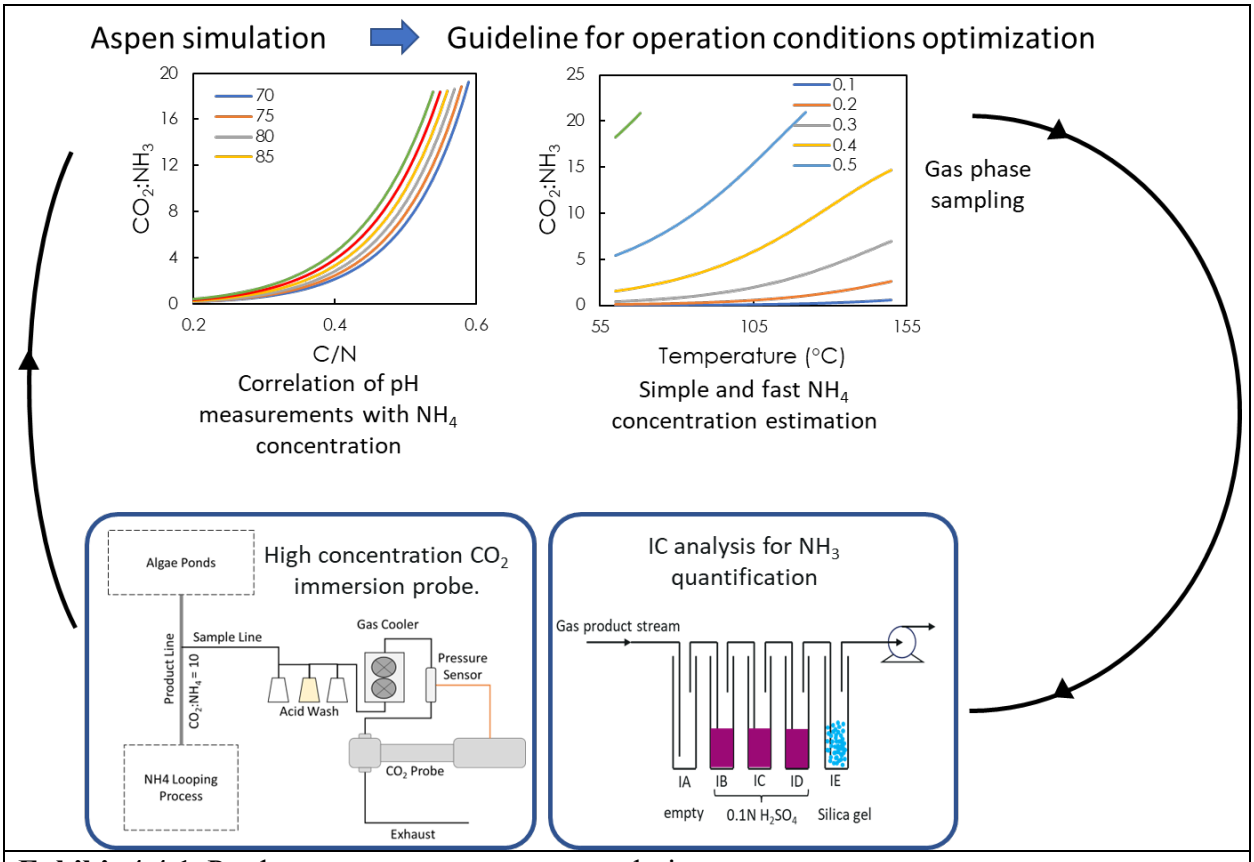

Exhibit 4.4.1. Product stream measurement evolution.

Real time product stream ratio testing

During the parametric and long-term campaigns regular gas sampling was conducted on the stripper product stream using the EPA method. Total ammonia was directly measured using ionic chromatography. Results for this method have a lengthy turnaround time and only give one data

point per collection. During the project, a real time continuous method was developed and tested, as shown in **Exhibit 4.4.2**

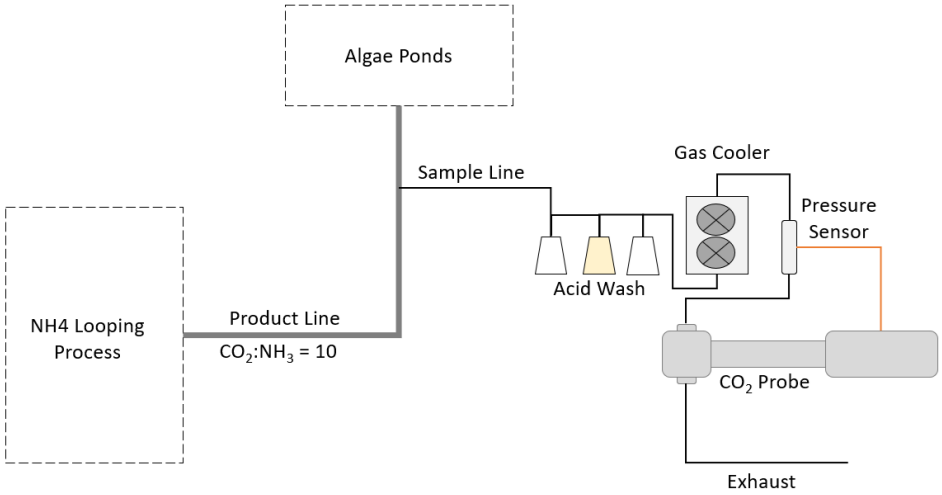

Exhibit 4.4.2. Real time product stream ratio testing setup.

In lieu of an impinger train a high concentration CO_2 and H_2O probe was installed. The probe can measure up to 100% gaseous CO_2 concentrations and water concentrations. Combined with an O_2 measurement, in case of atmospheric leakage, the ammonia content was derived. In line with the probe is a gas cooler to chill the hot product gas below 60°C—to prevent damaging the probe—a pressure sensor which provides pressure data to the probe for accurate measurements, an internal temperature sensor, and an optional acid wash. Testing results in **Exhibit 4.4.3** show that the CO_2 probe can be used for real time product stream measurements; while also showing how the ratio changes with inlet stripping temperature, as expected.

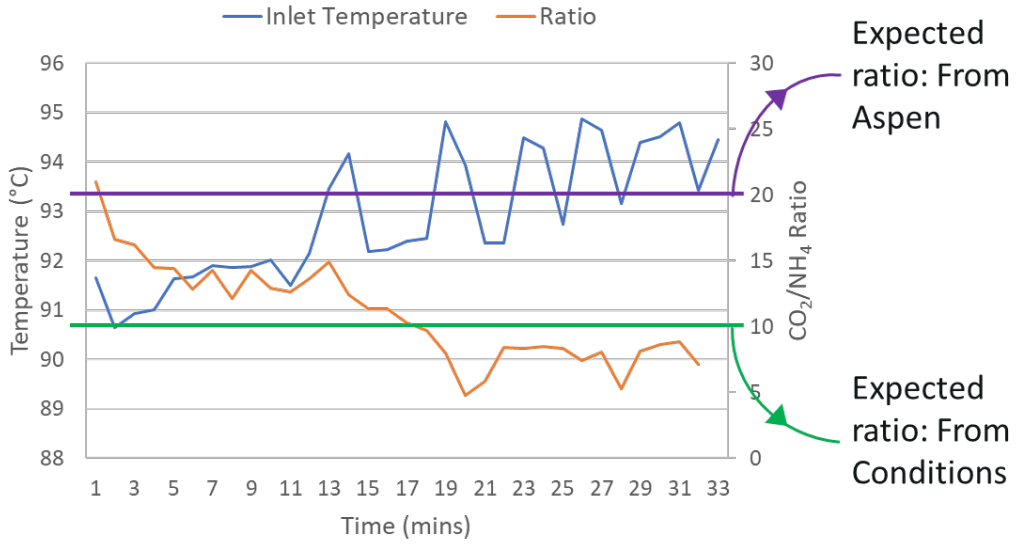

Exhibit 4.4.3. The expected ratio from Aspen was 20 but by adjusting experimental conditions, warm solvent flow to the top of the stripper and inlet stripping temperature, the target ratio of 10 was achieved.

4.5 Long-term Campaign, Process Performance

Following the parametric campaign completed in Task 10.0, UTEX B72 production has been demonstrated. Culturing in this campaign was carried out in ORPs (1100 L) equipped with probes for continuous measurement of dissolved O_2, pH, temperature, and turbidity. Two ponds were provided with CO_2:NH_3, while the other two ponds were operated conventionally as a reference, sparging with gaseous 3% CO_2:N_2 with CO_2 as the C source and urea as the N source. This permitted a direct comparison of system productivity, which was tracked as described for Task 5.0. 3% CO_2/N_2 was supplied from cylinders using a feed-on-demand approach, based on culture pH. The two systems were operated simultaneously for a minimum of 88 days. The resulting algae biomass was analyzed for protein, carbohydrate, and lipid content.

The experimental results of CO_2:NH_3 ratio were found to be 2.5 times lower than the simulation results obtained from Aspen. To investigate the root cause, additional experiments were performed to maximize the CO_2:NH_3 ratio. According to the simulation results from Aspen, the CO_2:NH_3 ratio tends to be higher at higher temperature and solvent C/N. As the Optimal CO_2:NH_3 mole ratio for algae growth lies in the range of 10:1-18:1, the C/N of solvent is preferably 0.4-0.6 with temperature inlet of 60-120 °C. To increase the feed ratio to the ORPs, the process was operated at higher loadings and higher inlet temperatures. Additionally, a spray nozzle was installed on the flash stripper solvent inlet line which will improve diffusion CO_2 into the product stream. Secondly, a cold rich inlet to the top of the flash stripper was installed. This has been shown in previous experiments to improve stripping efficiency by acting as an in-situ condenser.

Two separate solvent concentrations were tested, 0.5 mol/kg and 2.0 mol/kg and rich solvent carbon loading was varied between 0.4 and 0.7 C/N for each concentration. At both the higher and lower alkalinities, CO_2:NH_3 ratios of 10 or more were consistently achieved. The highest ratio was achieved with the use of the hot oil system set to 90°C, as shown in **Exhibit 2.5.2** run 4. Conversely, higher hot oil temperatures, as in run 10, lower the ratio, as the amount of gaseous and vaporous ammonia produced exceeds the knockout capacity of cold-rich-spilt-flow. This can be compensated for by increasing the flow rate of the cold-rich-split-flow but doing so will impact overall stripping.

(a)

Run	Hot Oil Setpoint (°C)	Stripper bottom temperature (°C)	Stripper top temperature (°C)	Rich feed temperature (°C)	Lean loading (mol C/mol N)	CO_2:NH_3 (exp mol/mol)
1	140	93	90	89	0.424	2.53
2	0	31	63	90	0.536	13.41
3	0	84	78	79	0.512	11.47
4	90	79	78	98	0.622	21.75

(b)

Run	Hot Oil Setpoint (°C)	Stripper bottom temperature (°C)	Stripper top temperature (°C)	Rich feed temperature (°C)	Lean loading (mol C/mol N)	CO_2:NH_3 (exp mol/mol)
5	0	36	45	68	0.548	13.8
6	0	51	68	91	0.491	4.78
7	0	52	98	92	0.454	4.21
8	0	32	64	91	0.511	7.09
9	0	54	64	92	0.504	5.84
10	100	85	81	95	0.514	1.8

Exhibit 4.5.2. (a) Experimental results for testing done with a solvent alkalinity at 0.5 mol/kg. (b) Similarly, results with a solvent alkalinity of 2 mol/kg.

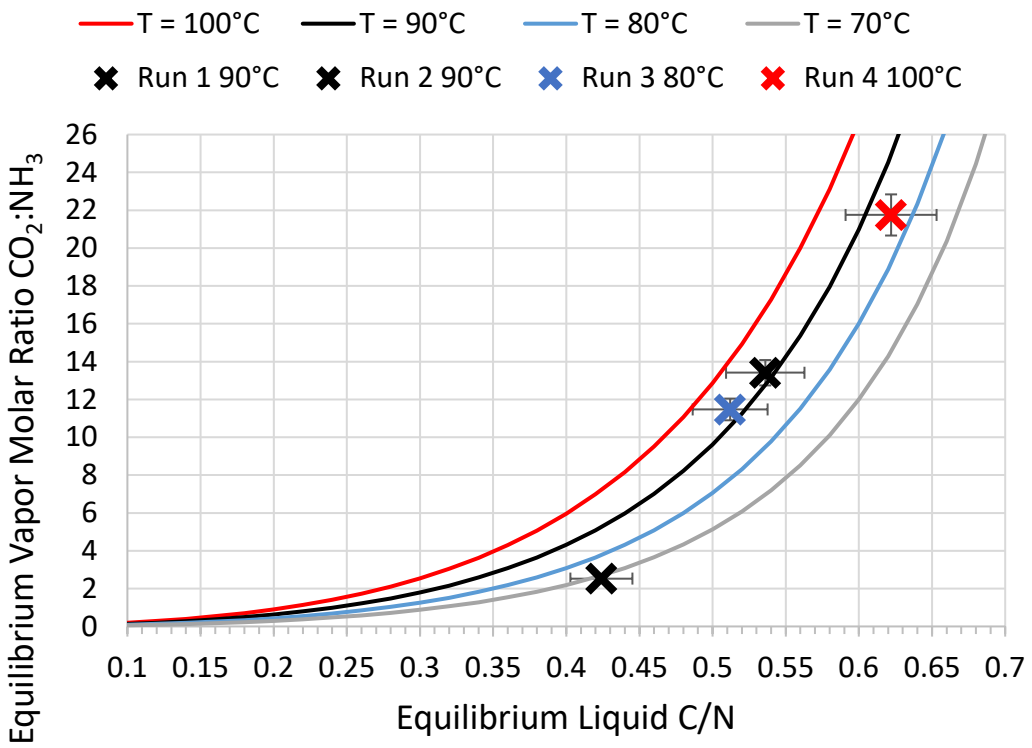

(a)

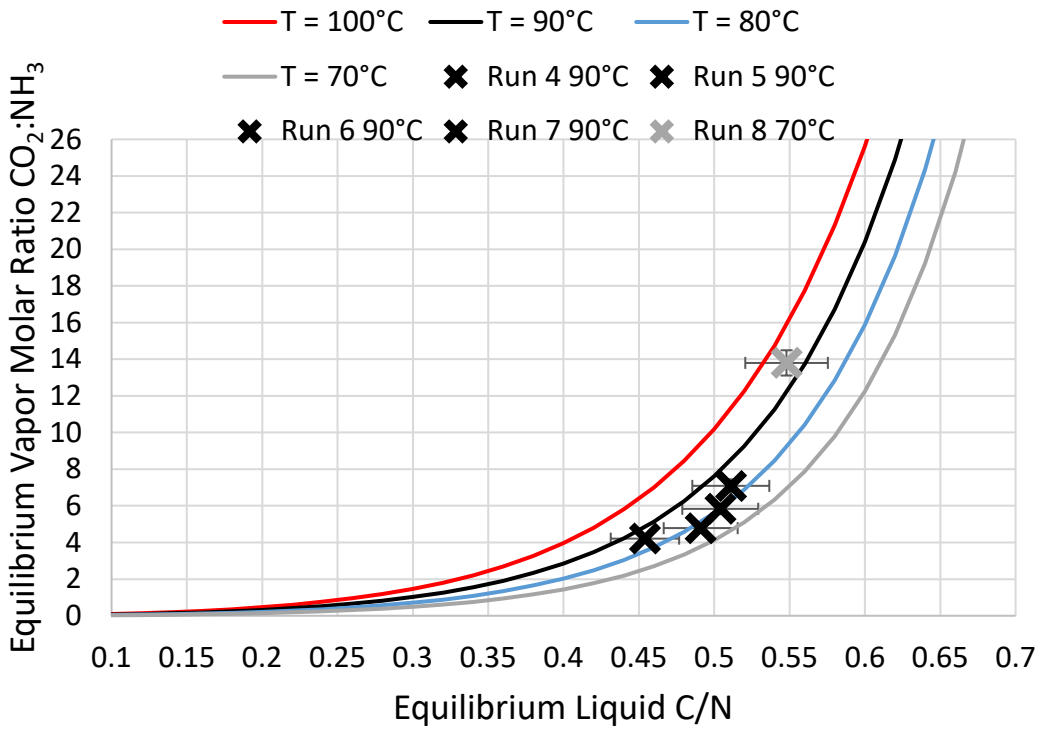

(b)

Exhibit 4.5.3. (a) 0.5 mol/kg Aspen simulation for stripping product CO_2:NH_3 ratio. (b) Aspen simulation with an alkalinity of 1.8 mol/kg.

Experimental results of the measured CO_2:NH_3 ratios for both high and low alkalinities were found to line up with simulation results obtained from Aspen, as shown in **Exhibit 4.5.3**. Previously, the experimental measurements remained unchanged with increasing carbon loading and stripping temperatures. This was due to excess NH_4 entering the gaseous/vapor phase, as shown in run 1 and 10. Additionally, experimental gas sampling methods were changed to minimize sudden pressure swings between the stripper and gas sampling vacuum pump. This subtle procedure changes greatly reduced the likelihood of pulling liquid solvent into sampling impingers.

Over the course of the long-term campaign the process delivered nutrients to the algae ponds. The total amount of the nutrients delivered are shown in **Exhibit 4.5.4.** During periods of non-operation the ponds were fed a solid nutrient source to keep ammonia levels consistent. Not once during the entire campaign was the process shut down for component failure. It was, however, shut down on weekends and during equipment modifications, such as the changes to the flash stripper.

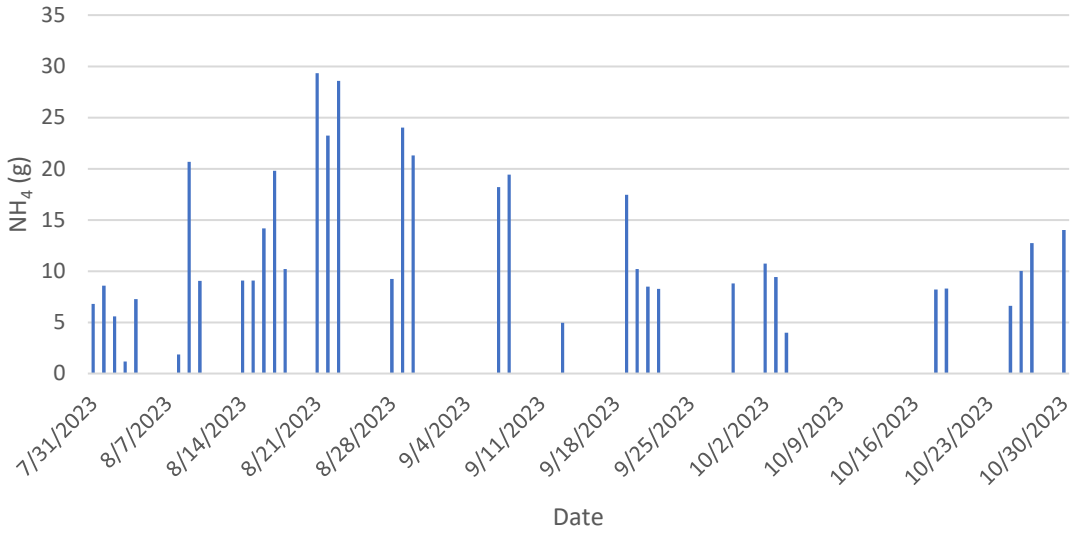

Exhibit 4.5.4. NH_4 delivery to the individual ponds throughout the long-term campaign.

4.6. Algae, Outdoor Evaluation

4.6.1. Overview

In Task 5.1, the feasibility of using gaseous CO_2/NH_3 as a C- and N-source for algae cultivation was assessed. *Scenedesmus acutus* was cultured in tubular PBRs using CO_2/NH_3 in mole ratios spanning the range from 7 to 18. Strong growth of the algae was observed, average growth rates typically exceeding those using 1% CO_2/N_2 and urea or $NaNO_3$ as the N-source.

In Task 5.2 effort focused on scaling up the cultivation of *Scenedesmus acutus* to 1100 L ORPs using CO_2 and NH_3 supplied from gas cylinders. Specific points of interest included the culture productivity, the levels of CO_2 and NH_3 utilization that could be attained, and the degree to which NH_3 was lost to the atmosphere as a consequence of outgassing from the ORPs.

4.6.2. Experimental

Algae Culturing

Scenedesmus acutus (UTEX B72) was initially grown indoors in 800 ml tubular glass PBRs, from which 10 L tubular glass PBRs were inoculated (also indoors). The light source consisted of T5 35-watt cool white fluorescent bulbs (90 μmol/m^2/s), cycling 24 hours a day. From there, the culture was inoculated into 30 x 10 L glass PBRs contained in a greenhouse and illuminated with natural light. In all cases BG-11 was used as the culture medium [45], the $NaNO_3$ component being omitted and replaced with $(NH_4)_2CO_3$ (17.6 mM). The PBRs were bubbled with 3% CO_2/N_2, the temperature being maintained at 23.3 ± 0.6 °C for indoor cultivation.
Outdoor cultivation of *Scenedesmus acutus* was performed in 4 x 1100 L fiberglass ORPs (Algae Lab Systems). Inoculation of the ponds was performed using culture from the 30 x 10 L PBRs, the initial biomass concentration in the ORPs being ~0.1 g/L. The ORPs were operated at an average depth of 23 cm, corresponding to a culture volume of 996 L in each ORP. Two ponds (denoted as ORP 1 and ORP 2) were fed in separate experiments with CO_2/NH_3 at 7:1 and 10:1 mole ratios. N_2 was used as a balance gas, the other gases used corresponding to 100% CO_2 and 4% NH_3/N_2 ($CO_2/NH_3/N_2$ flow = 0.11/0.015/2.58 L/min to each pond for CO_2/NH_3 = 7 and $CO_2/NH_3/N_2$ flow = 0.15/0.015/2.58 L/min to each pond for CO_2/NH_3 = 10). Two other ponds (ORP 3 and ORP 4) were operated as a reference, using pure CO_2 as the feed (0.15 L/min). All of the ponds were operated in open loop mode (i.e., with continuous CO_2 sparging). $NaNO_3$ functioned as the N-source in ponds 3 and 4, other essential nutrients in ORPs 1-4 being supplied according to the BG-11 nutrient recipe. ORP 1 was monitored continuously for dO_2 and temperature (Algae Lab Systems probes coupled to an ALS-SPARC-2 wireless monitoring and control system). Additional measurements were made for all ORPs three times daily (morning, noon and late afternoon) for pH, temperature and ambient photosynthetically active radiation (PAR). Samples of the cultures were taken for dry mass determination and UV-vis spectrophotometry measurements (absorption at 680 nm) three times per week (Monday, Wednesday and Friday), as well as for the determination of ammonium ion concentrations using ion chromatography.

Harvesting was performed when the algae concentration reached a minimum value of ~0.4 g/L, ~75% of the algae being removed at each harvest, i.e., the concentration after harvesting was ~0.1 g/L. In this manner, the cultures remained in the log phase of growth. After each harvest, the nutrients and water were replenished to the initial values, the added water being sterilized using a UV system.
Productivity (P, g/L/d) was obtained using the equation $P = (X_t - X_0)(t - t_0)^{-1}$ where X_t is the biomass concentration (g/L) at t (d) and X_0 is the biomass concentration at inoculation (t_0). Areal productivity values (g/m^2/d) were obtained by multiplying volumetric productivity values by the pond volume (996 L) and dividing by the pond area (4.33 m^2).

Analytical methods
Detection and quantitation of ammonium ions was performed as described for Task 5.1, as was the analysis of algae biomass.

Statistical analysis
Differences in the data reported as significant were compared at the 95% confidence level by a t-test.

4.6.3. Results and Discussion
Cultivation of Scenedesmus acutus using CO_2/NH_3 (7:1 mole ratio)

Cultivation of *Scenedesmus acutus* was performed outdoors using CO_2/NH_3 from gas bottles in two different mole ratios, namely, 7:1 and 10:1. In the first experiment, two ORPs (denoted as ORP 1 and 2) were fed with CO_2/NH_3 at a 7:1 mole ratio, corresponding to the approximate C:N stoichiometric ratio in algae biomass. Simultaneously, two reference ponds (ORP 3 and 4) were operated using excess CO_2 (10% CO_2/N_2) as the carbon source and dissolved $NaNO_3$ as the N-source (BG-11 medium). Culturing was performed for 15 days, after which ~75% of the biomass in the ponds was harvested and culturing continued for a further 11 days.

As shown in **Exhibit 5.2.1**, the behavior of ORP 1 and 2 – operated with continuous gas flow – mirrored that seen in our previously reported indoor experiments with respect to pH (Task 5.1). Initially the pH increased as the concentration of dissolved NH_3 increased, peaking at around pH 10.5. After approximately 5 days the pH started to decrease (as growth picked up and dissolved NH_3 was consumed), finally stabilizing at a value of ~8. Notably, in previous (unpublished) experiments conducted over the pH range 5.5 – 8.0, we have observed that a pH value of 8 was optimal for the growth of *Scenedesmus acutus* when using urea, KNO_3 or NH_4NO_3 as the N-source. Hence, when culturing using gaseous CO_2/NH_3, it is questionable if significant gains in algae productivity can be made by using a feedback loop to regulate the pH around a value of 8, given that the pH tends towards this value in any case.

In contrast, the pH for the reference ponds, after initial fluctuations, stabilized at a value of ~6.3. This reflects the saturation of the culture with CO_2 and is very similar to values observed previously by us when feeding cultures in open loop mode with similar CO_2 flow rates, either using 10% CO_2/N_2 or coal-derived flue gas [46].

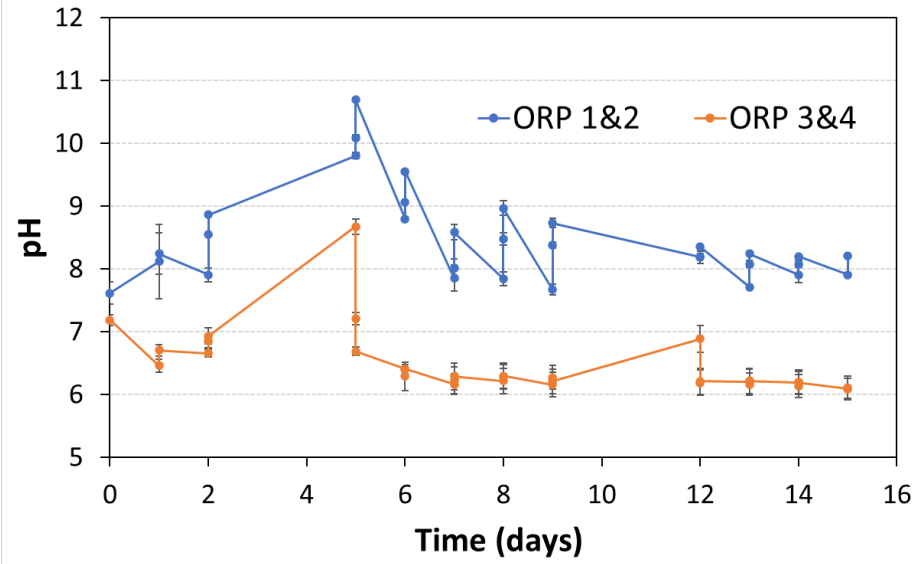

Exhibit 4.6.1. Average culture pH of ORP 1 and 2 and of ORP 3 and 4 as a function of time during 1st cultivation/harvest cycle (CO_2/NH_3 = 7). Error bars represent the st. dev. (n = 2). With the exception of the start and end dates, pH measurements were taken three times daily (early morning, noon and late afternoon). The increase in pH during the course of any given day reflects CO_2 consumption by the algae as a result of photosynthesis.

The density of the cultures as a function of time for the first and second cultivation/harvest cycles is reported in **Exhibit 4.6.2**. For the first cultivation/harvest cycle, net productivity averaged 5.2 ±

0.5 g/m^2/day for ORP 1 and 2, and 3.4 ± 0.2 g/m^2/day for ORP 3 and 4 on an ash-free dry basis (AFDB). For the second cycle, the algae growth rates dropped to 3.1 ± 0.9 g/m^2/day for ORP 1 and 2, and 2.2 ± 0.4 g/m^2/day for ORP 3 and 4, these decreases resulting from a deterioration in the weather at the start of the second cycle, as reflected in lower temperatures (see **Exhibit 4.6.3**) and decreased average PAR values. Overall, the treatment ponds (ORP 1 and 2) consistently showed better performance than the reference ponds (ORP 3 and 4), the difference for the first cultivation/harvest cycle being statistically significant ($p < 0.05$).

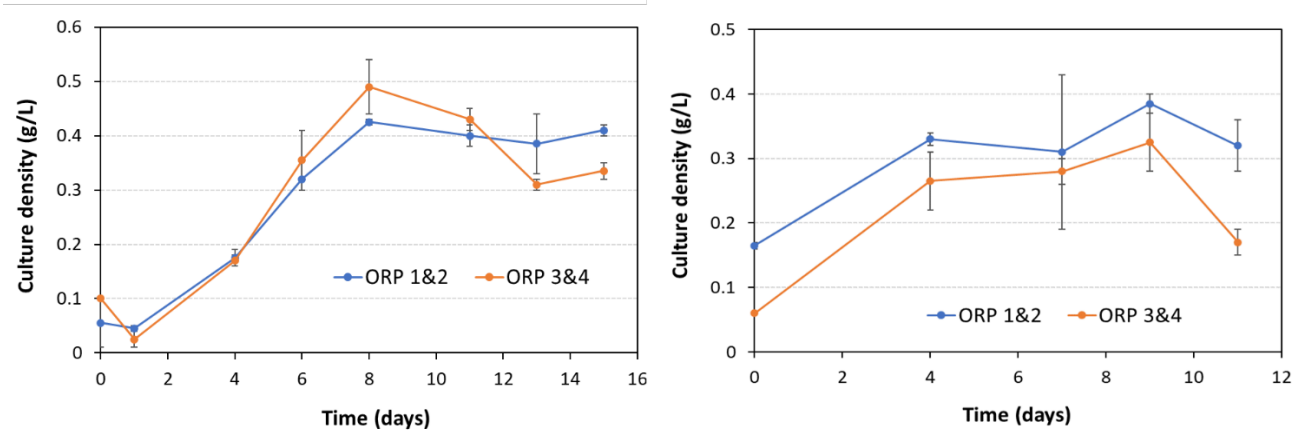

Exhibit 4.6.2. Culture density versus time. Left: 1st culture/harvest cycle; right: 2nd culture/harvest cycle. ORP 1 and 2 were fed with 7/1 CO_2/NH_3, and ORP 3 and 4 were fed with pure CO_2 and $NaNO_3$. The CO_2 flow rate to each pond was 0.15 L/min. Error bars represent the st. dev. (n = 2).

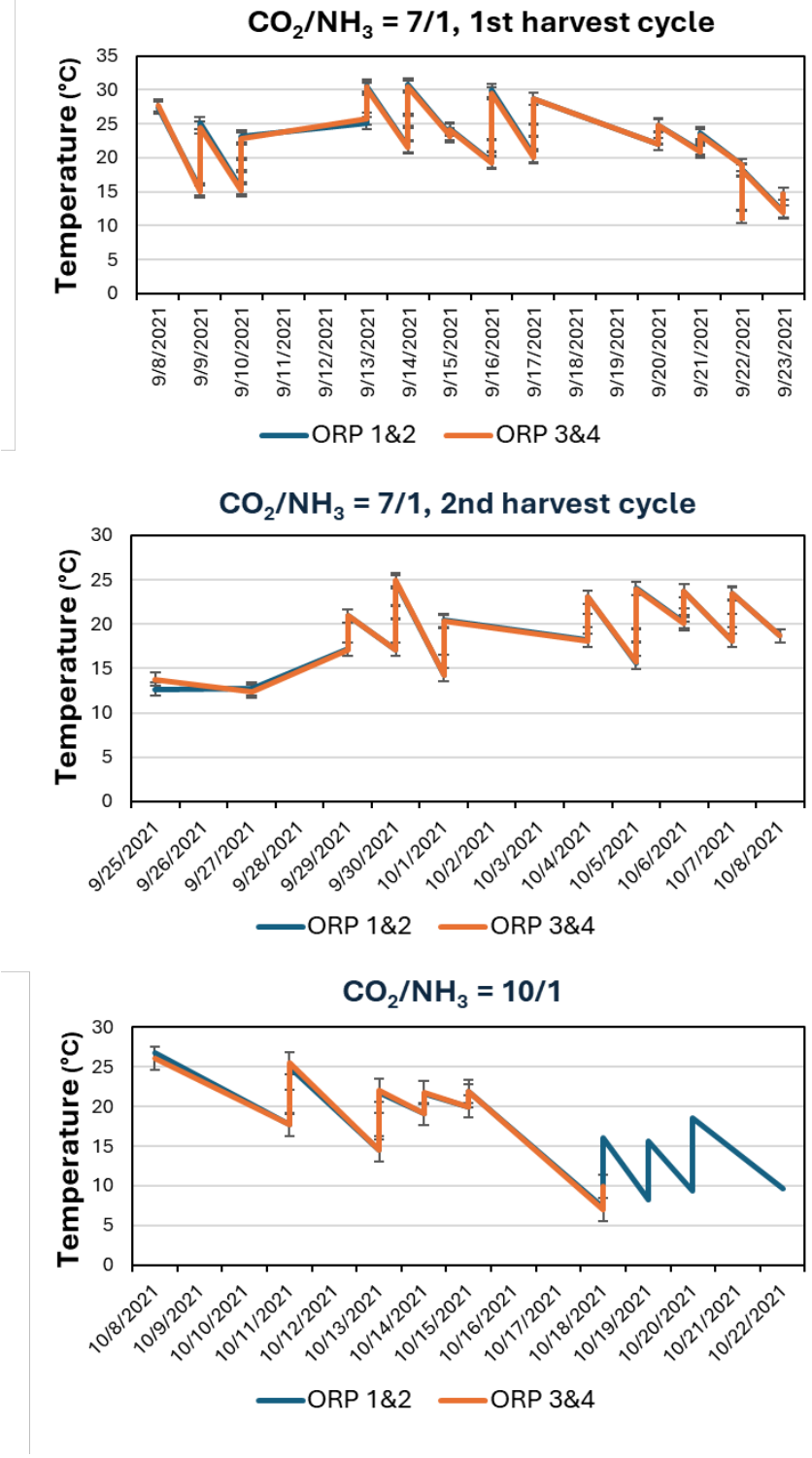

Exhibit 4.6.3. Daytime temperatures measured in ORPs 1-4 by run date. With the exception of the start and end dates, temperature measurements were taken three times daily (early morning, noon and late afternoon). Error bars represent the st. dev. (n = 2). Culturing in ORPs 3 and 4 was terminated on 10/18/21.

IC analysis was performed for samples collected from ORP 1 and 2 at the end of the second cultivation/harvest cycle. NH_4^+ concentrations of 27.9 ppm and 61.0 ppm NH_4^+ were found in ORP 1 and 2, respectively. Based on these values and the pH and temperature, the free ammonia concentration was calculated to be 87 µM and 69 µM for ORP 1 and 2, respectively, being within the safe limit of ~2 mM for green algae.

Algae biomass harvested at the end of the first and second cultivation/harvest cycles was analyzed for C and N by microcombustion. Combining the results with the algae productivity, the CO_2 and NH_3 utilization was calculated as described in section 2.3. The results of these calculations are summarized in **Exhibit 4.6.4.** Note that the calculation of CO_2 and NH_3 utilization is based on 24 h/day supply of CO_2 and NH_3 (as used in the experiment). As reported in the table, during the first cycle for ORP 1 and 2, the average CO_2 and NH_3 utilization efficiencies were only ~15%. The fact that the value is almost the same for CO_2 and NH_3 confirms that CO_2 and NH_3 were consumed by the algae in an approximate 7:1 mole ratio. The feed rate used in the experiment was equivalent to that used previously in the indoor photobioreactor (PBR) experiments in Task 5.1, designed to support a growth rate of up to 0.2 g/L/day. While such high growth rates are feasible in a PBR, growth rates in ponds are lower due to inherent limitations in mixing and penetration of light into the culture, as well as variations in temperature and PAR. Therefore, the CO_2/NH_3 feed rate was undoubtedly excessive, meaning that equivalent growth rates should be possible at lower feed rates, in turn increasing the utilization efficiencies.

Exhibit 4.6.4. Elemental analysis of algae biomass harvested from ORPs and calculated CO_2 and NH_3 utilization efficiency (CO_2/NH_3 mole ratio = 7)

	C (%)	N (%)	Ash (%)	Protein (%)	CO_2 utilizn. (%)	NH_3 utilizn. (%)
1st cultivation/harvest cycle						
ORP 1	49.64 ± 0.19	8.95 ± 0.05	5.4 ± 0.02	42.78 ± 0.23	15.0 ± 0.7	17.2 ± 0.8
ORP 2	49.78 ± 0.47	9.1 ± 0.09	6.64 ± 0.02	43.5 ± 0.43	15.8 ± 0.8	18.4 ± 1.0
ORP 3	48.38 ± 0.44	3.02 ± 0.06	6.85 ± 0.14	14.44 ± 0.3	0.8 ± 0.04	-
ORP 4	46.95 ± 0.49	2.66 ± 0.03	6.69 ± 0.11	12.71 ± 0.14	0.9 ± 0.05	-
2nd cultivation/harvest cycle						
ORP 1	49.08 ± 0.34	9.06 ± 0.05	5.6 ± 0.01	43.31 ± 0.24	5.8 ± 0.3	6.7 ± 0.3
ORP 2	46.86 ± 0.82	8.83 ± 0.2	6.54 ± 0.05	42.21 ± 0.10	10.0 ± 0.6	11.8 ± 0.7
ORP 3&4	49.06 ± 0.38	7.45 ± 0.06	6.79 ± 0.05	35.61 ± 0.3	5.8 ± 0.3	-

* AFDB = Ash-free dry base.

Cultivation of Scenedesmus acutus using bottled CO_2/NH_3 (10:1 mole ratio)

In the next experiment, a CO_2/NH_3 mole ratio of 10:1 was used, representing the optimal value determined from indoor culturing experiments (Task 5.1). **Exhibit 4.6.5** reports the measured pH values, the pH being rather unstable for the first 6 days, after which it tended towards a value of 8.

As expected, the reference ponds consistently showed lower pH values than ORP 1 and 2, due to the absence of NH_3.

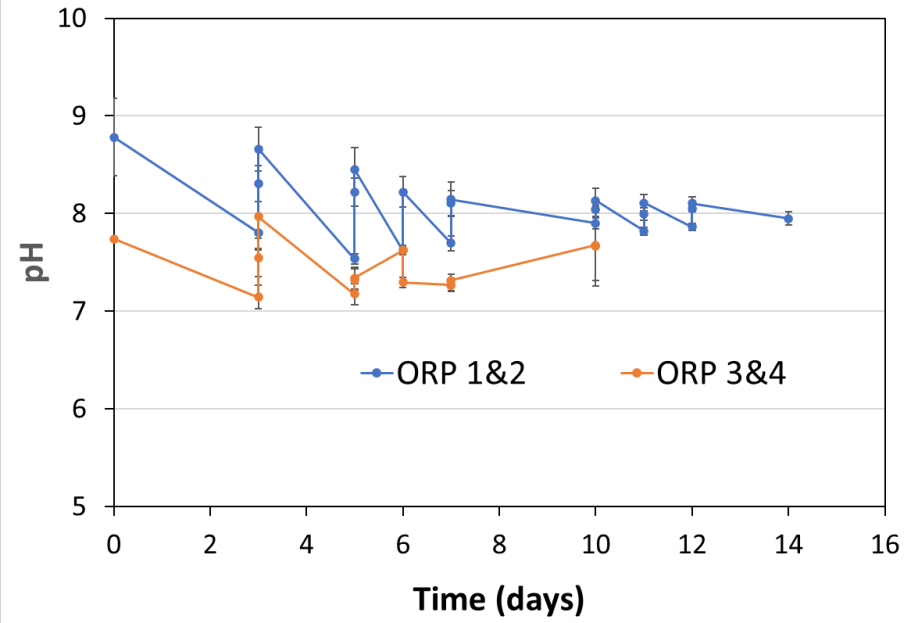

Exhibit 4.6.5. Average measured pH of ORP 1 and 2, and of 3 and 4, by run date. ORP 1 and 2 were fed with 10/1 CO_2/NH_3, and ORP 3 and 4 were fed with pure CO_2 and $NaNO_3$. The CO_2 flow rate to each pond was 0.15 L/min. Error bars represent the st. dev. (n = 2). With the exception of the start and end dates, pH measurements were taken three times daily (early morning, noon and late afternoon). The increase in pH during the course of any given day reflects CO_2 consumption by the algae as a result of photosynthesis.

Exhibit 4.6.6 depicts the culture density as a function of time. Note that only one cultivation/harvest cycle could be completed due to the onset of unseasonably poor weather. Consistent with the previously reported indoor PBR results (Task 5.1), increasing the CO_2/NH_3 mole ratio from 7 to 10 resulted in an improvement in the algae productivity averaged over the full duration of each experiment, albeit reliable comparisons are hampered by the changeable nature of the weather during the culturing period. Average productivity for ORP 1 and 2 amounted to 5.8 ± 0.6 $g/m^2/day$, representing a 12% improvement on the productivity obtained using the CO_2/NH_3 mole ratio of 7:1.

In the case of the reference ponds (ORP 3 and 4), the cultures underwent moderate growth for the first three days (**Exhibit 4.6.6**), after which the cultures crashed, evidenced by their brown appearance after 10 days (**Exhibit 4.6.7**). Microscopic examination revealed the cultures to be heavily contaminated with bacteria. This result highlights a potential benefit of maintaining a low concentration of free NH_3 in algae cultures, given that many invasive organisms such as rotifers and bacteria are inherently more sensitive to the toxic effects of NH_3 than are algae. Indeed, the addition of NH_3 to algae cultures has recently been suggested as a practical method of suppressing rotifers to ensure culture health.

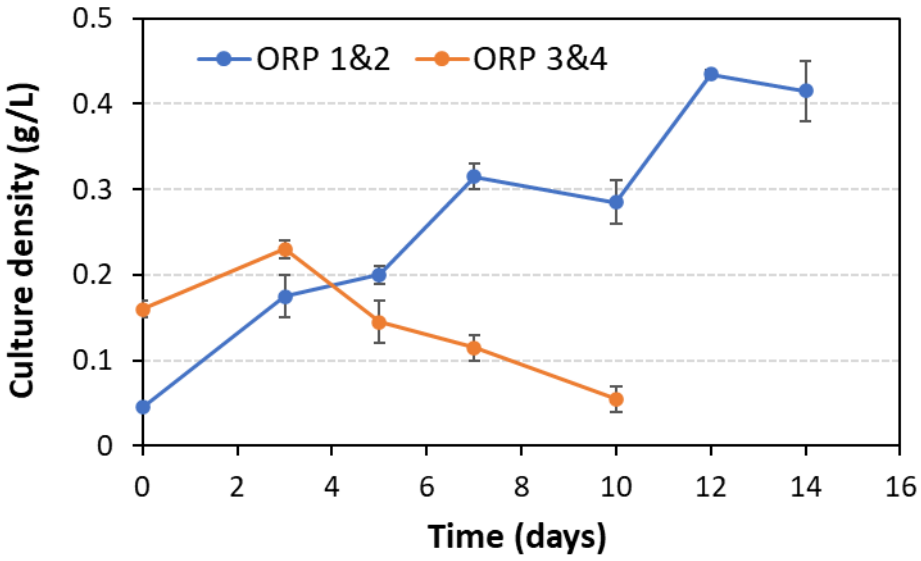

Exhibit 4.6.6. Culture density by run date: ORP 1 and 2 were fed with 10/1 CO_2/NH_3, and ORP 3 and 4 were fed with pure CO_2 and $NaNO_3$. The CO_2 flow rate to each pond was 0.15 L/min. Error bars represent the st. dev. (n = 2).

Exhibit 4.6.7. ORPs used for culturing experiments, 10 days after inoculation. Left: ORPs 1 and 2, fed with 10/1 CO_2/NH_3; right: ORPs 3 and 4, fed with pure CO_2 and $NaNO_3$; the cultures in ORPs 3 and 4 had crashed at this point. The CO_2 flow rate to each pond was 0.15 L/min.

Exhibit 4.6.8 shows the ammonium ion concentrations as analyzed by IC and the calculated free ammonia concentrations for experiments performed using a feed CO_2/NH_3 mole ratio of 10. From these results it is apparent that there was a gradual accumulation of NH_4^+ and free NH_3 in solution as culture cycle progressed, i.e., not all the NH_3 was consumed. However, the NH_3 concentration remained well below the safe limit of ~2 mM at all times, this being aided by the relatively low culture pH (<8.5).

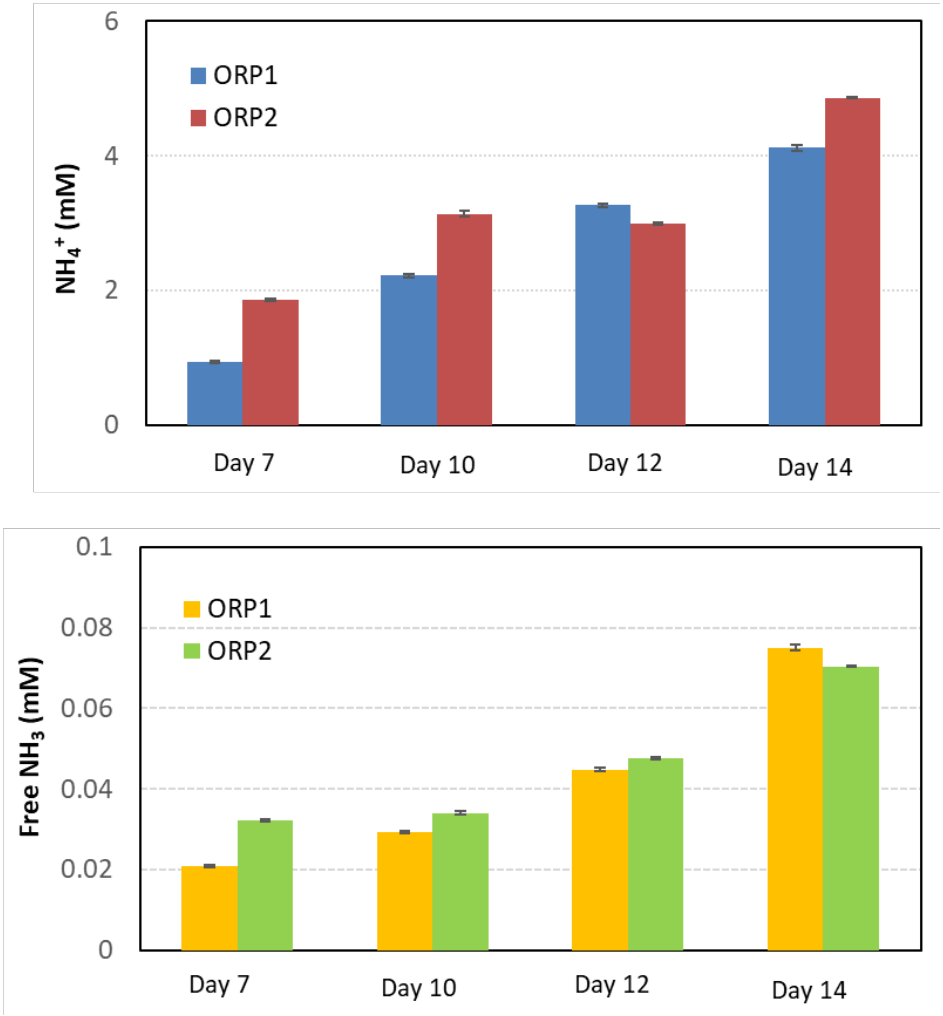

Exhibit 4.6.8. Top: Measured ammonium ion concentration during algae culturing in ORP 1 and 2. Bottom: Corresponding (calculated) free ammonia concentration. Feed CO_2/NH_3 ratio = 10. Error bars represent the st. dev. (n = 3).

Exhibit 4.6.9 summarizes the results of elemental analysis performed on the biomass from ORP 1 and 2, and the calculated NH_3 and CO_2 utilization efficiencies. Consistent with the results obtained from the indoor culturing experiments, the algae biomass is characterized by high protein and low ash content. At around 5 wt%, the ash content is higher than for indoor cultivation experiments (Task 5.1), although this is to be expected given the open nature of the ponds, and hence likely contamination form air-borne dust. Nevertheless, these results confirm the suitability of the biomass for use as a feedstock for the production of bioplastics or for use as animal feed, both of these uses benefiting from high protein and low ash contents. For the algae biomass produced using CO_2/NH_3 = 10, the esterifiable lipid profile was determined by means of simultaneous in situ transesterification and fatty acid methyl ester (FAME) extraction. Analysis of the FAME composition showed them to be almost exclusively polyunsaturated isomers of c-16 and c-18, in agreement with previous analyses [47]. Notably, the measured concentration of esterifiable lipids was <1%, much lower than the value previously reported by us for this organism (6.2 wt%) [47]. From this it can be concluded that the increased protein content of *Scenedesmus*

acutus grown using gaseous CO_2/NH_3 as the feed comes largely at the expense of decreased lipid content.

Exhibit 4.6.9. Elemental analysis of algae biomass harvested from ORPs and calculated CO_2 and NH_3 utilization efficiency (CO_2/NH_3 mole ratio = 10)

	C (%)	N (%)	Ash (%)	Protein (%)	CO_2 utilizn. (%)	NH_3 utilizn. (%)
ORP 1	51.95 ± 0.7	10.64 ± 0.06	5.20 ± 0.09	50.86 ± 0.29	13.1 ± 0.7	23.0 ± 1.1
ORP 2	50.57 ± 1.19	10.45 ± 0.17	5.19 ± 0.04	49.95 ± 0.80	10.3 ± 0.7	18.2 ± 1.0

As for **Exhibit 4.6.4**, the calculated NH_3 and CO_2 utilization efficiencies in **Exhibit 4.6.9** are based on 24 h/day supply of CO_2 and NH_3 (as used in the experiment). If the calculation is based on daylight hours only, average efficiencies correspond to ~24% for CO_2 and ~43% for NH_3, i.e., approximately double the values reported in **Exhibit 4.6.9**. The values for NH_3 utilization are higher than those for the $CO_2/NH_3 = 7$ experiment, reflecting the stronger growth of the cultures at the higher CO_2/NH_3 ratio and the higher amount of N incorporated in the biomass. In contrast the CO_2 utilization values are slightly lower as a consequence of the greater amount of CO_2 fed. As noted above, higher utilization efficiencies should be possible if a lower CO_2/NH_3 feed rate is used, at no detriment to the algae productivity (i.e., by better matching the feed rate to the growth rate of the algae).

Based on the amount of ammonium ions and free ammonia in solution (**Exhibit 4.6.8**) and the amount of biomass produced, coupled with its N content (**Exhibit 4.6.9**), the amount of ammonia that was lost from the ORPs during algae cultivation was estimated according to the equation:

$$N_{fed} = N_{biomass} + N_{soln} + N_{atmos} \quad \text{(Eqn. 5)}$$

where N_{fed} is the amount of N fed (as NH_3), $N_{biomass}$ is the amount of N captured in the algal biomass, N_{soln} is the amount of N accumulated in solution as NH_4^+ and NH_3, and N_{atmos} is the amount of NH_3 lost to the atmosphere.

In eqn. 5, the difference between the amount of N fed as ammonia and the amount of N captured in the biomass, plus N present in solution, is assumed to correspond to ammonia released to the atmosphere. **Exhibit 4.6.10** presents the results of this calculation for ORP 1 and 2, the amount of NH_3 in each category being expressed as a percentage of the NH_3 fed. In both cases, the percentage of NH_3 released from the ORPs was substantial, corresponding to 46.1% and 45.4%, respectively. These high NH_3 losses can be attributed to overfeeding, i.e., the CO_2/NH_3 feed rate to the ORPs was too high. Clearly, such NH_3 losses would be unacceptable from an environmental and economic standpoint, and they highlight the need for a control strategy that balances the CO_2/NH_3 supply with the algae growth rate. One such strategy would require real time monitoring of the culture for NH_4^+ ion concentration and pH, such that the concentration of free NH_3 could be tracked and adjustments made to the rate of CO_2/NH_3 delivery as necessary.

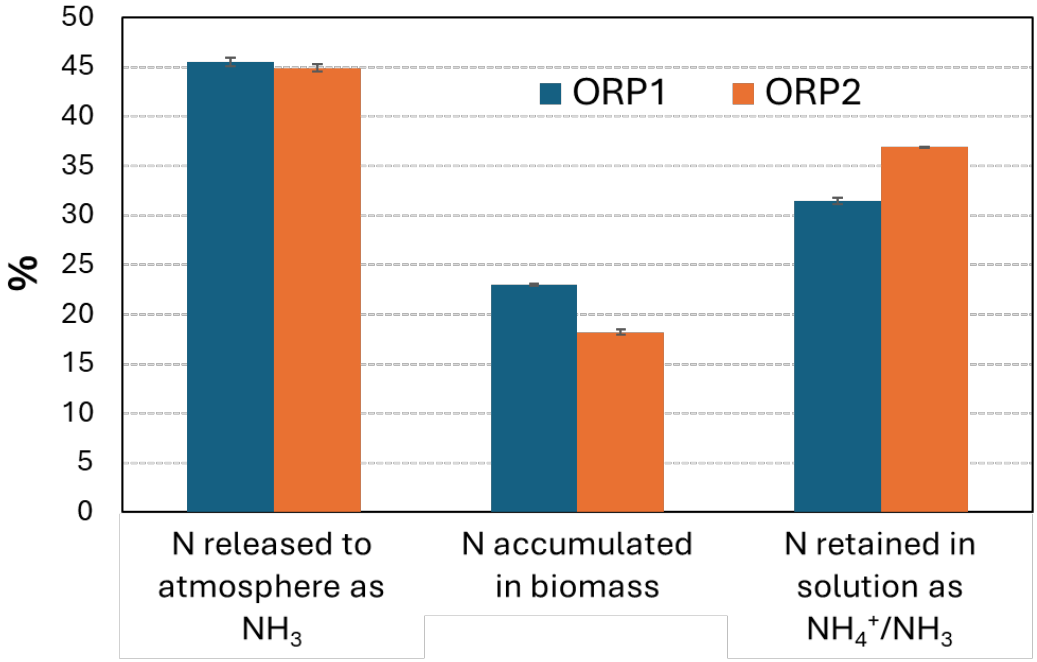

Exhibit 4.6.10. Calculated percentage of NH_3 released to atmosphere, accumulated in biomass and retained in solution for ORP 1 and ORP 2 during culturing at CO_2/NH_3 = 10. Error bars represent the st. dev. (n = 3).

4.6.4. Summary

Scenedesmus acutus was grown in open ponds using CO_2 and NH_3 supplied from gas cylinders at CO_2/NH_3 mole ratios of 7 and 10, the gas mixture employed acting as a surrogate for the output from a CO_2 scrubbing system using aqueous ammonia. Compared to *Scenedesmus acutus* grown in open ponds using gaseous CO_2 and $NaNO_3$ as the N-source, the ponds supplied with gaseous CO_2 and NH_3 displayed consistently higher productivity, in agreement with previously reported experiments conducted in indoor photobioreactors. The resulting biomass possessed a high protein and low ash content, rendering it particularly suitable for use as a bioplastic feedstock.

Ion chromatography revealed a gradual accumulation of NH_4^+ and free NH_3 in solution as culturing progressed, i.e., not all the NH_3 fed was consumed. However, the NH_3 concentration remained below levels toxic to the algae at all times, this being aided by the relatively low culture pH which stabilized at values of ~7.5-8.5, ensuring that the added NH_3 was mainly present as NH_4^+ ions. Depending on the culturing conditions and CO_2/NH_3 mole ratio, CO_2 utilization ranged up to 15.8% and NH_3 utilization to 23.0%. These rather low values reflect the fact that CO_2/NH_3 feed rate used was too high, suggesting that higher utilization efficiencies should be possible if the feed rate is better matched to the growth rate of the algae. This overfeeding also resulted in a substantial release of NH_3 from the ORPs (~45%), a finding that highlights the need for a control strategy that closely balances the CO_2/NH_3 supply with the algae growth rate.

4.7 Long-term Campaign, Algae Production

4.7.1. Introduction

The goal of this task was to demonstrate *Scenedesmus acutus* (UTEX B72) production using open raceway ponds (ORPs, 1100 L) fed with gaseous CO_2 and NH_3 from the membrane absorber

system. Experiments were performed with the objective of (i) confirming that good algae productivity can be obtained outdoors using NH_3 as a nutrient over a sustained period, (ii) assessing the degree of NH_3 utilization by the algae culture and (iii) determining the composition of the resulting algae biomass.

4.7.2. Experimental

To provide sufficient algae biomass for the inoculation of the ORPs, indoor culturing was initiated on agar plates and subsequently in 800 mL photobioreactors (PBRs). Culturing was then scaled up to 10 L PBRs housed indoors, the resulting biomass in turn providing inoculum for 30 x 10 L reactors housed in a greenhouse and illuminated by natural light. In this manner, the algae were gradually acclimated to outdoor conditions. In addition, ammonium carbonate was used in the culture medium (BG-11, without $NaNO_3$), in order to acclimate the algae to the use of ammonium ions as the nitrogen source.

Outdoor cultivation of *Scenedesmus acutus* (UTEX B72) was carried out in 4 x 1100 L fiberglass open raceway ponds (ORPs, Algae Lab Systems). One of the ORPs (ORP 1) was monitored continuously for pH and temperature (Algae Lab Systems probe coupled to an ALS-SPARC-2 wireless monitoring and control system), while additional measurements were made 3 times per day (morning, midday and late afternoon) for NH_4^+ concentration (Vernier Go Direct® ammonium ion-selective electrode) and ambient photosynthetically active radiation (PAR). Measurements of pH, temperature and NH_4^+ concentration were also performed manually 3 times daily for the other ORPs. In addition, samples of the culture were taken from each ORP for dry mass determination and UV-vis spectrophotometry measurements (absorption at 680 nm) every weekday. Samples were also taken from ORP 1 every weekday for the determination of ammonium ion concentration using ion chromatography. Dissolved NH_3 concentrations were calculated from measured NH_4^+ concentrations (and the corresponding pH and temperature values) as described in the literature.

Unless otherwise stated, the gas mixture fed to ORPs 1 and 2 from the membrane absorber system corresponded to 10% NH_3, 15% CO_2 and 75% H_2O, the flow rate to each ORP being varied between 100 and 300 ml/min. In order to control the CO_2:NH_3 ratio fed to the ponds, ORPs 1 and 2 were provided with a second continuous feed of 100% CO_2. This was necessitated by the fact that in initial operation of the membrane absorber system (during the period when the weather was suitable for algae cultivation) it proved challenging to attain CO_2:NH_3 mole ratios of much greater than 1, i.e., far below the ratio of ca. 7 required on the basis of typical algae composition; consequently, the addition of significant supplemental CO_2 was required. As a precaution, the initial flow rate of CO_2 was set to a value of 750 ml/min, giving an overall CO_2:NH_3 mole ratio of ≥ 25. This rather higher value was chosen in order to prevent excessive basification of the test ponds in the event of an operational upset of the membrane absorber system (that might result in excessive supply of NH_3). In later experiments the CO_2 flow rate was decreased to assess the effect of the reduced flow on the CO_2 utilization efficiency. **Exhibit 4.7.1** summarizes the gas flow rates to ORPs 1 and 2 as a function of time and shows the dates of harvests and of nitrogen supplementation using $(NH_4)_2CO_3$ (see below for a discussion of the latter).

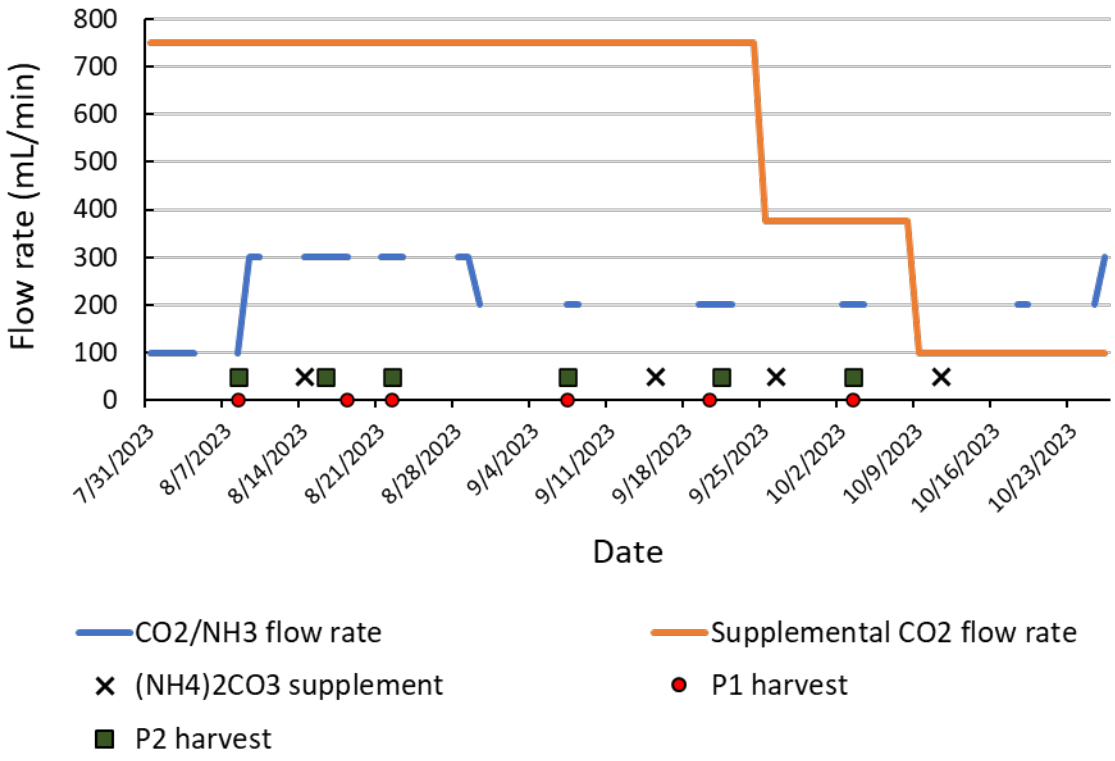

Exhibit 4.7.1. Gas flow rates, $(NH_4)_2CO_3$ supplementation and harvests vs. time for ORPs 1 and 2

ORPs 3 and 4 were operated as reference ponds, being fed continuously with pure CO_2 (750 ml/min). $NaNO_3$ functioned as the N-source in ORPs 3 and 4, other essential nutrients in ORPs 1-4 being supplied according to the standard BG-11 nutrient recipe.
Experiments were performed for multiple growth/harvest cycles, ≥50% of the algae being removed at each harvest. Harvesting was performed when the algae concentration reached a minimum value of ~0.5 g/L, the concentration after harvesting being ~0.2 g/L. In this manner, the cultures remained in the log phase of growth. After each harvest, the nutrients and water were replenished, the water being sterilized using a UV system.

4.7.3. Results and Discussion

Algae Cultivation

Exhibit 4.7.2 displays the culture density as a function of time for the four ORPs. Somewhat weak growth was observed for ORPs 1-3 immediately after inoculation of the ponds, this potentially reflecting the acclimatization of the cultures to outdoor conditions. Thereafter, all of the cultures showed strong growth, the only exception being ORP 4, which for unknown reasons displayed negative growth during the second harvest cycle, but which then recovered. **Exhibits 4.7.3** and **4.7.4** collect the calculated algae productivity for the four ORPs based on the complete dataset. For ORPs 3 and 4, the dataset spans the period between 7/31/23 and 10/27/23 (88 days). In the case of ORPs 1 and 2, harvest cycle #1 was excluded from the dataset, because the membrane absorber system supplying NH_3 to the cultures began operation after the cycle had commenced. Consequently, the dataset for ORPs 1 and 2 corresponds to a period of 80 days. **Exhibit 4.7.3** expresses the productivity of the ponds on an areal basis ($g/m^2/day$), while for completeness,

Exhibit 4.7.4 shows the corresponding data expressed on a volumetric basis (g/L/day). As shown, algae productivity ranged up to a maximum of 0.046 g/L/day, corresponding to a maximum areal productivity of slightly less than 8 g/m^2/day. Note that the foregoing volumetric productivity is significantly lower than that previously reported by us in indoor experiments conducted in simple tubular photobioreactors (~0.18 g/L/day). This difference can be ascribed to a number of factors, including the longer photoperiod for the indoor experiments (24 h/day), the superior gas/liquid mixing in the photobioreactors, as well as the shorter path length for the incident light, the lack of temperature fluctuations, and the absence of invasive organisms such as algae grazers.

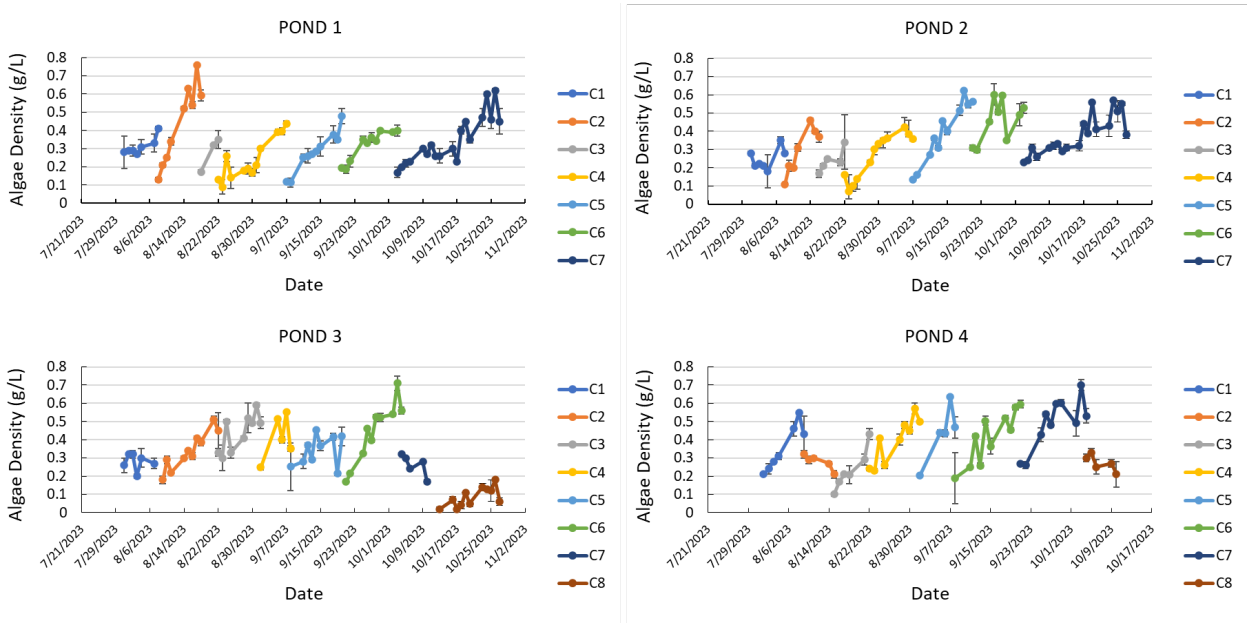

Exhibit 4.7.2. Culture density for ORPs 1-4 as a function of time. Error bars represent the st. dev. (n = 3). In each figure key, C1, C2, etc., refer to the harvest cycle (1st, 2nd, etc.).

According to the data in **Exhibit 4.7.3**, average algae productivity followed the order ORP 1 (4.6 ± 2.6 g/m^2/day) > ORP 2 (3.4 ± 1.9 g/m^2/day) > ORP 4 (3.1 ± 4.4 g/m^2/day) > ORP 3 (1.2 ± 3.7 g/m^2/day). Noticeably, there was some variability between the two sets of ponds. In the case of ORPs 1 and 2, this may reflect the fact that it proved challenging to ensure that both ponds received exactly the same gas flow from the membrane absorber system. In the case of ORPs 3 and 4, the latter pond consistently outperformed the former; this is at least in part attributable to the presence of rotifers that were consistently observed in ORP 3 (this is discussed further below in relation to **Exhibit 4.7.9**).

Overall, the algae growth rates reported above are lower than expected. This can be partly attributed to the fact that culturing continued well into October, at which point the weather was far from optimal. Indeed, the maximum productivity for ORPs 1 and 2 was observed in the month of August. Additionally, in the case of ORPs 1 and 2, algae growth was almost certainly nitrogen-limited during periods when the membrane absorber system was inoperative, such as during weekends. This is discussed further below in relation to **Exhibits 4.7.5** and **4.7.6**.

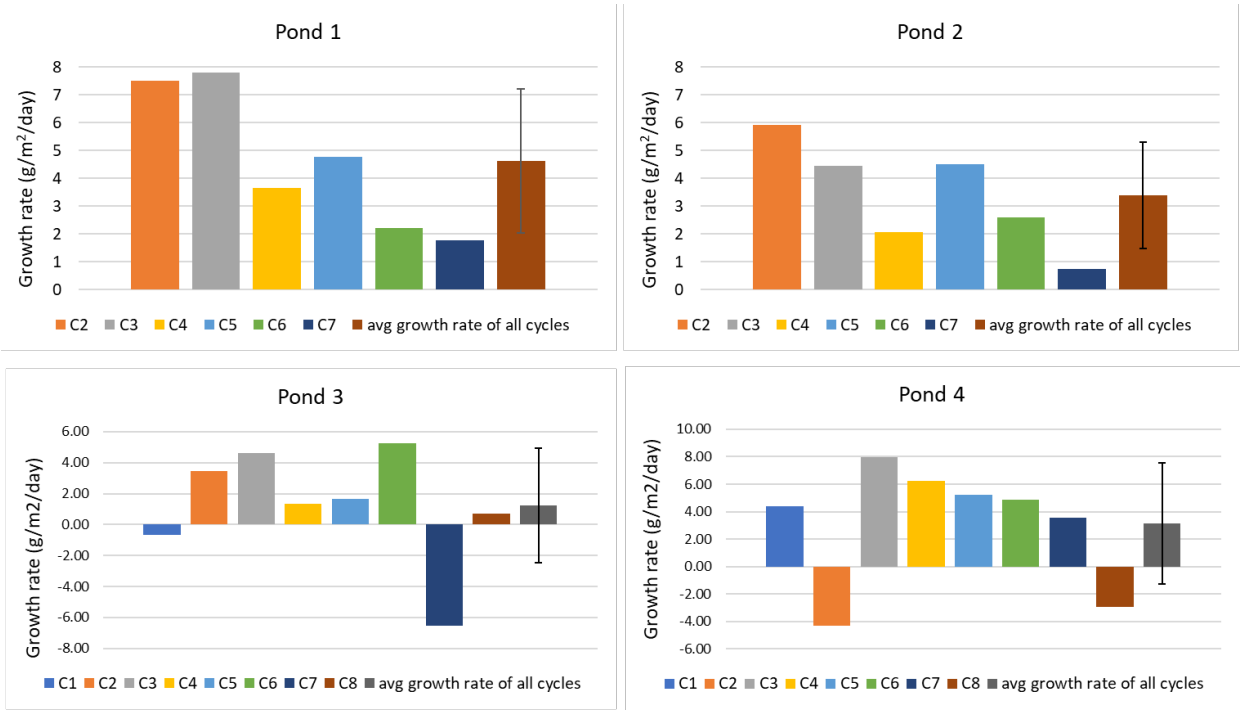

Exhibit 4.7.3. Areal algae growth rate for ORPs 1-4 by harvest cycle, based on complete dataset. Error bars represent the st. dev. (n = 6 for ORP 1 and 2, and n = 8 for ORP 3 and 4)

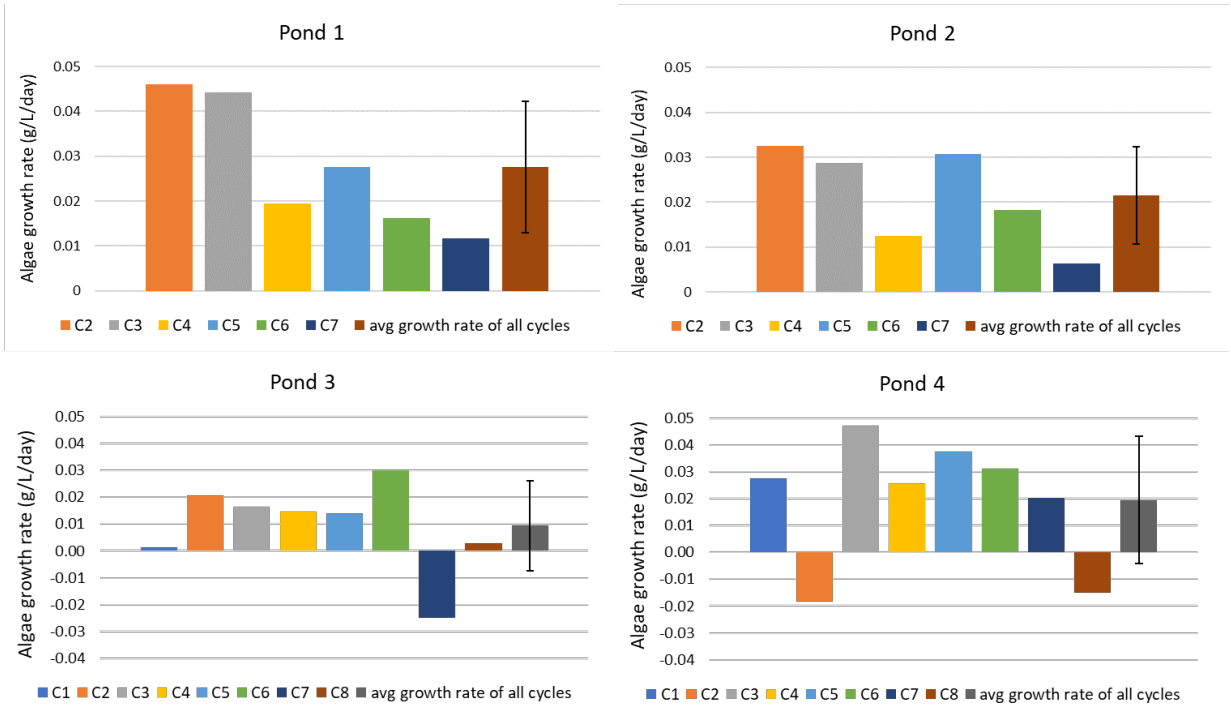

Exhibit 4.7.4. Volumetric algae growth rate for ORPs 1-4 by harvest cycle, based on complete dataset. Error bars represent the st. dev. (n = 6 for ORP 1 and 2, and n = 8 for ORP 3 and 4)

Due to the discontinuous operation of the membrane absorber system (no operation during weekends and some weekdays), the cultures in ORPs 1 and 2 were at times nitrogen-depleted. To

compensate for this, on 4 occasions (corresponding to weekdays, see **Exhibit 4.7.1**), supplemental nitrogen was added to these ponds in the form of $(NH_4)_2CO_3$ to maintain culture health. However, it was observed that during weekends, NH_4^+ concentrations in ORPs 1 and 2 typically dropped to low values due to ammonium ion consumption, likely limiting algae growth. For this reason, algae productivity was also calculated based on the periods when the membrane absorber was operational, excluding all other data points. In this manner, the comparison of algae productivity in ORPs 1 and 2 with the reference ORPs (3 and 4) should be fairer, given that none of the ponds should be N-limited in these periods. For the purposes of the calculation, any day on which the absorber system was operational for any amount of time (typically 3 - 5 h), was considered to represent one full day (24 h) of algae growth. The results of these calculations are depicted in **Exhibit 4.7.5**. Somewhat counter-intuitively, **Exhibit 4.7.5** shows that the values for algae growth in ORPs 1 and 2 calculated according to this methodology are actually lower than the values calculated across the whole dataset, as shown in **Exhibit 4.7.4**. This finding can be explained in terms of the typical lag effects observed in algae growth. Specifically, when feeding gaseous NH_3 to a N-depleted culture, depending on the amount of NH_3 fed each day, it may take several days for the dissolved N content to reach optimum levels and for the organism, having become acclimated to low N levels, to re-adjust to the new conditions. This results in a lag effect, with the consequence that growth rates calculated over the whole culturing period are more representative than those calculated for the relatively brief periods of time (1-4 days) corresponding to consecutive days of membrane absorber operation.

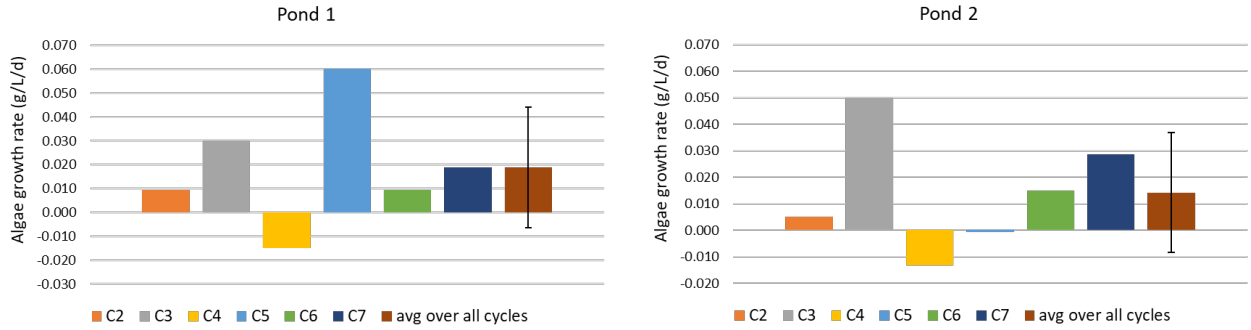

Exhibit 4.7.5. Volumetric algae growth rate for ORPs 1-4 by harvest cycle, based on periods when membrane absorber unit was operational. Error bars represent the st. dev. (n = 7)

Exhibit 4.7.6 summarizes the temperature and pH of ORPs 1 and 3 on a daily basis, with the exception of weekends; these plots are representative of the corresponding datasets for ORPs 2 and 4, respectively. In the case of ORP 3, relatively little variation in pH was observed, values generally spanning the range 7 – 8. However, in the case of ORP 1, the pH trace tends to be cyclical due to the periodic nature of membrane absorber operation. Specifically, the pH tended to decrease during the weekends (due to the consumption of NH_4^+/NH_3), sometimes to quite low values (~5.5 – 6.5), and then increased the following Monday when the membrane absorber system was restarted. This supports the inference that algae growth was likely nitrogen-limited during at least some portion of the weekends.

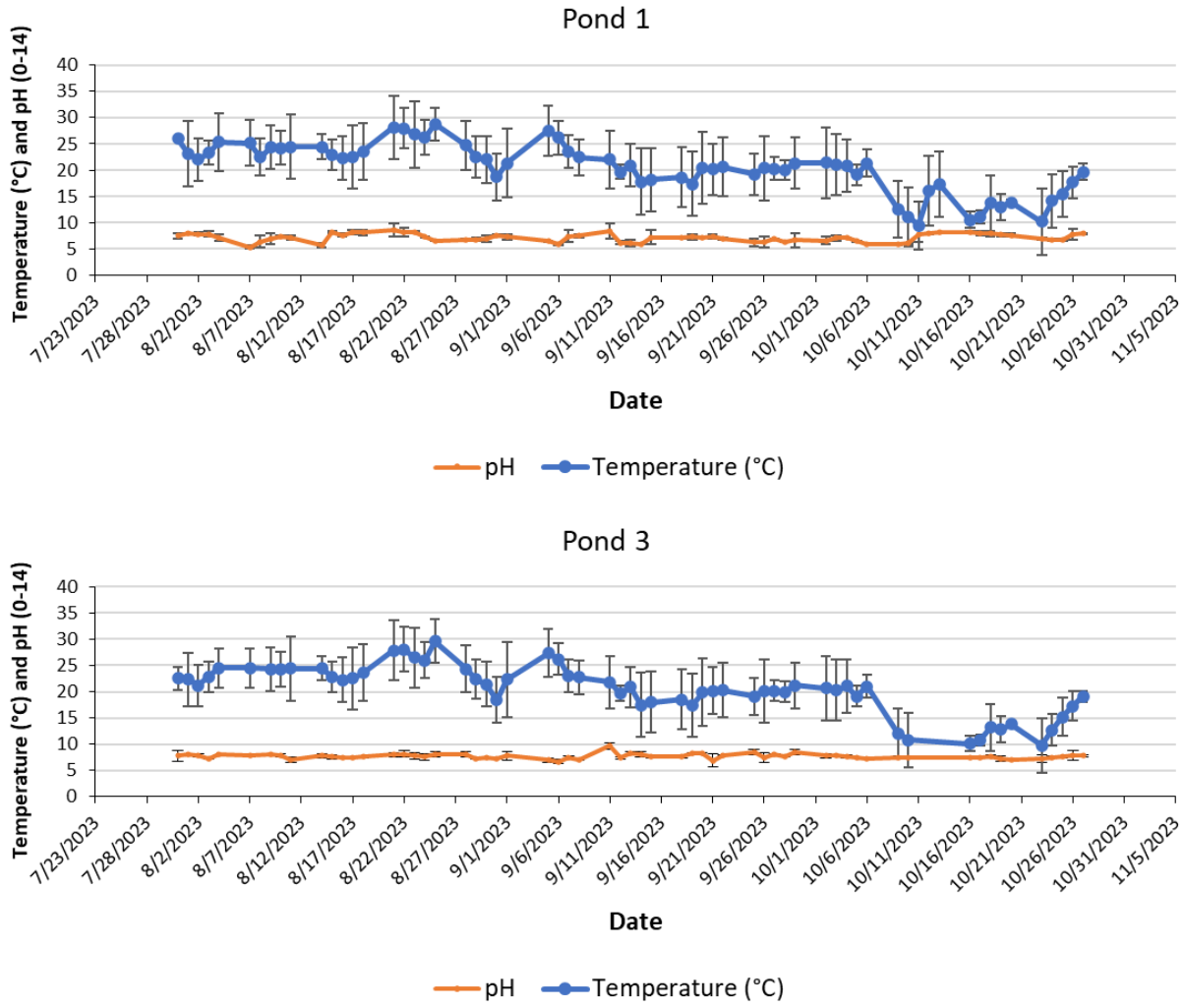

Exhibit 4.7.6. Measured pH and temperature for ORPs 1 and 3 as a function of time. Datapoints represent the average of three measurements performed daily at 9 am, 12 pm and 4 pm. Error bars represent the st. dev. (n = 3)

For completeness, **Exhibit 4.7.7** collects the measured PAR values, averaged for each day of culturing. Taken together with the temperature plots in **Exhibit 4.7.6**, the PAR data reflect the relatively good culturing conditions experienced in August, September and early October. After 10/6/23, conditions deteriorated (lower temperatures and PAR values), resulting in ORPs 3 and 4 crashing almost immediately (see **Exhibit 4.7.2**). In contrast, ORPs 1 and 2 continued to show moderate growth until 10/26/23.

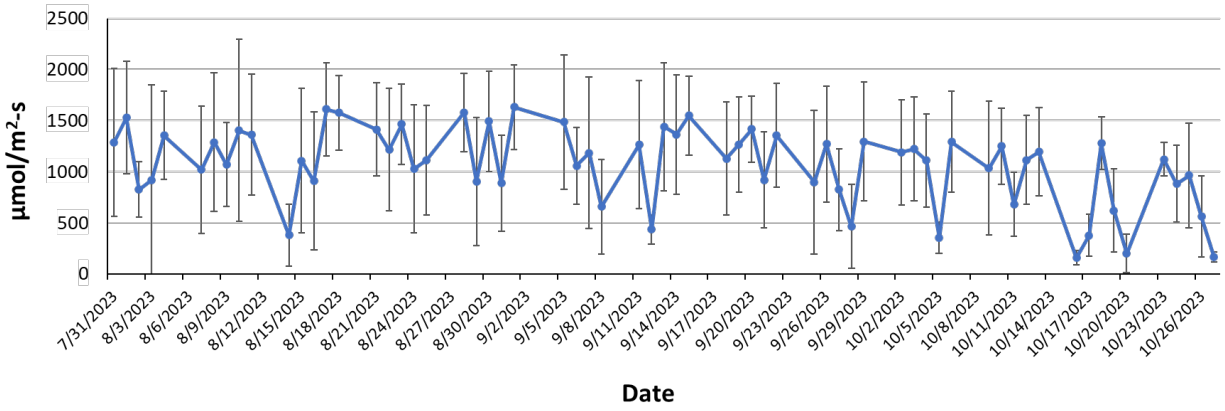

Exhibit 4.7.7. Measured PAR as a function of time. Data points represent the average of three readings taken each day at 9 am, 12 pm and 4 pm. Error bars represent the st. dev. (n = 3).

As noted above, ammonium ion concentrations were tracked in ORP 1 on a daily basis using ion chromatography (IC), while readings were also taken directly using an ammonium ion-selective electrode (ISE) in all of the ponds. While the latter represents a faster and more convenient method of determining NH_4^+ concentrations, it was found to give very inconsistent results; the reasons for this are not fully understood but are likely related to the charged nature of the algae cells and the high solids content of the algae cultures. Consequently, the resulting data are considered unreliable and are therefore not discussed further here. **Exhibit 4.7.8** shows the [NH_4^+] data obtained using IC for ORP 1, and the corresponding calculated NH_3 concentrations.

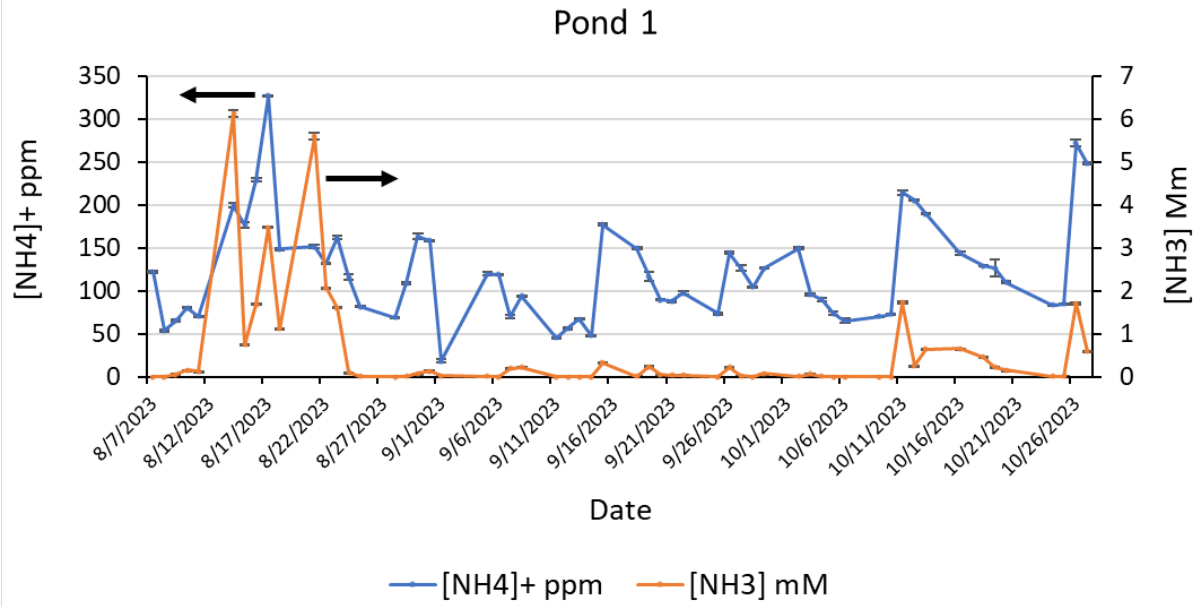

Exhibit 4.7.8. Measured NH_4^+ and calculated NH_3 concentrations in ORPs 1 and 2 as a function of time. NH_4^+ concentrations were determined by means of ion chromatography. Error bars represent the st. dev. (n = 3)

According to **Exhibit 4.7.8**, on three occasions in August the concentration of free NH_3 in ORP 1 spiked, reaching a maximum value of 6 mM on 8/14/23. These concentration spikes corresponded to periods when the NH_4^+ concentration reached rather high values (~250-400 ppm), accompanied

by elevated pH values (~9). As outlined for Task 5, the literature suggests that the threshold for NH_3 toxicity in some species of green algae is around 2 mM, although higher threshold concentrations have been reported for other green algae. However, in the present case the overall health of the culture was not seriously affected, as indicated by the strong growth observed in this period (see **Exhibit 4.7.2**). Thereafter, the NH_4^+ concentration remained at a lower level (<250 ppm), as did that of the free NH_3 (<2 mM).

It is also worth noting that the combined NH_4^+ and NH_3 concentration in ORP 1 dipped below 50 ppm on several occasions, corresponding to periods when the membrane absorber unit had been out of operation for several days. This depletion of dissolved nitrogen is likely to have impaired algae growth during these periods.

In order to monitor the health of the cultures, and in particular to check for the presence of rotifers (algae grazers), samples were taken for optical microscopy on a regular basis, hemocytometry being used to quantify rotifer numbers. The results of these measurements are summarized in **Exhibit 4.7.9**. As shown, the occurrence of rotifers in ORPs 1 and 2 was sporadic, rotifer numbers being fairly low relative to ORPs 3 and 4. In the case of ORP 3, rotifer infestations were common, the frequency of such events generally increasing in the second half of the experimental campaign. The numbers of rotifers detected during these infestations were also significantly higher than those in ORPs 1 and 2. While infestations were less common in ORP 4 than ORP 3, rotifer numbers again tended to increase sharply towards the end of the campaign. These findings are consistent with the known toxicity of NH_3 towards rotifers such as *Brachionus*. Indeed, it has been reported that *Brachionus* rotifer reproduction is inhibited at NH_3 concentrations of 0.14 mM, and complete mortality is observed at concentrations above 0.29 mM [48]. Moreover, exposure of algae cultures to NH_3 has recently been demonstrated as a practical method of suppressing rotifers to ensure culture health.

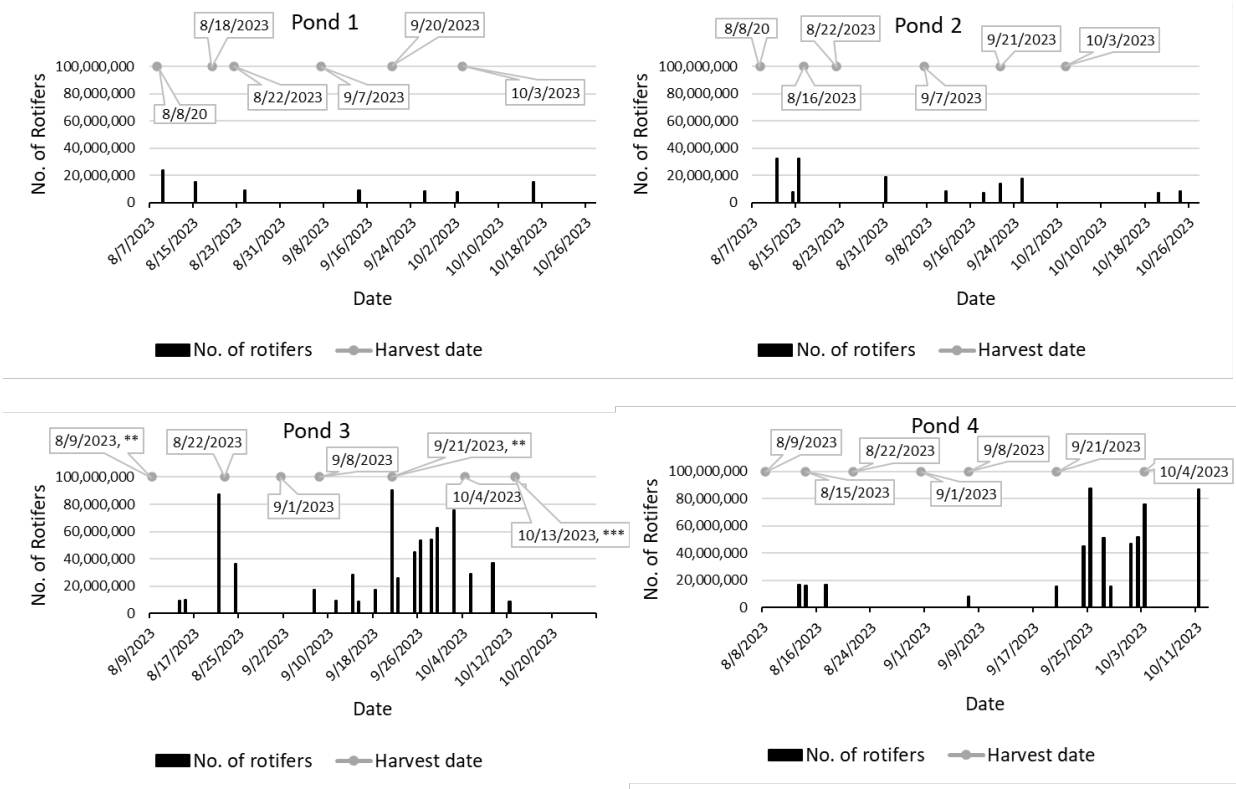

Exhibit 4.7.9. Rotifer populations per pond estimated by hemocytometry for ORPs 1-4 as a function of time. Harvest dates are shown in the text boxes.

Exhibit 4.7.10. Elemental analysis of algae biomass harvested from ORPs

	C (%)	N (%)	Ash (%)	Protein (%)
2nd harvest cycle				
ORP 2	48.1 ± 0.4	9.5 ± 0.1	6.0 ± 0.1	45.2 ± 0.1
ORP 4	48.6 ± 0.6	8.5 ± 0.1	n.d.	40.7 ± 0.1
3rd harvest cycle				
ORP 1	50.2 ± 0.5	9.7 ± 0.1	5.9 ± 0.1	46.6 ± 0.1
ORP 2	48.4 ± 0.5	9.2 ± 0.1	7.1 ± 0.2	43.9 ± 0.1
ORP 3	50.9 ± 0.4	8.6 ± 0.2	5.5 ± 0.1	41.1 ± 0.2
4th harvest cycle				
ORP 1	50.5 ± 0.1	9.2 ± 0.0	5.0 ± 0.1	43.9 ± 0.0
ORP 2	47.9 ± 0.2	9.0 ± 0.1	6.3 ± 0.1	42.9 ± 0.1
ORP 4	51.8 ± 0.1	9.1 ± 0.0	6.0 ± 0.1	43.6 ± 0.0
5th harvest cycle				
ORP 1	50.2 ± 0.3	9.5 ± 0.0	6.5 ± 0.1	45.2 ± 0.0
ORP 2	50.4 ± 0.3	9.9 ± 0.2	6.9 ± 0.1	47.3 ± 0.2

Shown in **Exhibit 4.7.10** are the results of elemental analysis performed on algae biomass harvested from the ORPs. No significant differences in carbon or ash content were observed between biomass harvested from the test and reference ponds. The ash content was consistently low and comparable to our previously reported values for outdoor cultivation experiments (Task 5.2), albeit it was higher than the ash content for the corresponding indoor cultivation experiments (Task 5.1). This is to be expected, given the open nature of the ponds and their likely contamination over time with airborne dust. The calculated protein content of the algae harvested from ORPs 1 and 2 (42.9-47.3%) is also similar to values observed previously during outdoor cultivation in this project (Task 5.2), but lower than that observed for indoor experiments (Task 5.1). This may be due to the higher continuous concentration of ammonium ions present in the indoor experiments, and/or the fact that such indoor conditions represent optimal culturing conditions generally.

NH_3 and CO_2 Utilization

Based on the C and N content of the biomass and the algae productivity, the CO_2 and NH_3 utilization was calculated according to Eqns. 1 and 2:

$$\eta_{CO2} = \frac{100 * m_{SA} * X_C}{m_{CO2}} \quad (1)$$

$$\eta_{NH3} = \frac{100 * m_{SA} * X_N}{m_{NH3}} \quad (2)$$

ηCO_2 is the $\%CO_2$ utilization, m_{SA} is the mass of algae produced, X_C is the C fraction in the algae, and mCO_2 is the mass of CO_2 fed. ηNH_3 is the $\%NH_3$ utilization, X_N is the N fraction in the algae, and mNH_3 is the mass of NH_3 fed. **Exhibits 4.7.11** and **4.7.12** report the calculated NH_3 and CO_2 utilization by harvest cycle, as well as the values averaged over all of the dataset. Note that for the two sets of calculations, cycle #1 data for ORP 1 and 2 was not included in utilization calculations since absorber operation only commenced during this harvest cycle.

Considering NH_3 utilization (**Exhibit 4.7.11**), values ranged from 30% - 98% by harvest cycle, the value for ORPs 1 and 2 averaged over the whole dataset amounting to 61 ± 2.4% (n = 2). This is significantly higher than the values reported for outdoor culturing reported in Task 5.2 (maximum of 23.0 ± 1.1%) and mainly reflects the higher amounts of NH_3 provided to the cultures in Task 5.2. Lesser contributing factors likely include the higher algae growth rates typically observed in Task 11.1 (due to better weather) and the higher effective CO_2:NH_3 ratios employed in Task 11.1 (increasing this ratio tends to lower the pH of the culture, thereby shifting the equilibrium between NH_4OH and NH_3 in favor of the former; this, in turn, should result in decreased NH_3 emissions to the atmosphere).

Periods of high NH_3 utilization corresponded to harvest cycles when algae growth was strongest. It should be noted that as shown in **Exhibit 4.7.1**, $(NH_4)_2CO_3$ supplementation was used on 4 occasions to maintain culture health (due to discontinuous nature of membrane absorber operation); this may have had the effect of depressing the utilization of NH_3 supplied from the membrane absorber when the absorber was re-started, suggesting that higher levels of NH_3 utilization should be possible.

In the case of CO_2 utilization (**Exhibit 4.7.12)**, it can be seen that CO_2 utilization efficiency was generally very low (< 2%). This was expected, given that emphasis in this study was placed on ensuring acceptable levels of NH_3 utilization. For this reason, high supplemental CO_2 flows were used, supplemental CO_2 being necessary in view of the typically low CO_2/NH_3 ratio (~1) provided by the membrane absorber during this phase of its operation in the project. Moreover, CO_2 was supplied 24 h/day, rather than simply during daylight hours, and, as discussed above, the discontinuous nature of membrane absorber operation limited algae productivity (i.e., algae productivity was nitrogen-limited during weekends) and therefore limited the utilization of the supplied CO_2. Supplemental CO_2 flow was decreased during harvest cycles #6 and #7 (from 750 ml/min to 375 ml/min during cycle 6 and then to 100 ml/min at the start of cycle #7); however, expected improvements in CO_2 utilization were largely off-set by lower algae productivity resulting from deteriorating weather conditions. In common with the superior productivity of ORPs 1 and 2 relative to the reference ponds, the former showed higher CO_2 utilization than the latter. It is also worth noting that in earlier work in this project, CO_2 utilization of up to 16% was achieved in ORPs when co-feeding CO_2 and NH_3 under non-optimized conditions. This indicates that higher CO_2 utilization is possible, providing that the supply of CO_2 is balanced with that of NH_3 and with the algae growth rate. Indeed, bearing in mind that a high degree of NH_3 utilization was obtained in this study, it follows that good CO_2 utilization efficiencies should be possible if the CO_2 is provided at a feed rate closer to that required in solution for the *ca.* CO_2/NH_3 mole ratio of 7 indicated by typical algae composition.

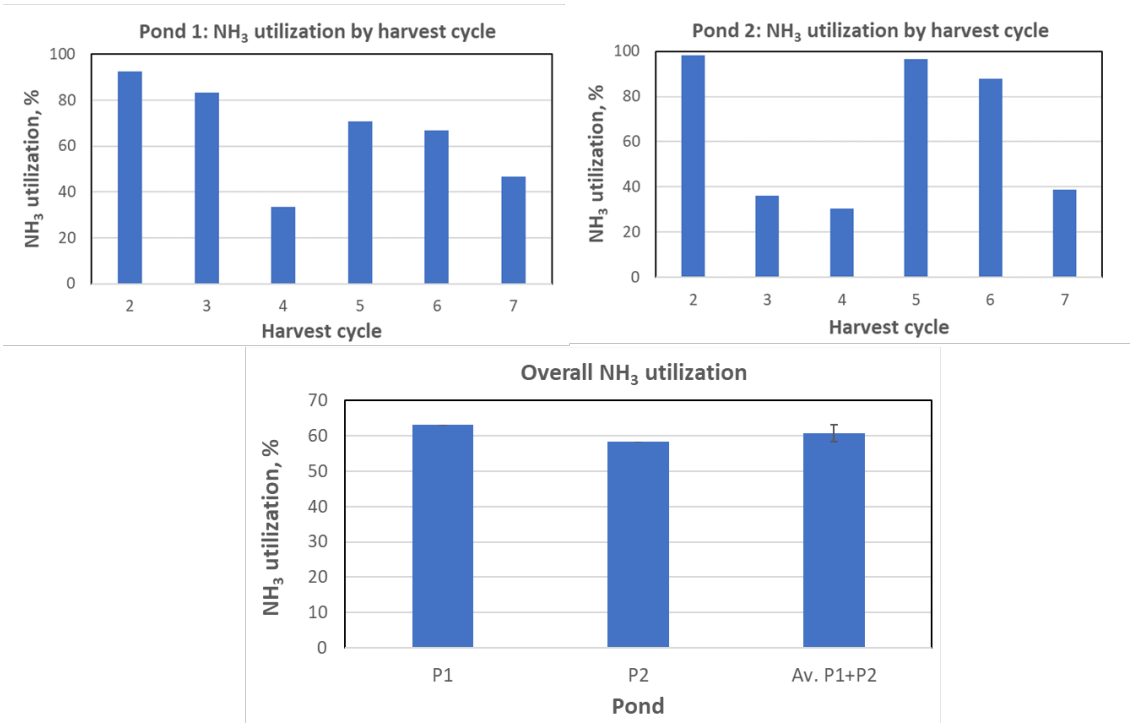

Exhibit 4.7.11. NH_3 utilization by harvest cycle for ORP 1 and 2 and corresponding values averaged over whole dataset. The error bar represents the st. dev. for the average of P1+P2 (n = 2).

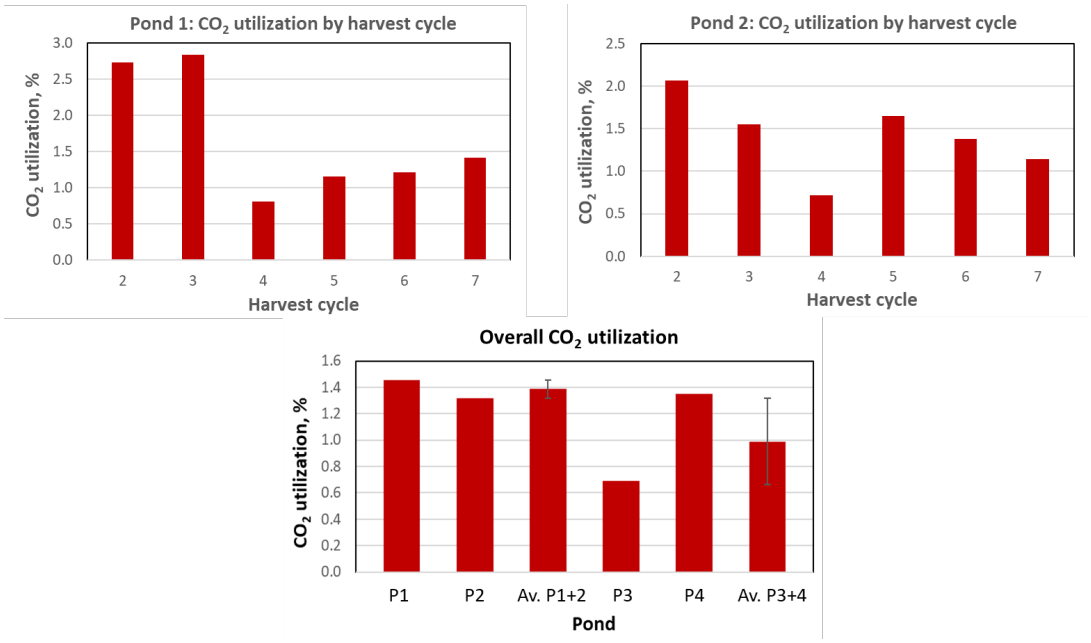

Exhibit 4.7.12. CO_2 utilization by harvest cycle for ORPs 1-2 and corresponding values averaged over whole dataset for ORPs 1-4. Error bars represent the st. dev. (n = 2).

4.7.4. Summary

In conclusion, the productivity of the test ponds (ORPs 1 and 2), when averaged over the whole dataset (80 days), exceeded that of the reference ponds (ORPs 3 and 4), validating our hypothesis concerning the benefits of using CO_2/NH_3 for algae culturing. Not only were algae growth rates higher in the test ponds, the algae cultures proved more robust with respect to the reference ponds. This can be attributed, in part at least, to the suppression of rotifers in the test ponds, resulting from the presence of free NH_3.

NH_3 utilization averaged 61% for ORPs 1 and 2 and higher values can be anticipated with continuous membrane absorber operation (negating the need for $(NH_4)_2CO_3$ supplementation). This is significantly higher than the values reported for outdoor culturing reported in Task 5.2 (maximum of $23.0 \pm 1.1\%$) and mainly reflects the higher amounts of NH_3 provided to the cultures in Task 5.2.

Owing to the high supplemental CO_2 flows used, CO_2 utilization efficiencies were very low in all of the ponds (< 2%). This was expected, given that emphasis in this study was placed on ensuring acceptable levels of NH_3 utilization. Moreover, the discontinuous nature of membrane absorber operation likely limited algae productivity in ORPs 1 and 2. Although the supplemental CO_2 flow was decreased during harvest cycles 6 and 7, expected improvements in CO_2 utilization were largely negated by lower algae productivity resulting from deteriorating weather conditions.

5. SUMMARY OF TECHNOLOGY MATURATION PLAN

Prior to this project, the technology readiness level (TRL) of the membrane contact reactor--for low-cross membrane pressure drop applications--was 3. CO_2 capture with just-in-time CO_2:NH_3 delivery was 2/3, along with ammonium looping process controls, and producing target CO_2/NH_3 ratios from stripping ammonium bicarbonate for end product use. It was the goal of this project to not only improve these TRL levels but combine the technologies into an integrated process using technologies with an already high TRL level as a basis, such as ammonium solvent regeneration which has a TRL of 7 and Algae PBR, ORPs which have a TRL of 7 and 9, respectively.

This integrated process consists of membrane absorption and stripping loops for continuous operation and an onsite liquid fuel boiler for CO_2 production. Downstream algae ORPs were integrated with the process for just-in-time nutrient delivery and CO_2 utilization for enhanced algae growth as well as an advanced automated process control scheme for delivering real time targeted CO_2/NH_3 ratios. This project was the first time solar thermal energy has been used in conjunction with ammonium solvent regeneration as well as a membrane absorber used with an ammonium solvent.

With the completion of this project, the TRL of the membrane absorber, production of target CO_2/NH_3 ratios, and ammonium looping process controls were all advanced to TRL 4/5 while the CO_2 capture with just-in-time CO_2:NH_3 delivery advanced to TRL 5. A bench scale absorption process was constructed, integrated into, and tested in conjunction with the existing IDEA bench CO_2 capture system with real combustion derived flue gas, which is a relevant, bench-scale environment. Additionally, the absorption process was integrated with a stripping loop and on site ORPs for algae production creating the fully integrated standalone bench scale ammonium looping process. CO_2 was absorbed from real natural gas-fired flue gas with commercial-scale operational parameters such as gas and solvent flow rates, velocities, temperatures, pressures, flu gas concentrations, alkalinities, and compositions. This project has established that the integrated process works, resulting in increased algae growth rates, and utilized CO_2.

6. SUMMARY OF TECHNOLOGY GAP ASSESSMENT

A technology gap assessment (TGA) was conducted, with a summary of the findings shown in **Exhibit 6.1**. Design changes for scaled application of both CO_2 capture membrane and nutrient delivery are needed.

Exhibit 6.1. Summary of the research and development gaps and approach to close the gaps.

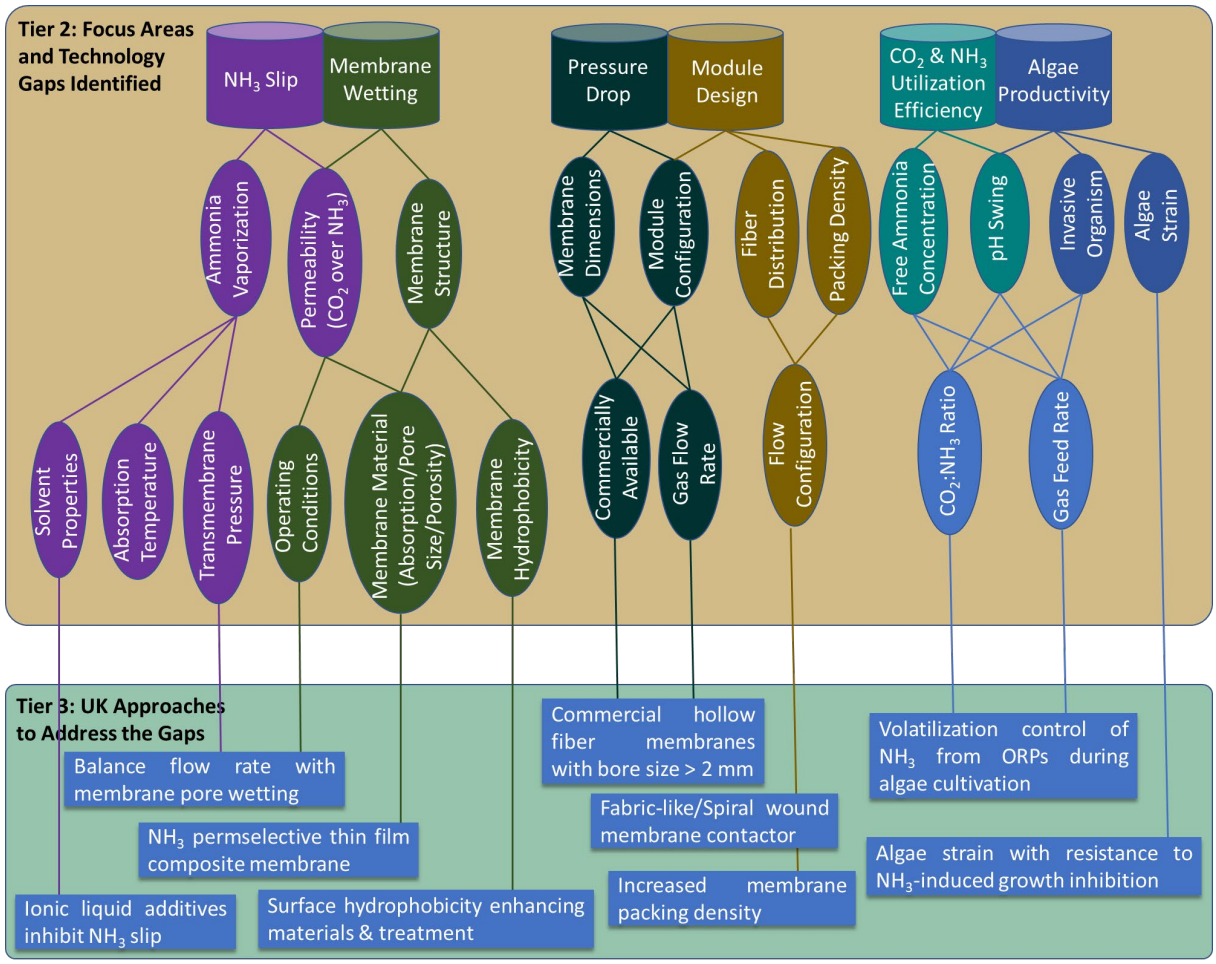

Technology Gap	Recommendation	Approach to closing gap
NH_3 slip	• Lower the energy penalty for recovering slipped ammonia • Decrease free ammonia concentration in solution • Increase the CO_2 permeability in membrane layer while depressing NH_3 mass transfer	• Indirect contact of liquid phase and gas phase • Use vapor suppressing additives with functional groups in absorbent solution to control ammonia volatility • Use selective composite membrane fiber made of a thin dense layer highly permeable to CO_2 but less permeable to NH_3

Membrane wetting	• Enhance hydrophobicity of the microporous membrane • Prevent the penetration of liquid water into the membrane pores by applying hydrophobic protective layer on membrane surface	• Fabricate hydrophobic microporous membranes • Apply surface modifications to change surface structures and properties • Utilize thin film composite membranes
Pressure drop	• Develop hollow fiber membranes with a large bore size • Identify appropriate operating conditions to decrease pressure drop	• Apply commercially available hollow fiber membranes with bore size > 2 mm • Optimize membrane bore size to balance mass transfer efficiency and energy consumption • Apply multichannel tubular membranes
Module design	• Apply uniform fiber distribution • Increase packing density • Apply appropriate flow configuration and module geometry	• Develop fabric-like structured hollow fiber membrane bundles • Increase packing density of membrane module • Apply counter-current flow mode • Use spiral wound membrane contactor
CO_2 & NH_3 utilization efficiency	• Control volatilization of NH_3 from ORPs during algae cultivation	• Feed just-in-time CO_2:NH_3 ratio to the algae pond based on the need of algae cultivation
Algae productivity	• Minimize invasive organism • Investigate effect of NH_3 on algal biomass composition	• Determine algae strain with resistance to NH_3-induced growth inhibition • Investigate the effect of NH_3 supplementation in conventional algae cultivation using predominantly $NaNO_3$ as the N-source to boost algae protein content

Membrane Performance

During this project, the CO_2 absorption membrane was studied extensively. Investigations were carried out, looking into reducing ammonia slip, reducing pressure drop, and experimenting with coatings. Testing and experimenting resulted in a customized flat sheet membrane module which showed great ammonia slip performance. For the integrated process this was swapped out for a hollow fiber membrane with a 9 times larger bore size (bore size = 1.8 mm) due to the limited membrane packing density and mass transfer capacity. This new membrane was acquired from Mann+Hummel and evaluated in the bench scale unit as shown in **Exhibit 6.2**, achieving pressure drop < 0.3 psi. This feature enables testing of the hollow fiber membrane at a feed flow rate similar to the flat sheet membrane, but with a higher CO_2 capture efficiency. Two membrane modules with different packing density (260 m^2/m^3 and 394 m^2/m^3) were applied in the bench-scale unit

and integrated system to investigate the effect of module configuration on the membrane performance. A 50% increase in the capture efficiency was attributed to longer residence time at the same feed gas flow rate.

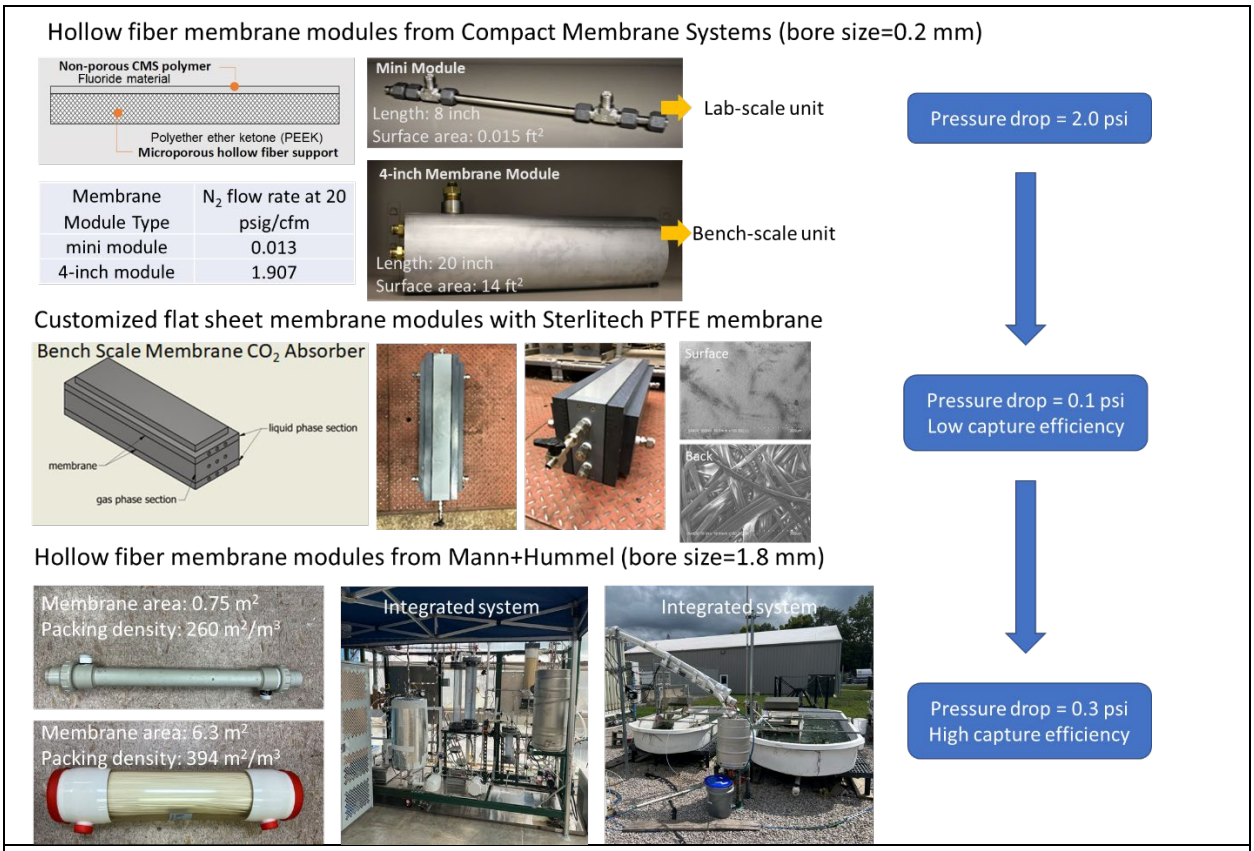

Exhibit 6.2. Effect of module configuration on the pressure drop and CO_2 capture efficiency.

Integrated System

At University of Kentucky, great efforts have been made towards developing a membrane contactor and algae cultivation process for carbon capture and utilization, which exhibit minimal ammonia emissions and enhanced algae productivity. Improvements in these areas translate into a practical, reliable, cost-effective, integrated system that can reduce capture capital and operating costs by 50% and boosts algae production by 50%. University of Kentucky successfully uses a "bottom-up" methodology (**Exhibit 6.3 & 6.4**) to develop an improved membrane absorber for carbon capture as follows. (1) Understand the impact of membrane material and solvent properties on the mass transfer of CO_2 and ammonia during absorption process, validate the concept of NH_3 slip inhibition by membrane modification and chelating additives at lab-scale, confirm the feasibility of using gaseous CO_2/NH_3 as a C- and N-source for algae cultivation and identify the optimal CO_2/NH_3 ratio and pH range for algae productivity. (2) Bench-scale level evaluation of the membrane performance, using existing carbon capture system and outdoor cultivation open raceway ponds, allows for testing and refinement of operation parameters under practical conditions. Commercially available hollow fiber membranes are deployed to build the membrane absorber and optimize solvent regeneration process to achieve controllable CO_2:NH_3 ratio in product stream. (3) The obtained CO_2 absorber and algae cultivation system are combined to

develop an integration system that serves as the foundation for process modelling and techno-economic/life-cycle analysis of the new technology.

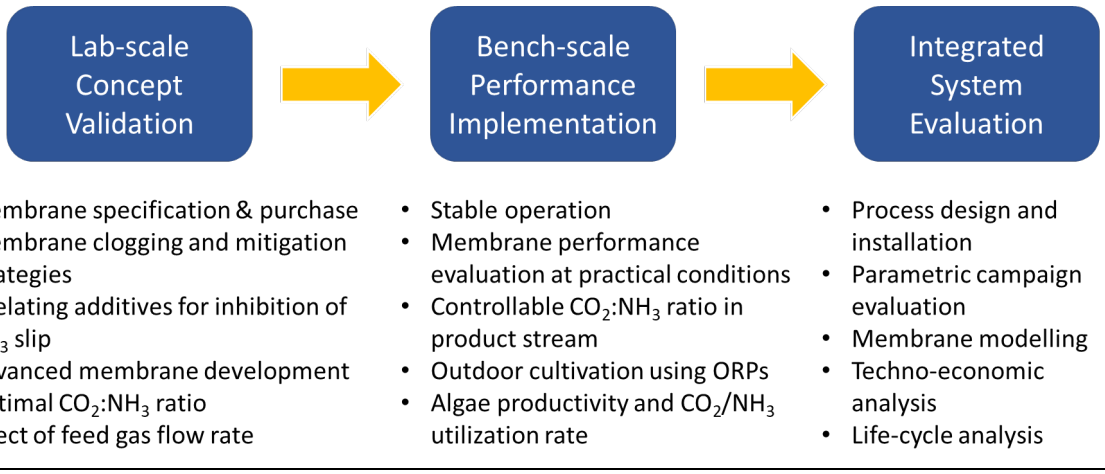

Exhibit 6.3. UK CO_2 capture and utilization technology development strategy.

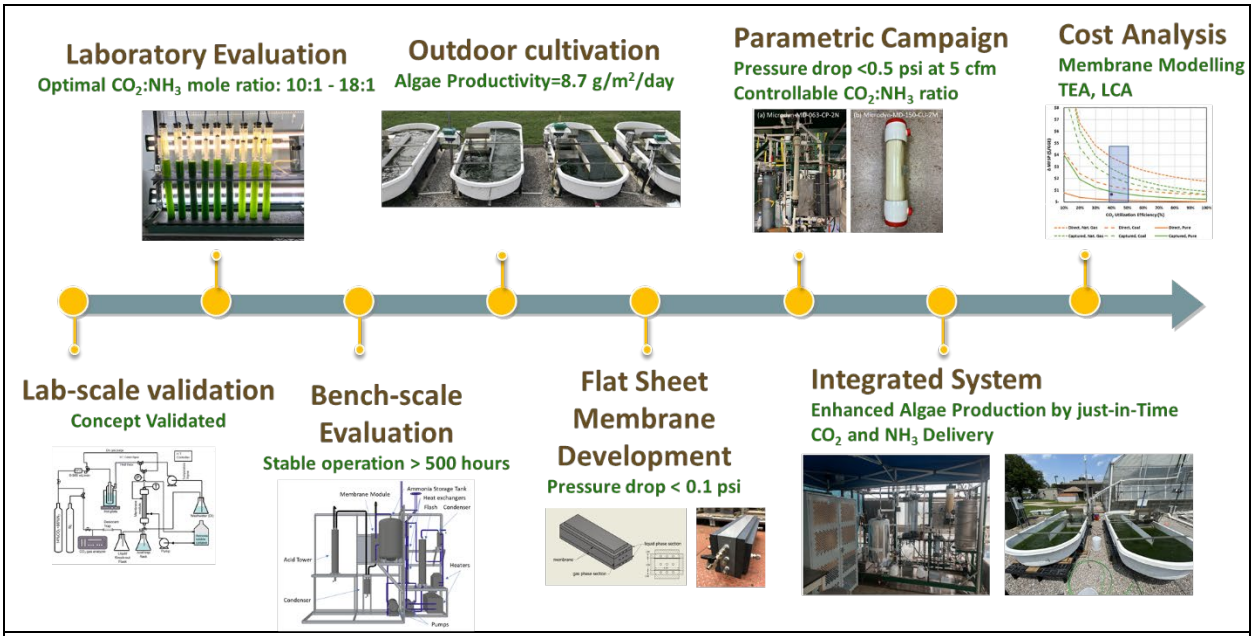

Exhibit 6.4. UK CO_2 capture and utilization technology development pathway.

Algae Productivity

The feasibility of using gaseous CO_2/NH_3 as a C- and N-source for algae cultivation was confirmed in both laboratory and outdoor experiments. In initial experiments, *Scenedesmus acutus* (UTEX B72) was cultured in 800 ml photobioreactors using a standard culture medium (BG-11 medium without a nitrogen source) with gaseous CO_2/NH_3 in mole ratios varying from 7 to 18. Excellent growth of *Scenedesmus acutus* was observed with the average growth rate for CO_2/NH_3 = 10 of 0.17 g L^{-1} day^{-1} exceeding values obtained using 1% CO_2/N_2 and $NaNO_3$ or urea as the N-source. From the long-term study, it was shown previously in this report that the average algae productivity

followed the order ORP 1 (4.6 ± 2.6 g/m^2/day) > ORP 2 (3.4 ± 1.9 g/m^2/day) > ORP 4 (3.1 ± 4.4 g/m^2/day) > ORP 3 (1.2 ± 3.7 g/m^2/day), where ORP 3 and 4 were the control ponds. ORP 1 and 2 showed significant increase in algae production with the integrated process, as well as protection from wild rotifers.

7. SUMMARY OF TECHNO- ECONOMIC ANALYSIS

A techno-economic analysis (TEA) conducted by Trimeric models an ammonium looping process at the pilot plant scale.
Colorado State University (CSU) proposed to use eight 2.2-acre ponds, totaling 17.6 acres. This pilot facility will have one central absorber unit with 8 satellite stripping units; one at each algae ORP for just-in-time delivery of nutrients. The algae are only active during sunlight hours and are significantly more active in summer months than in winter. Figure 7.1a shows algal utilization (derived from hourly sunlight intensity measured as Global Horizontal Irradiance (GHI) of CO_2 over the course of a year. The total annual utilization of CO_2 is 1,000 tonnes per year, or 114.2 kg/hr, in the time span of 4,611 hours annually, or roughly 53% of the time (corresponding to the annual hours when sunlight is sufficient for algae activity[2]). Therefore, the average utilization during sunlight hours is 216.9 kg/hr.

For this TEA, the CO_2 capture unit was sized to meet the peak CO_2 utilization rate of the algae during active sunlight hours (478 kg of CO_2/hr) based on the experimental data collected from the bench-scale integrated system constructed and studied under this award; after the design CO_2 capture rate was established by UKy and Trimeric, the peak CO_2 utilization rate was adjusted based upon algal productivity value provided by CSU based on EERE reference, backup algae requirements, and wetted pond acreage. Although there was a change in the peak CO_2 utilization rate, the CO_2 capture design rate was maintained.

Overall, the system will be capable of capturing 3,559 tonnes of CO_2 annually at peak design rate and 85% capacity factor but will be operated at 1,572 tonnes of CO_2 to algae ponds throughout the year at variable rates to meet the algae CO_2 demands. All this CO_2 is bubbled through the algae ponds, and approximately 1,000 tonnes are absorbed by the algae through photosynthesis, producing biomass. The remaining CO_2 (572 tonnes) bubbles out of the ponds and is exhausted to the atmosphere. Overall, the average utilization of CO_2 by the algae is 63%, which is specified by the UKy algae team and CSU experts. Figure 7.1b illustrates the daily average CO_2 capture requirements during active hours; this includes CO_2 utilized and CO_2 that bubbles through the algal ponds to atmosphere. Overall, the average annual capture rate is 179.5 kg/hr throughout the course of the year – and 340.9 kg/hr during annual sunlight hours.

[2] It is unclear if this estimate considers the effects of cloud cover or inclement weather

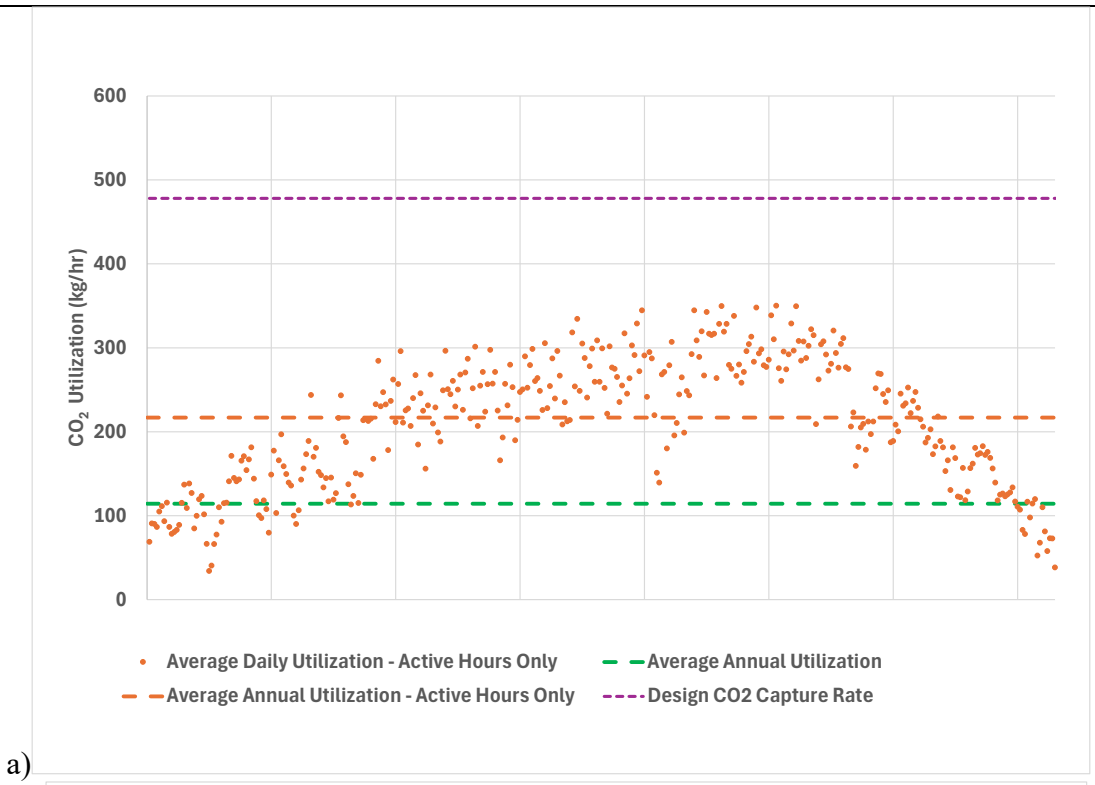

a)

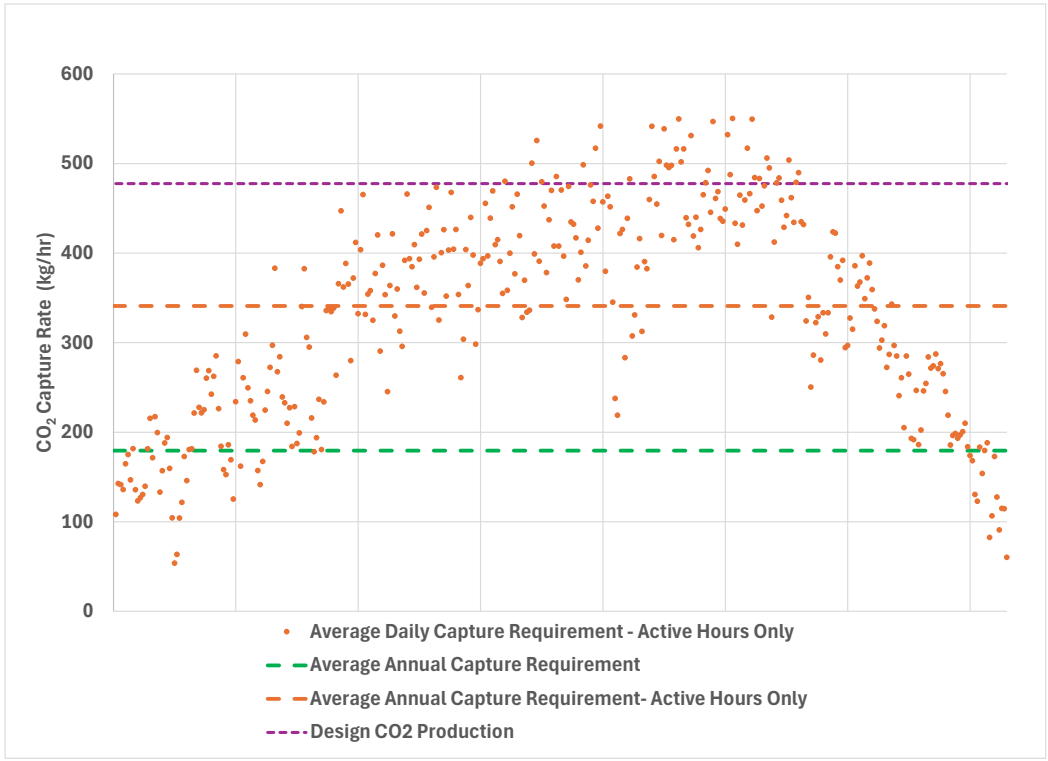

b)

Exhibit 7.1. a) Shows the CO_2 utilization rate over the course of a year, as influenced by the availability of sunlight. b) Same plot but shows CO_2 capture rate instead of Utilization. The process has been designed to accommodate algae feeding at peek sunlight availability conditions.

The general approach used for preliminary equipment sizing and associated cost estimation can be summarized as follows:

- Determine equipment type and estimate sizes of major equipment in the capture process.
    - Trimeric used standard engineering sizing methods, scaling from previous projects/internal sources, and bottom-up sizing to generate characteristic equipment sizing for all equipment. For the membrane contactor, input from UKy and Vanderbilt was explicitly used for sizing and costing.
- Identify a reference or baseline equipment cost with an associated equipment sizing metric, and use cost scaling exponents to estimate cost of the equipment in the UKy application as described in Equation 1:

$$\frac{C^{UKy}}{C^{REF}} = \left(\frac{A^{UKy}}{A^{REF}}\right)^{x} \left(\frac{CEPCI^{2024}}{CEPCI^{REF}}\right) \quad (1)$$

where:
C = Cost of equipment (REF = reference equipment)
A = Characteristic size of equipment used for cost-scaling
x = Cost-scaling exponent (0.6 is used as a general value when no other data are available)
CEPCI = Chemical Engineering Plant Cost Index (Base year for this report is 2024)

- Use Aspen Capital Cost Estimator to generate a cost estimate for key process equipment or those without a suitable reference cost for cost scaling.
- Summarize individual equipment costs to calculate total purchased equipment costs.
- Scale the purchased equipment costs (PEC) to total plant costs (TPC) using values based on Trimeric's experience with similar systems. The overall installation factor used for this project is three, as we expect that most of the equipment will be fabricated and assembled in the shop and shipped to site on skids. Field construction should be minimal.

Sizing and costing approaches for select key equipment or categories of equipment are summarized below (Exhibit 7.2). All equipment costs were estimated with stainless steel materials of construction (MOC).

Central Site Equipment List and Purchased Equipment Costs

Equipment	Purchased Equipment Cost (August '24)	Quantity	Total Purchased Equipment Cost
Rich Pump	$4,950	2	$9,900
Lean Booster Pump	$4,550	2	$9,100
Lean Cooler	$156,200	1	$156,200
DCC Water Pump	$3,450	2	$6,900
Ammonia Wash Water Pump	$3,450	2	$6,900
DCC Water Cooler	$86,600	1	$86,600
DCC Tower	$90,200	1	$90,200
Blower	$77,100	1	$77,100
Ammonia Wash Tower	$90,200	1	$90,200
Knockout Vessel	$6,500	1	$6,500

Membrane ($50/m^2)[3]	$237,600	1	$237,600
Total			**$777,200**

Modular Solvent Regeneration Unit Purchased Equipment Costs

Equipment	Purchased Equipment Cost (August '24)	Quantity	Total Purchased Equipment Cost
Lean Rich Solvent HX	$7,100	8	$56,800
PV Panels and Electric Immersion Heater	$54,500	8	$436,000
Regen Tower + Internals	$32,200	8	$257,600
Regen Tower Bottoms Pump	$3,200	16	$51,200
Total			**$801,600**

Total Plant Costs and Annualized Capital Costs

Purchased Equipment Costs	$1,578,800
Lang Factor	3
Total Plant Costs	$4,736,400
Annualized Capital Costs	$334,900

Exhibit 7.2. Capital costs for the central capture unit, satellite regeneration units, and total plant costs.

Maintenance material costs for the capture and utilization system were estimated at 2% of the total plant costs, in accordance with DOE reference materials [51], and that is the biggest operational cost at the scale used for this TEA study (over 50% of total operating costs). Chemical makeup costs were determined by calculating the required amount of ammonia makeup for the capture system. Ammonia leaves the capture system with CO_2 product via the overhead of the regeneration column in a 10:1 CO_2 to ammonia ratio (molar). The commercial price of anhydrous ammonia, as reported by the USDA in January 2025 [52], was used to estimate chemical makeup cost. The total operating costs for the peak design rate of 2,204 tonnes per year of CO_2 captured (478 kg/hr for 4,611 hours) are summarized in **Exhibit 7.3**. The total operating costs for the average capture rate of 1,572 tonnes per year (during operational daylight hours) are also summarized in **Exhibit 7.3**.

[3] Vanderbilt University provided a range of costs between $30 and $150 per m^2. UKy advised Trimeric to use a cost of $50 per m^2. More information on the membrane is available in a separate report authored by Vanderbilt.

Operating Costs at Design Capture Rates			
	Power	67.5	kW
	Uptime	4,611	hours
	Electricity Requirements	311,243	kWh
	Electricity Cost	0.075	$/kWh
	Yearly Electricity Cost	$23,300	$/yr
	Maintenance Cost (2% of plant cost)	$95,000	$/yr
	Ammonia Makeup	85.3	tonne/year
	Anhydrous Ammonia Cost	772	$/tonne
	Ammonia Makeup Cost	$65,800	$/yr
	Operating Costs	$184,000	$/yr
Operating Costs at Average Capture Rates			
	Power	25.8	kW
	Uptime	4,611	hours
	Electricity Requirements	118,964	kWh
	Electricity Cost	0.075	$/kWh
	Yearly Electricity Cost	$9,000	$/yr
	Maintenance Cost (2% of plant cost)	$95,900	$/yr
	Ammonia Makeup	60.8	tonne/year
	Anhydrous Ammonia Cost	772	$/tonne
	Ammonia Makeup Cost	$47,000	$/yr
	Operating Costs	$151,000	$/yr
Exhibit 7.3. Operating costs at design and average rates.			

Exhibit 7.4 summarizes the cost of CO_2 capture and the cost of CO_2 utilized by the algae. The high cost of CO_2 utilization is brought on by the project inefficiencies, including the following:

- Project scale
  - The current capture design needs to be at least one hundred times larger in scale to be commercially viable. This would require multiple 100+ acre algae ponds for commercial scale.
- CO_2 utilization
  - Approximately 36% of the CO_2 captured in the ammonium solvent is lost when it escapes the algal ponds. This increases the cost of CO_2 capture.
- CO_2 capture versus CO_2 utilization
  - The design capture rate (during operational hours) is approximately 2.2x the utilization rate due to the high CO_2 demand peak rates versus the daily average demand. Buffer storage of CO_2 may help reduce the design capture rate of CO_2, so that annual system utilization increases.
- System Utilization
  - The system operates for 53% of the year, often at rates well below the design capture rate. Overall, the system utilization is 44%; 1,572 tonnes per year of CO_2 captured relative to the 3,559 tonnes per year of CO_2 that could be captured if the capture system ran at design rates and 85% capacity factor for the entire

year. Once CO_2 utilization is considered, total system utilization is approximately 28%.

Cost of CO_2 Capture at Design Rates

Item	Value	Units
Annual Capital Payment	$334,900	$/yr
Annual Operating Costs	$151,000	$/yr
Total Annual Payment	$485,900	$/yr
CO_2 Capture Rate	1,572	tonne/yr
Cost of Capture	309	$/tonne
CO_2 Avoided	53	kg/MMBtu of natural gas
Heat Duty Replaced by Solar	9,591	MMBtu/yr
CO_2 Avoided	509	tonne/yr
Cost of Capture with CO_2 Avoided	233	$/tonne

Cost of CO_2 Utilized by Algae

Item	Value	Units
Annual Capital Payment	$334,900	$/yr
Annual Operating Costs	$151,000	$/yr
Total Annual Payment	$485,900	$/yr
CO_2 Utilization Rate	1,000	tonne/yr
Cost of Utilization	486	$/tonne
CO_2 Avoided	53	kg/MMBtu of natural gas
Heat Duty Replaced by Solar	9,591	MMBtu/yr
CO_2 Avoided	509	tonne/yr
Cost of Utilization with CO_2 Avoided	322	$/tonne

Exhibit 7.4. Cost of CO_2 capture and the cost of CO_2 utilized by the algae

Sensitivity cases were evaluated to understand how potential changes to the process configuration or cost assumptions will affect the overall cost of utilization. The two sensitivity cases and their results are summarized below. The first case uses solar power from the electrical grid in lieu of onsite solar production. The second sensitivity case analyzed the effect of increasing membrane costs from $50/m² to $100/m². The results are shown in **Exhibit 7.5**.

Sensitivity Case 1 Economic Analysis

Item	Value	Units
Annual Capital Payment	$242,400	$/yr
Annual Operating Costs	$438,000	$/yr
Total Annual Payment	$680,400	$/yr
CO_2 Utilization Rate	1,000	tonne/yr
Cost of Utilization	680	$/tonne
CO_2 Avoided	53	kg/MMBtu of natural gas
CO_2 Emitted by Grid Solar Power	12	kg/MMBtu
Heat Duty from Grid	9,591	MMBtu/yr

CO_2 Avoided	394	tonne/yr
Cost of Utilization with CO_2 Avoided	488	$/tonne

Case 2 Economic Analysis

Item	Value	Units
Annual Capital Payment	$385,300	$/yr
Annual Operating Costs	$166,000	$/yr
Total Annual Payment	550,300	$/yr
CO_2 Utilization Rate	1,000	tonne/yr
Cost of Utilization	550	$/tonne
CO_2 Avoided	53	kg/MMBtu of natural gas
Heat Duty Replaced by Solar	9,591	MMBtu/yr
CO_2 Avoided	509	tonne/yr
Cost of Utilization with CO_2 Avoided	365	$/tonne

Exhibit 7.5. Sensitivity cases looking at using grid solar power in lieu of onsite solar power generation and lowering the cost of the membrane absorber to the lower end.

Life Cycle Analysis

Both techno-economic analysis and life cycle assessment rely on an engineering process model that accurately represents mass and energy flows across the system. To support this effort, an engineering process model was developed to represent an algal farm with just-in-time CO_2 and ammonia with 10:1 ratio delivered from a UKy-IDEA's ammonium looping capture and utilization technology co-located with a biorefinery. The process model builds upon previous research to provide detailed and systematic evaluation of resource requirements, including energy and mass balances for algal cultivation, harvesting, dewatering, anaerobic storage, and subsequent biofuel conversion, **Exhibit 7.6**. This integrated approach enables a rigorous assessment of process efficiencies, cost drivers, and environmental impacts, informing the optimization of sustainable algal biofuel production pathways.

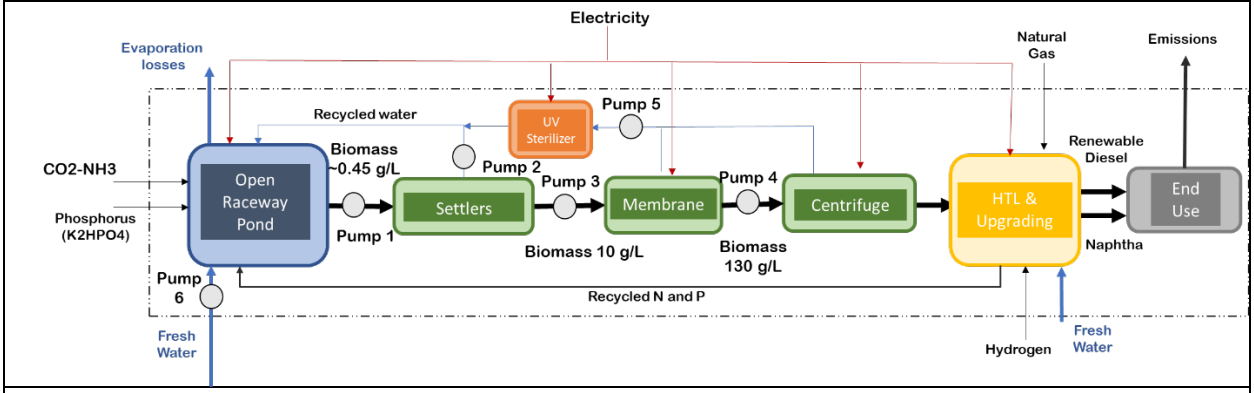

Exhibit 7.6. Process model for algal cultivation, harvesting, dewatering, anaerobic storage, and subsequent biofuel conversion.

The minimum biomass selling price (MBSP) was analyzed across different system scales, with costs broken down into key components, as shown in **Exhibit 7.7.a**. The results indicate that CO_2 costs remain one of the most significant cost drivers, particularly in smaller-scale operations such as the pilot-scale used in this analysis, where they contribute substantially to overall expenses. The 20-acre system exhibited the highest MBSP, exceeding $2,900 per tonne, primarily due to the high

per-unit cost of CO_2 with ammonia-embedded, and energy. As the system scales up to 500 acres, the MBSP decreases significantly, benefiting from economies of scale, reduced equipment costs, and improved resource utilization. The 500-acre system using ammonium looping demonstrates the lowest cost, achieving a substantial reduction in CO_2-related expenses by leveraging more efficient carbon capture and delivery methods. In contrast, the 500-acre system with CO_2 sparging remains more expensive, mainly due to increased energy demand and higher CO_2 costs, which result from the additional compression and sparging process. Beyond CO_2 costs, infrastructure investments such as pond construction, paddlewheel operation, and water delivery systems also contribute to MBSP, though these expenses become less pronounced at larger scales. Overall, the findings highlight the cost advantages of large-scale ammonium looping, which offers a more economical pathway for algal biomass production compared to conventional sparging-based systems.

The MFSP, shown in **Exhibit 7.7.b**, was determined to be highest for the 20-acre system, reaching nearly $8.25 per liter of gasoline equivalent (LGE) in 2024 USD. The results highlight the significant impact of capital expenses (CAPEX) and operational expenses (OPEX) on total costs, with cultivation-related OPEX being the largest contributor. High operational costs are primarily driven by CO_2 supply and energy inputs, making cultivation the dominant cost factor. In comparison, conversion-related costs, including hydrothermal liquefaction (HTL) and upgrading, represent a smaller fraction, contributing to less than 20% of the total MFSP. As the system scales up to 500 acres, MFSP decreases substantially due to economies of scale, leading to lower per-unit costs for infrastructure, labor, and energy consumption. The 500-acre system using ammonium looping achieves the lowest MFSP, benefiting from cost-efficient CO_2 delivery and lower energy intensity. Conversely, the 500-acre sparging system remains more expensive, as higher CO_2 compression and energy costs offset some of the benefits of scale. These findings underscore the importance of reducing cultivation costs, particularly CO_2 supply expenses, to achieve cost parity with petroleum-based fuels.
The GWP analysis, presented in **Exhibit 7.8.a**, evaluates the net greenhouse gas emissions of the biofuel by considering life cycle emissions, reported in CO_2 equivalent (CO_{2e}). The results show that a significant amount of carbon is sequestered by the biomass during cultivation (-109 g CO_{2e} MJ^{-1}). However, most of this sequestered carbon is redistributed across different HTL product streams, with portions released in the gas-phase (13 g CO_{2e} MJ^{-1}) and aqueous-phase (23 g CO_{2e} MJ^{-1}). When considering fuel combustion emissions (71 g CO_{2e} MJ^{-1}), a net carbon sequestration credit of 1 g CO_{2e} MJ^{-1} was calculated, which represents the carbon in the biochar phase of HTL. In addition to these inherent process emissions, the life cycle impacts of other system inputs—including ammonia, DAP, natural gas, hydrogen, and electricity—were accounted for, resulting in a net GWP of 57 g CO_{2e} MJ^{-1}. Among the embodied emissions in the CO_2,feedstock were identified as a major contributor, accounting for 51% of net emissions.

The GWP was further disaggregated to assess the contributions of different process stages and to compare the ammonium looping system with the conventional CO_2 compression and sparging method, as shown in **Exhibit 7.8.b**. The results indicate that cultivation-related emissions, particularly those linked to CO_2 capture and delivery, are the largest contributors to overall GWP. The CO_2 sparging scenario exhibits significantly higher emissions from cultivation due to its greater energy intensity, stemming from the compression and sparging process required for CO_2 delivery. In contrast, the ammonium looping system benefits from emissions offsets through

carbon sequestration in biochar and the recovery of ammonia in the aqueous phase of HTL, both of

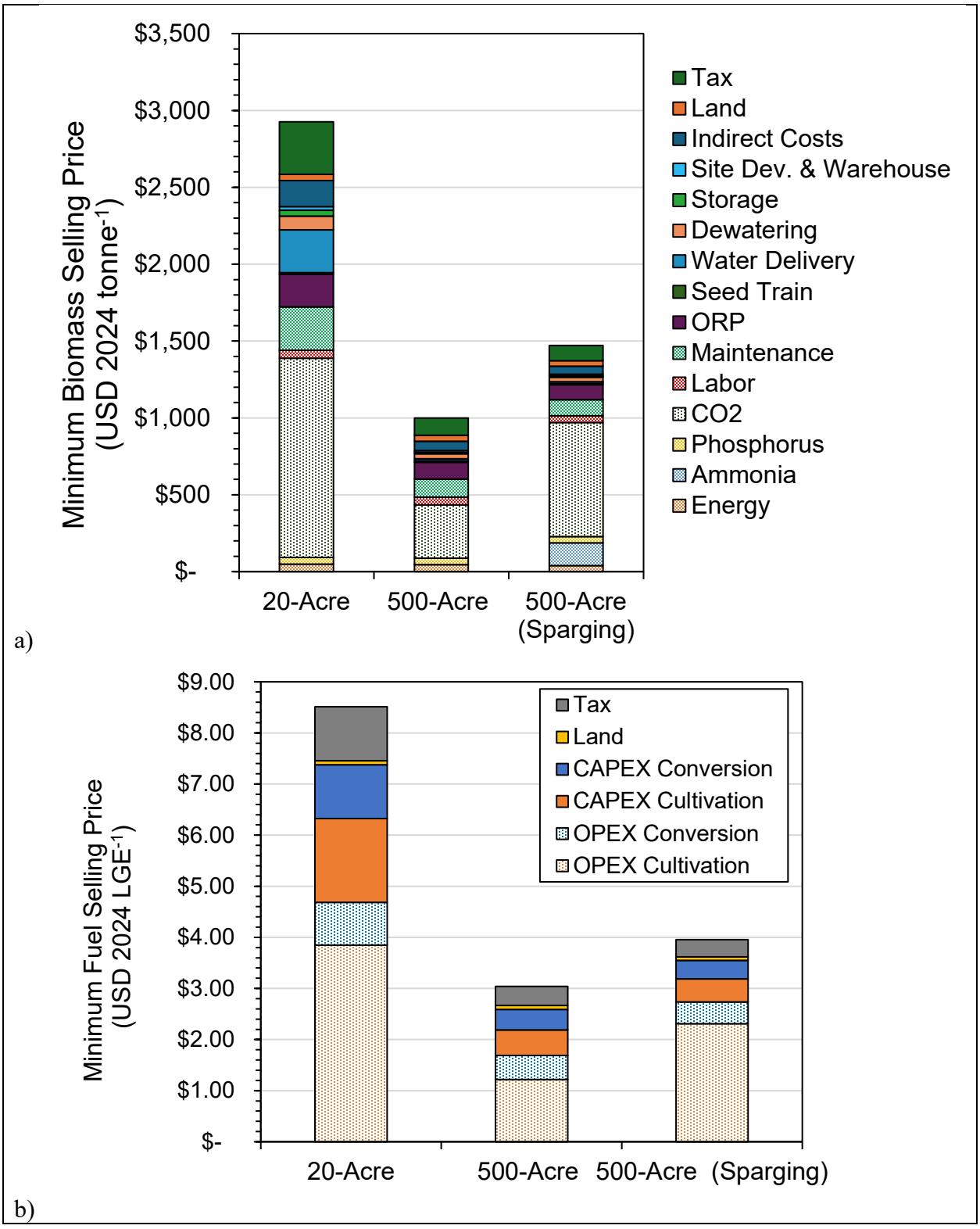

Exhibit 7.7. a) Minimum biomass selling price for a 20- and 500-acre farm. The economics of scale drastically reduce the biomass selling price at the 500-acre scale. b) Minimum fuel selling price.

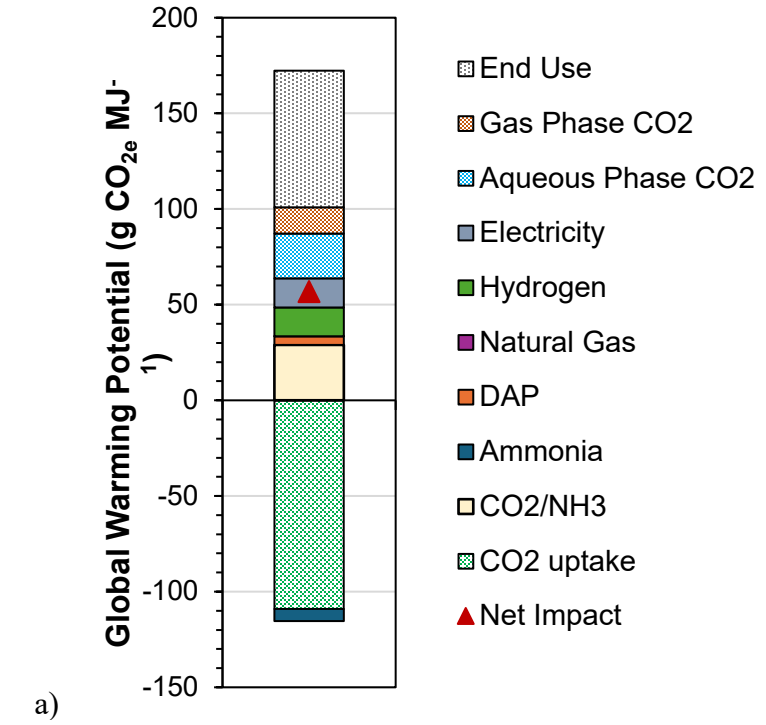

a)

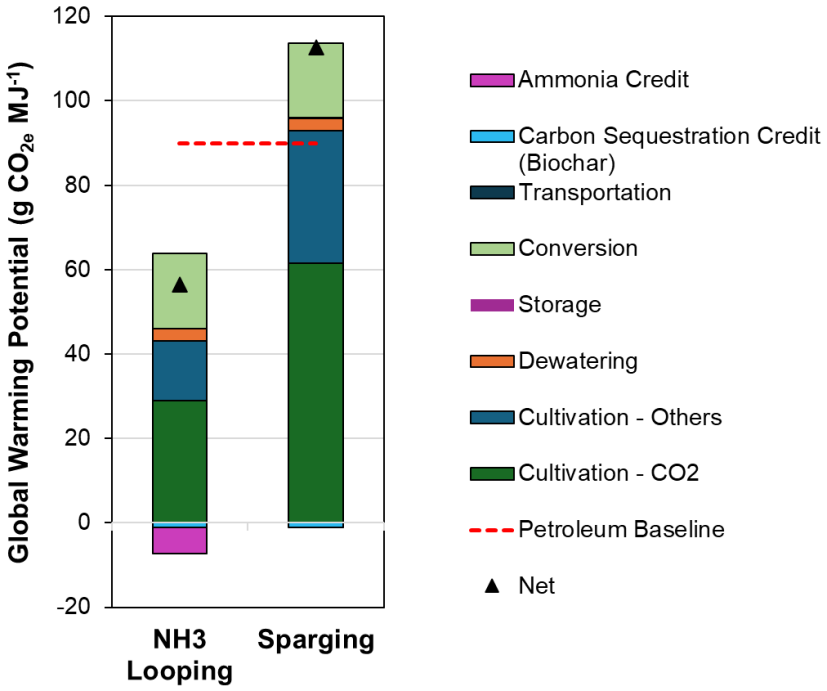

b)

Exhibit 7.8. a) GWP analysis. b) Ammonium looping vs sparging GWP analysis.

which help reduce its net impact. Conversion and transportation emissions remain relatively similar across both scenarios, contributing to 30% of the total net GWP in the ammonium looping system. Overall, results indicate that the net GWP of ammonium looping is substantially lower than that of CO_2 sparging, and it also falls well below the petroleum baseline of 90 g CO_2e MJ^{-1}.

8. LESSONS LEARNED

Four key learnings from this project have been identified.

1) Efficient and simple hollow fiber membranes with a low ammonia slippage are commercially available. Improvements can be made on these membranes; the bore size can be adjusted for optimal performance and manufacturing methods can improve. Studying how these membrane scale for larger production can be done for accurate technological economic assessments. Using the moisture entrained in the flue gas to wash the membrane of ammonium carbamate proved to be an effective strategy and is being implemented on other membrane applications at UK IDEA.

2) Using a solar thermal water heater to provide heat for regeneration proved very effective at the bench/pilot scale testing, and commercial scale. However, at medium scales there is no mature commercial market for this technology, so it has to be replaced with another method, such as solar electric panels.

3) Maintaining a consistent CO_2/NH_3 ratio of 10 while meeting the product quantity demands of the algae pounds is delicate balance. Increasing rich/lean solvent flow is one way but could lower capture, making stripping less efficient. Another method is to increase stripping to release more CO_2 while condensing excess ammonia vapor in the product line. The latter method has the advantage of keeping capture high. An effective method for condensing excess ammonia vapor is to inject colder rich solvent--≈ 20°C cooler than the inlet hot rich—into the top of the stripper via a spray nozzle. This condenses excess vapor while also cooling the outlet product stream, keeping heat inside the stripper and improving efficiency. This is a method that has been used in other UK IDEA processes and continues to be a proven solution and valuable learned lesson.

4) Algae cultivation is a dynamic process that is dependent on many factors, primarily the weather and the conditions of the current crop. These factors, along with many others impacts the nutrient need on a day-by-day basis. To optimize CO_2 and NH_3 delivery to the algae ponds it was determined that a smart monitoring and process control system would be needed, with live instantaneous feedback on product stream ratio and crop conditions. UK IDEA has developed such a system that is functional and operates as intended on a bench/pilot scale. The need for dynamic control systems is quickly becoming more and more important as CO_2 capture is adapted into real industrial scenarios. It is now UK IDEA's policy to evaluate the need for advanced control schemes and implement them if required, for all projects moving forward.

9. TECHNICAL BENEFITS AND SHORTCOMINGS

Benefits of the technology that have been incorporated into plans for UK IDEA CO_2 capture process for demonstration at the engineering and large pilot scales. The primary advantage of this technology is the on-site utilization of CO_2, which removes the cost of vacuum pumping, liquifying, transportation, and storage of CO_2 from the total cost of mitigation.

Current TEA estimates for this technology suggest that it is heavily impacted by cost-of-scale. But current larger scales are limited to the size of algae growth ponds and how many are at any given site.

10. FUTURE DEVELOPMENT

Currently there are plans in motion to scale this process up to a larger pilot scale. For future commercial applications, industries which use algae in their production chain have been solicited to take part in pilot studies. Generally, this process can be used for any algae production chain, see **Exhibit 10.1**.

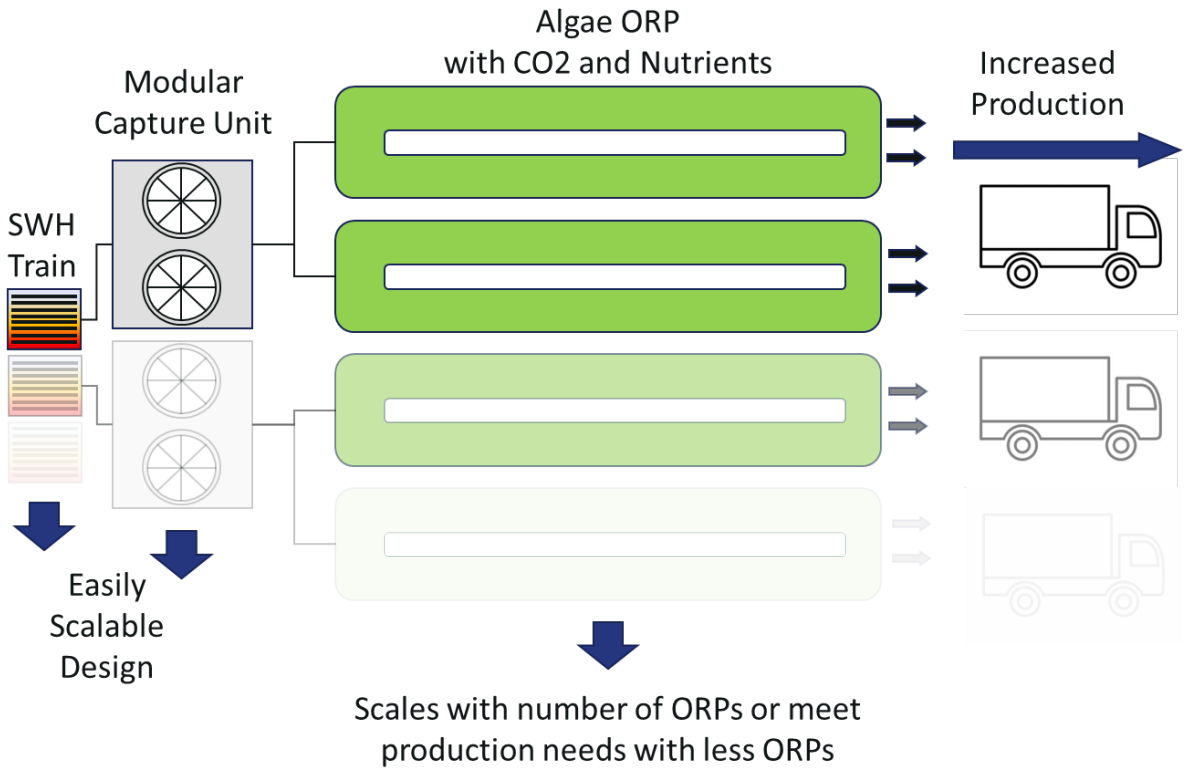

Exhibit 10.1. Algae growers can expect to increase production with the adaptation of an ammonium looping process to their growth ponds. Not only will the ammonia and CO_2 nutrients increase growth rate by 50% but the ammonia will also act as a protectant against foreign rotifers. Shown is an example of a potential direct air capture set up.

11. References

1. Diao, N., Li, Q. and Fang, Z. 2004. Heat transfer in ground heat exchangers with groundwater advection. *International Journal of Thermal Sciences*, 43: 1203-1211.
2. He, Q., Chen, M., Meng, L., Liu, K., and Pan, W. 2004. Study on Carbon Dioxide Removal from Flue Gas by Absorption of Aqueous Ammonia. Western Kentucky University
3. Yeh, A.C., and Bai, H. 1999. Comparison of ammonia and monoethanolamine solvents to reduce CO_2 greenhouse gas emissions. *The Science of the Total Environment*. 228: 121-133.

4. Villeneuve, K., Roizard, D., Remigy, J., Iacono, M., and Rode, S.. 2018. CO_2 capture by aqueous ammonia with hollow fiber membrane contactors: Gas phase reactions and performance stability. *Separation and Purification Technology*, 199: 189-197.
5. Toro Molina, C., and Bouallou, C. 2016. Carbon dioxide absorption by ammonia intensified with membrane contactors. *Clean Technologies and Environmental Policy*, 18: 2133–2146.
6. Makhloufi, C., E. Lasseuguette, J.C. Remigy, B. Belaissaoui, D. Roizard, and E. Favre. 2014. Ammonia based CO_2 capture process using hollow fiber membrane contactors. *Journal of Membrane Science*, 455: 236-246.
7. Berman, T. 1999. Algal growth on organic compounds as nitrogen sources. *Israel Oceanographic*, 21: 1423-1437.
8. Finlay, K., Leavitt, P. R., Wissel, B., and Prairie, Y. T.. 2009. Regulation of spatial and temporal variability of carbon flux in six hard-water lakes of the northern Great Plains. *Limnology and Oceanography*, 54: 2553–2564.
9. Beal CM, Gerber LN, Sills DL, Huntley ME, Machesky SC, Walsh MJ, Tester JW, Archibald I, Granados J, Greene CH (2015) Algal biofuel production for fuels and feed in a 100-ha facility: A comprehensive techno-economic analysis and life cycle assessment. Algal Res 10:266–279. https://doi.org/10.1016/j.algal.2015.04.017
10. Davis R, Fishman D, Frank ED, Wigmosta MS, Aden A, Coleman AM, Pienkos PT, Skaggs RJ, Venteris ER, Wang MQ (2012) Renewable Diesel from Algal Lipids: An Integrated Baseline for Cost, Emissions, and Resource Potential from a Harmonized Model. ANL/ESD/12-4; NREL/TP-5100-55431; PNNL-21437. doi:https://dx.doi.org/10.2172/1044475.
11. Frank E, Pegallapati AK, Davis R, Markham J, Coleman A, Jones S, Wigmosta MS, Zhu Y (2016) Life-cycle analysis of energy use, greenhouse gas emissions, and water consumption in the 2016 MYPP algal biofuel scenarios. Argonne National Laboratory (ANL), 2016. http://www.osti.gov/scitech/biblio/1281137.
12. Huntley ME, Johnson ZI, Brown SL, Sills DL, Gerber L, Archibald I, Machesky SC, Granados J, Beal C, Greene CH (2015) Demonstrated large-scale production of marine microalgae for fuels and feed. Algal Res 10:249–265. https://doi.org/10.1016/j.algal.2015.04.016
13. Pate R, Klise G, Wu B (2011) Resource demand implications for US algae biofuels production scale-up. Appl Energy 88:3377–3388. https://doi.org/10.1016/j.apenergy.2011.04.023
14. Quinn JC, Catton KB, Johnson S, Bradley TH (2013) Geographical Assessment of Microalgae Biofuels Potential Incorporating Resource Availability. BioEnergy Res 6:591–600. https://doi.org/10.1007/s12155-012-9277-0
15. Quinn JC, Davis R (2015) The potentials and challenges of algae based biofuels: A review of the techno-economic, life cycle, and resource assessment modeling. Bioresource Tech 184:444-452. https://doi.org/10.1016/j.biortech.2014.10.075
16. Venteris ER, Skaggs RL, Wigmosta MS, Coleman AM (2014) A national-scale comparison of resource and nutrient demands for algae-based biofuel production by lipid extraction and hydrothermal liquefaction. Biomass Bioenergy 64:276–290. https://doi.org/10.1016/j.biombioe.2014.02.001

17. Somers MD, Quinn JC (2019) Sustainability of carbon delivery to an algal biorefinery: A techno-economic and life-cycle assessment. J CO_2 Util 30:193-204. https://doi.org/10.1016/j.jcou.2019.01.007
18. Y-K Lee, H-K Hing (1989) Supplying CO_2 to photosynthetic algal cultures by diffusion through gas-permeable membranes. Appl Microbiol Biotechnol 31:298-301. https://doi.org/10.1007/BF00258413
19. Carvalho AP, Malcata FX (2001) Transfer of Carbon Dioxide within Cultures of Microalgae: Plain Bubbling versus Hollow-Fiber Modules. Biotechnol Prog 17(2):265-272. https://doi.org/10.1021/bp000157v
20. Putt R, Singh M, Chinnasamy S, Das KC (2011) An efficient system for carbonation of high-rate algae pond water to enhance CO_2 mass transfer. Bioresource Technol., 102(3): 3240-3245. https://doi.org/10.1016/j.biortech.2010.11.029
21. Kumar K, Mishra SK, Shrivastav A, Park MS, Yang JW (2015) Recent trends in the mass cultivation of algae in raceway ponds. Renew Sustain Energy Rev 51:875-885. https://doi.org/10.1016/j.rser.2015.06.033
22. Könst P, Mireles IH, van der Stel R, van Os P, Goetheer E (2017) Integrated system for capturing CO_2 as feedstock for algae production. Energy Procedia 114:7126-7132. https://doi.org/10.1016/j.egypro.2017.03.1856
23. Hazlebeck D, Rickman B, Corpuz R (2020) Algae Production CO_2 Absorber with Immobilized Carbonic Anhydrase. United States. https://doi.org/10.2172/1581442
24. Nikolic H, Liu K, Crocker M (2020) NH_4OH Looping with Membrane CO_2 Absorber and Distributed Stripper for Enhanced Algae Growth. United States. https://doi.org/10.2172/1722918. https://www.osti.gov/servlets/purl/1722918.
25. Liu K, Crocker M, Nikolic H (2023) CO_2 capture and utilization system and method. US Patent Application US20230021734A1.
26. Diao Y, Zheng X, He B, Chen C, Xu X (2004) Experimental Study on Capturing CO_2 Greenhouse Gas by Ammonia Scrubbing. Energy Convers Manag 45:2283-2296. https://doi.org/10.1016/j.enconman.2003.10.01
27. He Q, Chen M, Meng L, Liu K, Pan WP (2004) Study on Carbon Dioxide Removal from Flue Gas by Absorption of Aqueous Ammonia, Institute for Combustion Science and Environmental Technology. https://www.semanticscholar.org/paper/Study-on-Carbon-Dioxide-Removal-from-Flue-Gas-by-of-He-Chen/4994d1230f70482e0b2fa8abbecd9a1daedfd5e0
28. Myers J (1951) Physiology of the algae. Ann Rev Microbiol 5:157-180.
29. Park J, Jin H-F, Lim B-R, Park K-Y, Lee K (2010) Ammonia removal from anaerobic digestion effluent of livestock waste using green alga *Scenedesmus* sp. Bioresource Technol 101:8649-8657. https://doi.org/10.1016/j.biortech.2010.06.142
30. Zheng H, Wu X, Zou G, Zhou T, Liu Y, Ruan R (2019) Cultivation of *Chlorella vulgaris* in manure-free piggery wastewater with high-strength ammonium for nutrients removal and biomass production: Effect of ammonium concentration, carbon/nitrogen ratio and pH. Bioresource Technol 273:203-211. https://doi.org/10.1016/j.biortech.2018.11.019
31. Townsend SA, Schult JH, Douglas MM, Skinner S (2008) Does the Redfield ratio infer nutrient limitation in the macroalga *Spirogyra fluviatilis*? Freshwater Biol 53(3):509-520. https://doi.org/10.1111/j.1365-2427.2007.01916.x

32. Collos Y, Harrison PJ (2014) Acclimation and toxicity of high ammonium concentrations to unicellular algae. Marine Pollution Bull 80:8-23. https://doi.org/10.1016/j.marpolbul.2014.01.006
33. Crofcheck C, E X, Shea A, Montross M, Crocker M, Andrews R (2013) Influence of flue gas components on the growth rate of *Chlorella vulgaris* and *Scenedesmus acutus*. Transactions of the ASABE, 56(6):1421-1429. https://doi.org/10.13031/trans.56.10094
34. Kang J, Wen Z (2015) Use of microalgae for mitigating ammonia and CO_2 emissions from animal production operations — Evaluation of gas removal efficiency and algal biomass composition. Algal Res 11:204-210. https://doi.org/10.1016/j.algal.2015.06.020
35. Abeliovich A, Azov Y (1976) Toxicity of ammonia to algae in sewage oxidation ponds. Appl Environ Microbiol 31:801–806. https://doi.org/10.1128/aem.31.6.801-806.1976
36. Azov Y, Goldman JC (1982) Free Ammonia Inhibition of Algal Photosynthesis in Intensive Cultures. Appl Environ Microbiol 43(4):735-739. https://doi.org/10.1128/aem.43.4.735-739.1982
37. de Araujo A, Snell TW, Hagiwara A (2000) Effect of unionized ammonia, viscosity and protozoan contamination on the enzyme activity of the rotifer *Brachionus plicalitis*. Aquac Res 31:359–365. https://doi.org/10.1023/A:1017567226012
38. Schlüter M, Groeneweg J (1985) The inhibition by ammonia of population growth of the rotifer, *Brachionus rubens*, in continuous culture. Aquaculture 46:215–220. https://doi.org/10.1016/0044-8486(85)90207-8
39. Thomas PK, Dunn GP, Passero M, Feris KP (2017) Free ammonia offers algal crop protection from predators in dairy wastewater and ammonium-rich media. Bioresource Technol 243:724-730. https://doi.org/10.1016/j.biortech.2017.07.008
40. Mohler D, Wilson MH, Kesner S, Schambach JY, Vaughan D, Frazar M, Stewart J, Groppo J, Pace R, Crocker M. (2019) Beneficial re-use of CO_2 emissions using microalgae: Demonstration assessment and biomass characterization. Biores Technol 293:122014. https://doi.org/10.1016/j.biortech.2019.122014
41. Greque de Morais M, Costa JAV (2007) Biofixation of carbon dioxide by *Spirulina* sp. and *Scenedesmus obliquus* cultivated in a three-stage serial tubular photobioreactor. J Biotechnol 129:439–445. https://doi.org/10.1016/j.jbiotec.2007.01.009
42. Calculation of Un-ionized Ammonia in Fresh Water, Florida Department of Environmental Protection, Tallahassee, Chemistry Laboratory Methods Manual, Rev. 2, 02/12/2001. https://floridadep.gov/sites/default/files/5-Unionized-Ammonia-SOP_1.pdf Accessed 4 April 2022
43. Lourenço SO, Barbarino E, Lavín PL, Lanfer Marquez UM, Aidar E (2004) Distribution of intracellular nitrogen in marine microalgae: calculation of new nitrogen-to-protein conversion factors. Eur J Phycol 39:17–32. https://doi.org/10.1080/0967026032000157156
44. Beckstrom BD, Wilson MH, Crocker M, Quinn JC (2020) Bioplastic production from microalgae with fuel co-products: A techno-economic and life-cycle assessment. Algal Res 46:101769. https://doi.org/10.1016/j.algal.2019.101769
45. UTEX Culture Collection of Algae. bg-11-medium.pdf (utexas.edu)

46. Wilson MH, Mohler DT, Groppo JG, Grubbs T, Kesner S, Frazar EM, Shea A, Crofcheck C, Crocker M. (2016) Capture and recycle of industrial CO_2 emissions using microalgae. Appl. Petrochem. Res. 6: 279–293.
47. Santillan-Jimenez E, Pace R, Marques S, Morgan T, McKelphin C, Mobley J, Crocker M (2016) Extraction, characterization, purification and catalytic upgrading of algae lipids to fuel-like hydrocarbons. Fuel 180:668-678.
48. Schluter M, Groeneweg J (1985) The inhibition by ammonia of population growth of the rotifer, Brachionus rubens, in continuous culture. Aquaculture 46:215–220.
49.
50. Sutter, D., M. Gazzani, and M. Mazzotti. 2015. Formation of solids in ammonia-based CO_2 capture processes — Identification of criticalities through thermodynamic analysis of the CO2–NH3–H2O system. Chemical Engineering Science. Volume 133, 8 September 2015, Pages 170-180.
51. "Oklahoma Production Cost Report (Bi-Weekly)," USDA, 2025.
52. "Sunshot 2030," US DOE, [Online]. Available: “Sunshot 2030,” Energy.gov, https://www.energy.gov/eere/solar/sunshot2030#:~:text=During%20this%20time%2C%20the%20solar,that%20highlights%20the%202030%20goals.

12. LIST OF ACRONYMS

BP – Budget Period
Compact Membrane Systems (CMS
carbon dioxide (CO2
CO2 capture system (CCS
CPVC – Chlorinated Polyvinylchloride
carbon utilization efficiency (CUE
direct contact cooler (DCC
DOE – Department of Energy
EH&S – Environmental, Health & Safety
global warming potential (GWP
hydrothermal liquefaction (HTL
IC – Ion Chromatography
life-cycle analysis (LCA
MEA – Monoethanolamine
NG – Natural Gas
ORP – Open Raceway Pond
polyester (PET
polytetrafluoroethylene (PTFE
Process Flow Diagrams (PFDs
piping and instrumentation diagrams
post-combustion (PC
state-of-the-art (SOA
TEA – Techno-Economic Analysis

TGA – Technology Gap Analysis
TMP –
TRL – Technology Readiness Level
UK – University of Kentucky
University of Kentucky Center for Applied Energy (UK CAER
University of Kentucky Institute for Decarbonization and Energy Advancement (UK IDEA
VFD – Variable Frequency Drive